

UNIVERSIDADE ESTADUAL DE MARINGÁ
CENTRO DE CIÊNCIAS BIOLÓGICAS
DEPARTAMENTO DE BIOQUÍMICA
PROGRAMA DE PÓS-GRADUAÇÃO EM CIÊNCIAS BIOLÓGICAS

GABRIELA BUENO FRANCO SALLA

**EFEITOS METABÓLICOS, DISTRIBUIÇÃO E INTERAÇÕES COM A BICAMADA
LIPÍDICA MEMBRANAR DOS HERBICIDAS DINOSEB, 2,4-D E PICLORAM NO
FÍGADO**

Maringá
2018

GABRIELA BUENO FRANCO SALLA

**EFEITOS METABÓLICOS, DISTRIBUIÇÃO E INTERAÇÕES COM A BICAMADA
LIPÍDICA MEMBRANAR DOS HERBICIDAS DINOSEB, 2,4-D E PICLORAM NO
FÍGADO**

Tese apresentada à Universidade Estadual de Maringá, como requisito parcial para a obtenção do título de doutor.

Orientador: Adelar Bracht

Coorientadora: Lívia Bracht

Maringá
2018

Dados Internacionais de Catalogação na Publicação (CIP)
(Biblioteca Central - UEM, Maringá, PR, Brasil)

S168e Salla, Gabriela Bueno Franco
Efeitos metabólicos, distribuição e interações com a bicamada lipídica membranar dos herbicidas Dinoseb, 2,4-D e Picloram no fígado. / Gabriela Bueno Franco Salla. -- Maringá, 2018.
92 f. : il., color., figs., tabs.

Orientador(a): Prof. Dr. Adelar Bracht.
Co-orientador(a): Prof^a. Dr^a. Lívia Bracht.
Tese (doutorado) - Universidade Estadual de Maringá, Centro de Ciências Biológicas, Departamento de Bioquímica, Programa de Pós-Graduação em Ciências Biológicas, 2018.

1. Herbicidas. 2. Metabolismo hepático. 3. Perfusão hepática. 4. Ratos Wistar. 5. Compostos tóxicos. I. Bracht, Adelar, orient. II. Bracht, Lívia, coorient. III. Universidade Estadual de Maringá. Centro de Ciências Biológicas. Departamento de Bioquímica. Programa de Pós-Graduação em Ciências Biológicas. IV. Título.

CDD 21.ed. 572.4

AHS-CRB-9/1065

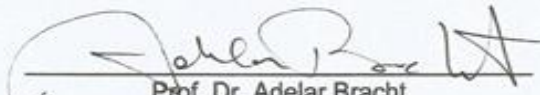
GABRIELA BUENO FRANCO SALLA

**EFEITOS METABÓLICOS, DISTRIBUIÇÃO E INTERAÇÕES COM A BICAMADA
LIPÍDICA MEMBRANAR DOS HERBICIDAS DINOSEB, 2,4-D E PICLORAM NO
FÍGADO**

Tese apresentada à Universidade Estadual de
Maringá, como requisito parcial para a obtenção
do título de doutor.

Aprovado em: 21/06/2018

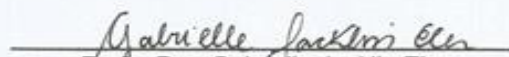
BANCA EXAMINADORA



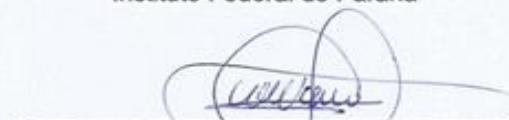
Prof. Dr. Adelar Bracht
Universidade Estadual de Maringá



Profa. Dra. Andrea de Oliveira Valoto
Centro Universitário Integrado



Profa. Dra. Gabrielle Jacklin Eler
Instituto Federal do Paraná



Prof. Dr. Jurandir Fernando Comar
Universidade Estadual de Maringá



Prof. Dr. Róberto Barbosa Bazzote
Universidade Estadual de Maringá

BIOGRAFIA

Gabriela Bueno Franco Salla nasceu em Penápolis/SP em 07/03/1989. Possui graduação em Ciências Biológicas – Licenciatura (2011) e Bacharelado (2012) pela Universidade Estadual do Norte do Paraná, *campus* Luiz Meneguel, Bandeirantes/PR. Durante a graduação realizou estágios na área da Biologia da Conservação da ictiofauna, como bolsista de Iniciação Científica pelo CNPq. No final da graduação, recebeu o “Prêmio Campus Luiz Meneghel”, atingindo a maior média e o 1º Lugar no curso de Ciências Biológicas formandos 2011. Possui mestrado em Genética (2014), pelo programa de Pós-Graduação em Genética da UNESP/IBILCE, *campus* de São José do Rio Preto/SP. Desenvolveu doutorado pelo programa de Pós-Graduação em Ciências Biológicas (Área de Concentração de Biologia Celular e Molecular) da UEM, Maringá/PR, sob a orientação do professor Dr. Adelar Bracht, no Laboratório de Metabolismo Hepático, Departamento de Bioquímica.

AGRADECIMENTOS

Agradeço acima de tudo o imenso amor de Deus em minha vida. Em cada momento vivido durante o doutorado, sei que pude contar com Suas bênçãos, proteção e amparo.

Agradeço meu orientador, Prof. Dr. Adelar Bracht por essa oportunidade e pelos ensinamentos, conselhos, paciência e dedicação constante para fornecer as melhores condições para realização deste trabalho. Minha admiração por ser um profissional extremamente dedicado e competente.

À minha coorientadora, Profa. Dra. Lívia Bracht pelos ensinamentos, ajudas e pela amizade. Além de orientar, ela compartilhou muitas lições e conhecimentos que levarei para minha vida pessoal e profissional.

Aos professores Jurandir e Anacharis pelos ensinamentos, amizades e apoio científico.

Aos técnicos do laboratório, Irene e Luis, que sempre estavam dispostos a ajudarem.

Agradeço os meus amigos de trabalho Ana Paula, Angela, Mariana, Cristiane, Juliana, Lorena, Heloisa, Geferson, Lucas, Juliany, Amanda S, Amanda M, Maiara, Gisele, Mellina, Vanesa, Marcos, Heloisa, Francielle e Luciana pelo companheirismo, pelas ajudas, conversas, risadas, desabafos e apoio.

Também quero agradecer aos meus pais, Adalberto e Mary, irmãos, Vinícius e Vivian e a toda minha família, que me apoiaram e me ajudaram a vencer todos os obstáculos encontrados ao longo do caminho. Obrigada por cada incentivo e conselho, pelo amor e pelas orações em meu favor.

Agradeço meu esposo, Alex, que de forma generosa me deu força e coragem, me apoiando nos momentos de dificuldades. Meu sincero agradecimento pelo companheirismo, dedicação, paciência e amor.

E ao apoio financeiro do CNPq e da CAPES.

APRESENTAÇÃO

Este é um trabalho realizado no Laboratório de Metabolismo Hepático do Departamento de Bioquímica da Universidade Estadual de Maringá, apresentado na forma de dois artigos científicos originais, em consonância com as regras do Programa de Pós-graduação em Ciências Biológicas.

Artigo 1:

Gabriela Bueno Franco Salla, Lívia Bracht, Anacharis Babeto de Sá-Nakanishi, Angela Valderrama Parizotto, Fabrício Bracht, Rosane Marina Peralta, Adelar Bracht. **Distribution, lipid-bilayer affinity and kinetics of the metabolic effects of dinoseb in the liver.** Department of Biochemistry, University of Maringá, 87020900 Maringá, Brazil.

Publicado na revista Toxicology and Applied Pharmacology, 329, 259–271, 2017; <https://doi.org/10.1016/j.taap.2017.06.013>).

Artigo 2:

Gabriela Bueno Franco Salla, Lívia Bracht, Angela Valderrama Parizotto, Rosane Marina Peralta, Fabrício Bracht, Adelar Bracht. **Actions of two organo-chlorinated herbicides, 2,4-dichlorophenoxyacetic acid and picloram, on liver metabolism.**

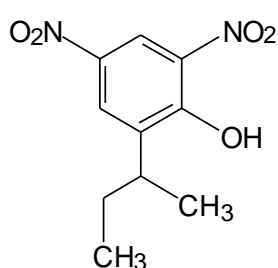
Department of Biochemistry, University of Maringá, 87020900 Maringá, Brazil.

LIST OF ABBREVIATIONS AND ACRONYMS

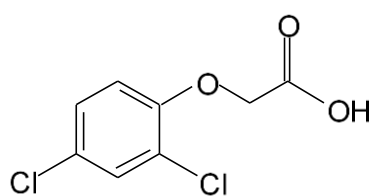
2,4-D	2,4-dichlorophenoxyacetic acid
ADP	adenosine diphosphate
AMP	adenosina monofosfato
ATP	adenosine triphosphate
C_e	extracellular concentration
C_i	intracellular concentration
DMSO	dimethylsulphoxide
EC_{50}	half-maximal stimulatory concentration
HPLC	high-performance liquid chromatography
IC_{50}	half-maximal inhibitory concentration
k_{met}	coefficient for metabolic transformation
LD_{50}	amount of a toxic agent that is sufficient to kill 50 percent of a population of animals
NAD+	nicotinamide adenine dinucleotide
PMF	potential mean force
POPC	1-palmitoyl-2-oleoyl-sn-glycero-3-phosphocholine
R	universal gas constant
S(t)	experimental outflow profile of a substance upon constant infusion into the portal vein
S'_{water}	the first derivative of the [3H]water outflow profile corrected for the time $\{[(t - t_0)/[(1 + \Phi) + t_0]]\}$
Φ	ratio of the extra, real or apparent, space occupied by a given substance divided by the aqueous space of the liver
T	absolute temperature
t	time
t_0	transit time in the large vessels of the liver plus that in the tubing system before and after the liver
θ	ratio of the cellular to the extracellular water space

RESUMO GERAL

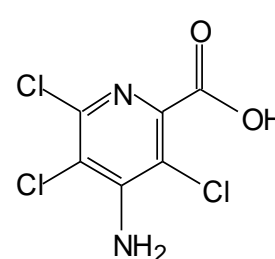
INTRODUÇÃO: Os herbicidas são amplamente utilizados na agricultura moderna. A maioria deles apresenta certa toxicidade para os mamíferos e os que apresentam alto grau de toxicidade já foram banidos em muitos países, fato que não impede seu uso em outros. Mesmo quando levemente tóxicos, raramente são completamente inertes para as funções celulares. Muitos deles já foram investigados usando sistemas subcelulares, como mitocôndrias isoladas ou microsomas, por exemplo. Alguns deles também foram extensivamente investigados em sistemas celulares intactos, como o diuron. Herbicidas que têm sido muito estudados em mitocôndrias isoladas, mas não em sistemas celulares intactos, compreende o dinoseb, o 2,4-D e o picloram. Suas estruturas químicas são mostradas abaixo.



Dinoseb



**Ácido 2,4-diclorofenóxi-acético
(2,4-D)**



Picloram

Os três compostos afetam a transdução de energia em mitocôndrias isoladas. O dinoseb age predominantemente como um desacoplador da fosforilação oxidativa. Sua ação protonofórica em mitocôndrias isoladas é exercida em concentrações de até 1 μM . O 2,4-D também age como um desacoplador, porém é menos potente que o dinoseb. Além disso, também inibe o fluxo de elétrons na cadeia respiratória. Os efeitos do picloram nas mitocôndrias são menos claros, especialmente porque os seus efeitos foram frequentemente caracterizados utilizando a formulação comercial Tordon[®], que é uma mistura de quatro partes do 2,4-D e uma parte do picloram. Há evidências, no entanto, de que o picloram também pode afetar a transdução de energia em mitocôndrias de mamíferos. Os três compostos são absorvidos quando ingeridos e suas concentrações nas células do fígado são significativas. Sabe-se que a transformação metabólica destes compostos é lenta, mas ainda não se conhece como eles afetam o metabolismo hepático. Por este motivo, o presente estudo tem como objetivo caracterizar as ações dos três compostos sobre o metabolismo hepático utilizando principalmente o fígado de rato em perfusão isolada. Além disso, também é interessante quantificar a distribuição destes compostos sobre as células hepáticas e como eles interagem com as membranas celulares.

MÉTODOS: O sistema experimental utilizado foi o fígado de rato em perfusão isolada. Ratos Wistar machos (200-260 g) foram alimentados *ad libitum* com dieta padrão de laboratório. Os animais foram anestesiados com injeção intraperitoneal de tiopental sódico (50 mg/kg) para o procedimento cirúrgico de preparação do fígado. Após a canulação das veias porta e cava, o fígado foi posicionado em uma câmara de acrílico e perfundido no sistema não recirculante. O líquido de perfusão foi o tampão Krebs/Henseleit-bicarbonato (pH 7,4), saturado com uma mistura de O_2 e CO_2 (95: 5) por meio de um oxigenador de membrana e simultaneamente aquecido a 37 °C. Metabólitos no perfusado eflu-

ente foram analisados por meio de procedimentos enzimáticos padrões. A concentração de oxigênio no perfusado efluente foi monitorada polarograficamente. O dinoseb, o 2,4-D e o picloram foram dissolvidos diretamente no líquido de perfusão nas concentrações desejadas. AMP, ADP e ATP, extraídos do tecido hepático, foram separados e quantificados por meio de cromatografia líquida de alta eficiência (HPLC; Shimadzu HPLC system, Japan). A detecção foi espectrofotométrica a 254 nm. Dinoseb, 2,4-D e picloram no perfusado efluente também foram separados e quantificados por HPLC. Os comprimentos de onda de detecção foram 370, 280 e 228 nm, respectivamente. As mitocôndrias do fígado foram isoladas por centrifugação diferencial e utilizadas para medir o consumo de oxigênio, a atividade ATPásica e para experimentos de ligação à membrana celular. Para calcular o potencial de força média (PMF) dos herbicidas ao cruzar as membranas das bicamadas lipídicas, utilizou-se o método de amostragem "umbrella sampling", seguido de uma análise das coordenadas de reação através do histograma ponderado das distribuições das distâncias resultantes. Os perfis de saída do dinoseb, 2,4-D e picloram resultantes da infusão constante de cada composto foram analisados por meio de um modelo espaço-distribuído com tempos variáveis de trânsito. Este modelo fornece a seguinte equação,

$$S(t) = \int_0^t \left[\frac{1}{1 + \Phi} \right] \cdot S'_{\text{água}} \left(\frac{(t - t_0)}{(1 + \Phi)} + t_0 \right) \cdot e^{-k_{\text{met}}(t-t_0)} dt$$

em que $S(t)$ é a curva experimental no perfusado efluente, resultante de uma infusão constante na veia porta, t é o tempo de infusão, $(1 + \Phi)$ é a relação entre o espaço de distribuição aparente da substância infundida para o espaço de distribuição da água marcada, t_0 o tempo de trânsito uniforme nos grandes vasos, $S'_{\text{água}}$ é a primeira derivada da curva da $[^3\text{H}]$ água corrigido para o tempo $[(t - t_0)/(1 + \Phi) + t_0]$ e k_{met} o coeficiente de transformação metabólica. O ajuste da equação à curva experimental foi feito usando um procedimento não-linear de mínimos quadrados, com programas específicos escritos em Turbo-Basic.

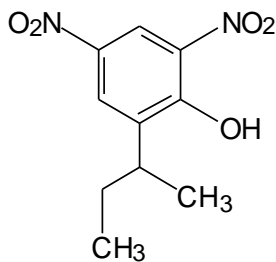
RESULTADOS: Os resultados mais importantes foram os seguintes: 1) O dinoseb e o 2,4-D aumentaram a glicólise, o primeiro na concentração até 10 μM e o segundo na faixa de 10 a 400 μM . O picloram não aumentou a glicólise no intervalo até 1 mM. A razão lactato/piruvato, indicativa do potencial redox do par citosólico NAD^+ -NADH, também foi aumentada pelo dinoseb e 2,4-D. O dinoseb aumentou adicionalmente a produção de glicose derivada da glicogenólise, um efeito ausente para o 2,4-D. 2) Os três compostos inibiram a gliconeogênese do lactato. A sequência crescente de potência foi picloram < 2,4-D << dinoseb. A inibição desta via pelo dinoseb foi completa na concentração de 10 μM ; as inibições causadas pelo 2,4-D e pelo picloram foram incompletas, no máximo 46% e 23%, respectivamente. Nenhum sinergismo entre o 2,4-D e o picloram foi detectado com referência à inibição da gliconeogênese. 3) O dinoseb inibiu a síntese de glicose a partir de alanina e frutose. Também inibiu a síntese de ureia a partir de alanina e aumentou a produção de amônia. 4) O consumo de oxigênio foi estimulado pelo dinoseb em todas as condições em concentrações até 10 μM : em fígados de ratos alimentados sob perfusão livre de substrato e em fígados de ratos em jejum na presença de lactato, alanina ou frutose como substratos. Metade do estímulo máximo do consumo de oxigênio no fígado intacto ocorreu em concentrações (2,8-5,8 μM) pelo menos dez vezes acima daquelas que produzem o mesmo efeito em mitocôndrias isoladas (0,28 μM). O 2,4-D, por outro lado, estimulou o consumo de oxigênio em fígados de ratos alimentados

sob perfusão livre de substrato, começando na concentração de 10 μM . Nenhum efeito significativo do 2,4-D foi encontrado em fígados de ratos em jejum na presença de lactato. O picloram, por fim, apresentou uma tendência em inibir o consumo de oxigênio nos fígados de ratos em jejum na presença de lactato, porém sem significância estatística ao nível de 5%. 5) Todos os compostos diminuíram os níveis de ATP celular. A sequência crescente de potência foi picloram < 2,4-D << dinoseb. 6) As transformações do dinoseb, 2,4-D e picloram foram lentas. Para cada um dos três compostos, a distribuição foi limitada pelo fluxo, isto é, ocorreu a taxas elevadas. O espaço de distribuição real ou aparente em relação ao espaço da água foi muito pronunciado para o dinoseb ($\Phi = 27,05 \pm 4,89$) e menos para o 2,4-D ($\Phi = 5,34 \pm 0,82$) e picloram ($\Phi = 1,69 \pm 0,20$). Para concentrações extracelulares de 10 μM , esses valores resultaram em concentrações intracelulares de equilíbrio de 438,7, 94,62 e 27,79 μM , para o dinoseb, 2,4-D e picloram respectivamente, quando expressos em termos de espaço físico aquoso. 7) As simulações de dinâmica molecular revelaram que o dinoseb apresentou alta afinidade pela região hidrofóbica das bicamadas lipídicas da membrana, com um coeficiente de partição de $3,75 \times 10^4$ (a 37 °C) entre as fases hidrofóbica e hidrofílica. Assim, o elevado espaço de distribuição aparente do dinoseb provavelmente reflete sua ligação às membranas celulares. O 2,4-D, por outro lado, apresentou uma afinidade muito baixa para as bicamadas lipídicas hidrofóbicas. Os coeficientes de partição foram de $6,27 \times 10^{-14}$ e $1,25 \times 10^{-9}$ para as formas aniônica e protonada, respectivamente. Isso sugere que o espaço de distribuição relativamente alto do 2,4-D reflete sua ligação a outras estruturas, como proteínas, por exemplo.

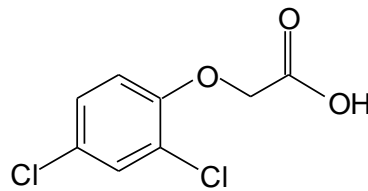
CONCLUSÕES: Pode-se concluir que todos os compostos estudados afetam o metabolismo energético nas células intactas do fígado. Isto é indicado principalmente pelas suas ações inibidoras sobre as vias anabólicas (por exemplo, a gliconeogênese) e em ações na estimulação em vias catabólicas (por exemplo, a glicólise e o consumo de O_2). O dinoseb é também um forte inibidor da detoxificação da amônia. O picloram, por outro lado, é de longe o menos ativo. Embora a sequência crescente de potência nas células do fígado (picloram < 2,4-D << dinoseb) corresponda àquela relatada para as mitocôndrias isoladas, existem muitas singularidades que sugerem diferenças substanciais no comportamento das três substâncias. Por exemplo, a ação do dinoseb nas células do fígado ocorre em uma faixa de concentração que é uma ordem de grandeza superior à faixa que afeta as mitocôndrias isoladas. O 2,4-D, no entanto, começa a atuar nas células do fígado em concentrações para as quais ainda não ocorrem efeitos nas mitocôndrias isoladas. Estes e outros fenômenos podem estar ligados ao comportamento bastante diferente do dinoseb e do 2,4-D. Enquanto o primeiro é altamente solúvel nas membranas celulares, este último tem pouca afinidade por essas estruturas e seu espaço de distribuição aparente relativamente alto sugere a ligação com outras macromoléculas celulares. Estudos ainda são necessários para se investigar como essa ligação poderia possivelmente afetar sua atividade. A inibição do metabolismo energético é certamente um componente importante da toxicidade do dinoseb e do 2,4-D, embora o primeiro seja muito mais potente que o segundo. Os fenômenos aqui descritos são certamente consistentes com a maior toxicidade do dinoseb quando comparado a vários outros desacopladores naturais ou sintéticos.

GENERAL ABSTRACT

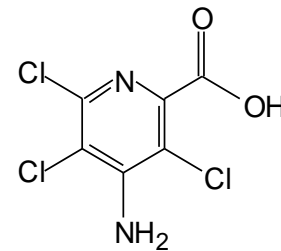
INTRODUCTION: Herbicides are widely used in modern agriculture. Most of them present at least a certain degree of toxicity to mammals. Some of those presenting high degrees of toxicity have been banned in many countries, a fact that does not prevent their use in others. Even when mildly toxic, they are seldom completely inert on cellular functions. Most of them have been investigated using subcellular systems, as isolated mitochondria or microsomes, for example. A few of them have also been extensively investigated in intact cell systems, as diuron, for example. A group that has been extensively investigated in isolated mitochondria, but incompletely in intact cell systems, comprises dinoseb, 2,4-D and picloram. Their chemical structures are shown below.



Dinoseb



**2,4-Dichlorophenoxyacetic acid
(2,4-D)**



Picloram

The three compounds affect energy transduction in isolated mitochondria. Dinoseb acts predominantly as an uncoupler of oxidative phosphorylation. Its protonophoric action in isolated mitochondria is exerted at concentrations up to 1 μ M. 2,4-D also acts as an uncoupler, but is less potent than dinoseb. In addition it also inhibits the electron flow in the respiratory chain. The effects of picloram on mitochondria are less clear, especially because its effects have often been characterized using the commercial formulation Tordon[®], which is a mixture of four parts of 2,4-D and one part of picloram. There is evidence, however, that picloram also affects energy transduction in mammal mitochondria. All three compounds are absorbed when ingested and their concentration in the liver cells is appreciable. It is known that metabolic transformation is slow, but how these compounds affect hepatic metabolism is largely unknown. For this reason, the present study aims to characterize the actions of the three compounds on liver biochemistry using mainly the isolated perfused rat liver. Furthermore, it is also of interest to quantify the distribution of the compounds over the hepatic cells and how they interact with the cellular membranes.

METHODS: The basic experimental system was the isolated perfused rat liver. Male Wistar rats (200-260 g) were fed *ad libitum* with a standard laboratory diet. Animals were anesthetized by intraperitoneal sodium thiopental injection (50 mg/kg) for the surgical procedure of liver preparation. After cannulation of the portal and cava veins the liver was positioned in a plexiglass chamber and perfused in the non-recirculating system. The perfusion fluid was Krebs/Henseleit-bicarbonate buffer (pH 7.4), saturated with a mixture of O₂ and CO₂ (95:5) by means of a membrane oxygenator and simultaneously heated to 37°C. Metabolites in the outflowing perfusate were assayed by means of standard enzymatic procedures. Oxygen concentration in the outflowing perfusate was monitored polarographically. Dinoseb, 2,4-D and picloram were dissolved directly into the perfusion fluid at the desired concentrations. AMP, ADP and ATP, extracted from the liver tissue, were separated and quantified by means of high

performance liquid chromatography (HPLC; Shimadzu HPLC system, Japan). Detection was spectrophotometric at 254 nm. Dinoseb, 2,4-D and picloram in the outflowing perfusate were also separated and quantified by HPLC. The detection wavelengths were 370, 280 and 228 nm, respectively. Liver mitochondria were isolated by differential centrifugation and used for measuring oxygen consumption and ATPase activity and for binding experiments. For calculating the potential mean force (PMF) of the herbicides when crossing membrane lipid-bilayers, the umbrella sampling method was used, followed by a weighted histogram analysis of the resulting distance distributions. The outflow profiles of dinoseb, 2,4-D and picloram resulting from step inputs of each compound were analyzed by means of a space-distributed and variable transit times model. This model yields the following equation,

$$S(t) = \int_0^t \left[\frac{1}{1 + \Phi} \right] \cdot S'_{\text{water}} \left(\frac{(t - t_0)}{(1 + \Phi)} + t_0 \right) \cdot e^{-k_{\text{met}}(t-t_0)} dt,$$

in which $S(t)$ is the experimental outflowing curve resulting from a step input into the portal vein, t is the infusion time, $(1 + \Phi)$ is the ratio of the apparent distribution space of the infused substance to the distribution space of labeled water, t_0 the uniform transit time in the large vessels, S'_{water} the first derivative of the [^3H]water outflow profile corrected for the time $[(t - t_0)/(1 + \Phi) + t_0]$ and k_{met} the coefficient for metabolic transformation. Curve fitting was done using a non-linear least-squares procedure, with specific programs written in Turbo-Basic.

RESULTS: The most important results were the following: 1) Dinoseb and 2,4-D increased glycolysis, the former in the range up to 10 μM and the latter in the range from 10 to 400 μM . Picloram did not increase glycolysis in the range up to 1 mM. The lactate to pyruvate ratio, indicative of the redox potential of the cytosolic NAD^+ -NADH couple was also increased by dinoseb and 2,4-D. Dinoseb additionally increased glucose output derived from glycogenolysis, an effect that was absent for 2,4-D. 2) All three compounds inhibited lactate gluconeogenesis. The sequence of increasing potency was picloram < 2,4-D << dinoseb. Inhibition by dinoseb was virtually complete at the concentration of 10 μM ; the inhibitions caused by 2,4-D and picloram were incomplete, maximally 46% and 23%, respectively. No synergism between 2,4-D and picloram was detected with reference to gluconeogenesis inhibition. 3) Dinoseb inhibited glucose synthesis from alanine and fructose. It also inhibited urea synthesis from alanine and increased ammonia output. 4) Oxygen uptake was stimulated by dinoseb under all conditions in the concentration range up to 10 μM : in livers from fed rats under substrate-free perfusion and in livers from fasted rats in the presence of lactate, alanine or fructose as substrates. Half-maximal stimulation of oxygen uptake in the whole liver occurred at concentrations (2.8–5.8 μM) at least ten times above those in isolated mitochondria (0.28 μM). 2,4-D, on the other hand stimulated oxygen uptake in livers from fed rats under substrate-free perfusion starting at the concentration of 10 μM . No significant effects of 2,4-D were found in livers from fasted rats in the presence of lactate. Picloram, finally, presented a tendency of inhibiting oxygen uptake in livers from fasted rats in the presence of lactate, however, without statistical significance at the 5% level. 5) All three compounds diminished the cellular ATP levels. The sequence of increasing potency was picloram < 2,4-D << dinoseb. 6) Transformations of dinoseb, 2,4-D and picloram were slow. For each of the three compounds the distribution was flow-limited, i.e., occurred at high rates. Uptake into a real or apparent space in

excess to the water space was very pronounced for dinoseb ($\Phi = 27.05 \pm 4.89$) and less so for 2,4-D ($\Phi = 5.34 \pm 0.82$) and picloram ($\Phi = 1.69 \pm 0.20$). For extracellular concentrations of 10 μM , these Φ values resulted in equilibrium intracellular concentrations of dinoseb, 2,4-D and picloram of 438.7, 94.62 and 27.79 μM , respectively, when expressed in terms of physical aqueous space. 7) Molecular dynamics simulations revealed that dinoseb presented high affinity for the hydrophobic region of the membrane lipid bilayers, with a membrane/aqueous phase partition coefficient of 3.75×10^4 (at 37 °C). Thus, the high apparent distribution space of dinoseb most likely reflects binding to cellular membranes. 2,4-D, on the other hand, presented a very low affinity for the hydrophobic lipid bilayers. The membrane/aqueous phase partition coefficients were 6.27×10^{-14} and 1.25×10^{-9} for the anionic and protonated forms, respectively. This suggests that the relatively high distribution space of 2,4-D reflects binding to other structures such as proteins, for example.

CONCLUSIONS: It can be concluded that all three compounds affect energy metabolism in the intact liver cells. This is indicated mainly by their inhibitory action on anabolic pathways (e.g., gluconeogenesis) and stimulating action on catabolic pathways (e.g., glycolysis and O_2 uptake). Dinoseb is also a strong inhibitor of ammonia detoxification. Picloram, on the other hand, is by far the least active. Although the sequence of increasing potency in the liver cells (picloram < 2,4-D << dinoseb) corresponds to that reported for isolated mitochondria, there are many singularities suggesting substantial differences in behavior for the three substances. For example, the action of dinoseb occurs in the liver cells at a concentration range that is one order of magnitude superior to that in isolated mitochondria. 2,4-D, however, begins to act in the liver cells at concentrations for which still no actions in isolated mitochondria occur. These and other phenomena may be linked to the quite different behavior of dinoseb and 2,4-D. Whereas the former is highly soluble in the cellular membranes, the latter has little affinity for these structures, its relatively high apparent distribution space suggesting binding to other cellular macromolecules. How such binding could be possibly affecting its activity remains to be elucidated. Inhibition of energy metabolism is certainly an important component of the toxicity of both dinoseb and 2,4-D, although the former is far more potent than the latter. The phenomena described herein are certainly consistent with the higher toxicity of dinoseb when compared to several other natural or synthetic uncouplers.

Distribution, lipid-bilayer affinity and kinetics of the metabolic effects of dinoseb in the liver

Gabriela Bueno Franco Salla, Livia Bracht, Anacharis Babeto de Sá-Nakanishi, Angela Valderrama Parizotto, Fabrício Bracht, Rosane Marina Peralta and Adelar Bracht*

Department of Biochemistry, University of Maringá, 87020900 Maringá, Brazil

Corresponding author:

Adelar Bracht

Department of Biochemistry

University of Maringá

5790 Avenida Colombo

87020900 Maringá, Brazil

Email: adebracht@uol.com.br; abracht@uem.br

Abstract

Dinoseb is a highly toxic pesticide of the dinitrophenol group. Its use has been restricted, but it can still be found in soils and waters in addition to being a component of related pesticides that, after ingestion by humans or animals, can originate the compound by enzymatic hydrolysis. As most dinitrophenols, dinoseb uncouples oxidative phosphorylation. In this study, distribution, lipid bilayer affinity and kinetics of the metabolic effects of dinoseb were investigated, using mainly the isolated perfused rat liver, but also isolated mitochondria and molecular dynamics simulations. Dinoseb presented high affinity for the hydrophobic region of the lipid bilayers, with a partition coefficient of 3.75×10^4 between the hydrophobic and hydrophilic phases. Due to this high affinity for the cellular membranes dinoseb underwent flow-limited distribution in the liver. Transformation was slow but uptake into the liver space was very pronounced. For an extracellular concentration of $10 \mu\text{M}$, the equilibrium intracellular concentration was equal to $438.7 \mu\text{M}$. In general dinoseb stimulated catabolism and inhibited anabolism. Half-maximal stimulation of oxygen uptake in the whole liver occurred at concentrations ($2.8\text{-}5.8 \mu\text{M}$) at least ten times above those in isolated mitochondria ($0.28 \mu\text{M}$). Gluconeogenesis and ureagenesis were half-maximally inhibited at concentrations between 3.04 and $5.97 \mu\text{M}$. The ATP levels were diminished, but differently in livers from fed and fasted rats. Dinoseb disrupts metabolism in a complex way at concentrations well above its uncoupling action in isolated mitochondria, but still at concentrations that are low enough to be dangerous to animals and humans even at sub-lethal doses.

Key words: herbicides; hepatic metabolism; hepatic perfusion; isolated mitochondria.

Introduction

Dinitrophenols are a class of compounds that exert several biological and toxic effects. The main action is impairment of energy metabolism, an effect that can be extremely harmful depending on its degree and intensity (Heusinkveld et al., 2016; Zaharia et al., 2016). Dinitrophenols can be and has been used in agriculture as herbicides and pesticides that persist in contaminated soils and waters. Although several of them have been officially banned in many countries, their use as pharmaceutical agents has also been proposed, especially for weight loss purposes and at least one of them, 2,4-dinitrophenol, can be purchased in the internet. Many death cases have been reported as accidents in agriculture or as overdoses in weight-loss diets (Zaharia et al., 2016).

The potency by which these compounds exert their activity varies considerably. The perhaps most toxic of them seems to be 2-(butan-2-yl)-4,6-dinitrophenol, more commonly known as dinoseb (MacBean, 2012). Dinoseb has been used mainly as an herbicide for weed-control in the production of crops like soybeans, vegetables, fruits and nuts, or citrus. It was also used as an insecticide to protect grapes. In the present, dinoseb is banned in the European Union and United States due to its high toxicity. However, it is still used in other countries and routinely found in rain- and drinking water (Heusinkveld et al., 2016; Zaharia et al., 2016; Guan et al., 2013). Furthermore, especially in China, large quantities of the acetate ester of dinoseb (dinoseb acetate) are manufactured annually, a compound that is equally used as pesticide (ProfResearch Reports, 2014). Dinoseb acetate can be easily transformed into dinoseb by simple hydrolysis of the ester bond, a phenomenon that is catalyzed by non-specific esterases (Preiss et al., 1988). In animals highly active esterases exist (Eler et al., 2013), leading to rapid hydrolysis of dinoseb acetate into dinoseb (MacBean, 2012). Another dinitrophenol that is rapidly metabolized in animals into dinoseb is binapacryl (the 3,3-dimethylacrylic acid ester of dinoseb), a compound used as acaricide and fungicide (MacBean, 2012).

The LD₅₀ values for orally administrated dinoseb are relatively low and vary between 14 to 114 mg/Kg, depending on the species (MacBean, 2012; Zaharia et al., 2016). Preceding death the poisoning symptoms include, prostration and convulsions, hyperventilation and hyperthermia. It is generally assumed that the main mechanism behind the deleterious effects of dinoseb is

uncoupling of mitochondrial oxidative phosphorylation (MacBean, 2012). In plants dinoseb is also an uncoupler of photophosphorylation (Oettmeier and Masson, 1980). Dinoseb is a potent uncoupler, considerably superior to the classical uncoupler 2,4-dinitrophenol. Half-maximal stimulation of oxygen uptake driven by succinate in isolated rat liver mitochondria (state IV respiration), for example, has been reported to occur at a concentration of 0.12 μM dinoseb (Palmeira et al., 1994a). For 2,4-dinitrophenol the corresponding concentration is 15–20 μM (Chappell, 1964; Hanstein and Hatefi, 1974). In mechanistic terms dinoseb seems to be a classical inhibitor, i.e., a compound that acts as a protonophore, thus dissipating the proton gradient across the mitochondrial membrane as well as the membrane potential (Palmeira et al., 1994a). Such an action, when potent enough, inevitably leads to decreased levels of cellular ATP (Palmeira et al., 1994b), leading ultimately to energetic failure of the whole organism.

ATP depletion by dinoseb has already been demonstrated in isolated hepatocytes (Palmeira et al., 1994b). However, impairment of energy metabolism has several consequences for basic metabolic pathways, such as glycolysis and gluconeogenesis (Saling et al., 2011; Moreira et al., 2013), which in the case of dinoseb have not yet been characterized. The distribution space of dinoseb in the liver has also not yet been measured. Based on these premises we decided to undertake a systematic study on the distribution (transport), lipid bilayer affinity and kinetics of the metabolic effects of dinoseb in the liver. The experimental system was the isolated perfused rat liver in which microcirculation and cell polarity are both preserved in addition to the cell integrity. Preservation of the microcirculation may be important for characterizing the cellular uptake of dinoseb, especially if intense interactions with the cellular lipidic environment occur. In addition to obtaining experimental data, molecular dynamics simulations were also done with the purpose of broadening the theoretical basis for interpretation. The results should bring additional information about the interactions of dinoseb with the liver which could be important if one considers that dinitrophenols in general still trigger both health and legal issues worldwide (MacBean, 2012; Zaharia et al., 2016).

Material and methods

Materials

The liver perfusion apparatus was built in the workshops of the University of Maringá. A schematic representation of this apparatus can be seen Fig. S1 (Supplementary Material). Dinoseb (2-(butan-2-yl)-4,6-dinitrophenol) was purchased from Sigma Chemical Co. (St Louis, USA). All enzymes and coenzymes used in the enzymatic assays were purchased from Sigma Chemical Co. (St Louis, USA). All standard chemicals were from the best available grade (98-99.8 % purity).

Animals

Male Wistar rats, weighing 240–260 g, were used in the experiments. The rats were housed in individual cages, maintained on a regulated light–dark cycle and fed *ad libitum* with a standard laboratory diet (Nuvilab[®], Colombo, Brazil). When required the rats were starved for 18 h prior to the experiments. Preparation of the liver for perfusion was done under sodium thiopental anesthesia, which was injected intraperitoneally (50 mg/kg). Lack of body or limb movement in response to a standardized tail clamping stimulus was the criterion of anesthesia. Experiments were done in accordance with the worldwide accepted ethical guidelines for animal experimentation and were previously approved by the Ethics Committee of Animal Experimentation of the University of Maringá (protocol number 8172271015).

Liver perfusion

Hemoglobin-free, non-recirculating perfusion was performed (Scholz and Bücher, 1965; Kelmer-Bracht et al., 1984). After cannulation of the portal and cava veins the liver was transferred to a plexiglass chamber. See Fig. S1 (Supplementary Material) for a schematic representation of the perfusion apparatus. Constant flow perfusion was done using a peristaltic pump (Minipuls 3, Gilson, France). The flow rate was adjusted between 30 and 32 mL/min, depending on the liver weight (Scholz and Bücher, 1965; Kelmer-Bracht et al., 1984). The perfusion fluid was Krebs/Henseleit-bicarbonate buffer (pH 7.4) containing 25 mg/100 mL bovine-serum albumin, saturated with a mixture of oxygen and carbon dioxide (95:5) by means of a membrane oxygenator with

simultaneous temperature adjustment (37 °C). The composition of the Krebs/Henseleit-bicarbonate buffer is the following: 116 mM NaCl, 25 mM NaHCO₃, 5.9 mM KCl, 1.2 mM Na₂SO₄, 1.18 mM MgCl₂, 1.24 mM NaH₂PO₄ and 2.5 mM CaCl₂. The perfusion fluid enters the liver via a cannula inserted into the portal vein and leaves the organ via a cannula inserted into the cava vein. Samples of the effluent perfusion fluid were collected and analyzed for their metabolite contents. Substrates and dinoseb were added to the perfusion fluid according to the experimental protocols. Due to its low water solubility, dinoseb was added to the perfusion fluid as a dimethylsulfoxide solution to achieve the desired final concentration. It is already amply documented that dimethylsulfoxide does not significantly affect liver metabolism, at least not when infused at rates up to 32 µL/min (Acco et al., 2004), a limit that was never surpassed in the present work.

Metabolites assays

Samples of the effluent perfusion fluid were collected according to the experimental protocol and analyzed for their metabolite contents. The following compounds were assayed by means of standard enzymatic procedures: glucose, lactate, pyruvate, ammonia and urea (Bergmeyer, 1974). The oxygen concentration in the outflowing perfusate was monitored continuously, employing a teflon-shielded platinum electrode adequately positioned in a plexiglass chamber at the exit of the perfusate (Kelmer-Bracht et al., 1984). Metabolic rates were calculated from input-output differences and the total flow rates and were referred to the wet weight of the liver.

The hepatic contents of the adenine nucleotides were measured by HPLC after freeze-clamping the perfused liver with liquid nitrogen (Mito et al., 2014). Two gram of the freeze-clamped liver were macerated in liquid nitrogen until homogeneity. To the powdered liver 6 mL of 0.6 M perchloric acid was added and the suspension was homogenized in a van Potter-Elvehjem homogenizer. The resulting homogenate was centrifuged at 4000g for 10 minutes and the resulting homogenate neutralized with fixed volumes of potassium carbonate (0.5 M). Extraction with perchloric acid has the advantage that the resulting insoluble potassium perchlorate salt can be eliminated by precipitation (Bergmeyer, 1974). The precipitated potassium perchlorate was eliminated by filtration and the filtrate used for the adenine nucleotides determinations. The

HPLC system (Shimadzu, Japan) consisted of a system controller (SCL-10AVP), two pumps (model LC10ADVP), a column oven (model CTO-10AVP) and an UV-Vis detector (model SPD-10AV). A reversed-phase C18 CLC-ODS column (5 μ m, 250 \times 4.6 mm i.d., Shimadzu) protected with a CLC-ODS precolumn (5 μ m, 4 \times 3 mm i.d., Phenomenex) was used with a gradient from reversed-phase 0.044 mol/L phosphate buffer solution, pH 6.0, to 0.044 mol/L phosphate buffer solution plus methanol (1.1), pH 7.0. In percent methanol, the gradient was the following: at 0 min, 0%; at 2.5 min, 0.5%; at 5 min, 3%; at 7 min, 5%; at 8 min, 12%; at 10 min, 15%; at 12 min, 20%; at 20 min, 30%. The temperature was kept at 35 °C, and the injection volume was 20 μ L with a flow rate of 0.8 mL/min. Monitoring was performed spectrophotometrically at 254 nm. Identification of the peaks of the investigated compounds was carried out by a comparison of their retention times with those obtained by injecting standards under the same conditions. The concentrations of the compounds were calculated by means of the regression parameters obtained from the calibration curves. The calibration curves were constructed by separating chromatographically standard solutions of the compounds. Linear relationships were obtained between the concentrations and the areas under the elution curves.

Dinoseb and [³H] assays

The quantification of dinoseb was firstly done by HPLC in order to investigate the possible presence of metabolites. The same apparatus and column systems described in the preceding sub-section was used. The mobile phase was 70% methanol and 30% water. Monitoring was done spectrophotometrically at 370 nm, with a flow rate of 1 mL/min at a temperature of 35 °C. Identification of the dinoseb peak was done by comparison of its retention time with that obtained by injecting standard dinoseb under the same conditions. The concentrations were calculated by means of the regression parameters obtained from a calibration curve. After verifying that the presence of metabolites would not interfere the dinoseb concentration in the outflowing perfusate was assayed by measuring its absorbance at 370 nm ($\epsilon = 1.27 \times 10^4 \text{ M}^{-1} \text{ cm}^{-1}$).

Quantification of ³H present in the perfusate samples as [³H]H₂O was done by liquid scintillation counting (TriCarb 2810 TR International model from Perkin Elmer Health science). A commercial scintillation liquid formed by an aqueous

biodegradable emulsion (BCS®, Biodegradable Counting scintillant, Amersham) was used.

Experiments with isolated mitochondria

For isolating mitochondria fasted rats were decapitated and their livers removed immediately and placed in ice-cold buffer containing 200 mM mannitol, 75 mM sucrose, 0.2 mM ethylene glycol tetraacetic acid (EGTA), 2 mM tris (hydroxymethyl)amino-methane (Tris-HCl), pH 7.4 and 50 mg% bovine serum albumin. The tissue was minced, washed with the buffer and homogenized in the same medium by means of a van Potter homogenizer for lysing the cells. After homogenization, the mitochondria were isolated by differential centrifugation and suspended in the same medium, which was kept at 0–4 °C (Voss et al., 1961; Bracht et al., 2003).

For measuring oxygen uptake freshly prepared intact mitochondria at a concentration of 0.5 mg protein/mL were incubated in the oxygraph chamber at 37 °C (Voss et al., 1961; Bracht et al., 2003). The medium (2 mL) contained 120 mM KCl, 5 mM KH₂PO₄, 3 mM Hepes (pH 7.2), 1 mM EGTA, 5 µM rotenone and 1 µg/mL oligomycin. Respiration was initiated by adding succinate to a final concentration of 4 mM. Dinoseb was added as DMSO solutions with different concentrations to ensure a constant amount of solvent (20 µL).

The mitochondrial ATPase activity was measured in medium containing 0.2 M sucrose, 50 mM KCl, and 20 mM Tris-HCl (pH 7.4) plus 0.2 mM EGTA and 5.0 mM ATP and 1.0 mg protein/mL of intact mitochondria (Bracht et al., 2003). The incubation time was 20 min at 37 °C. Dinoseb was added as DMSO solutions with different concentrations to ensure a constant amount of solvent (20 µL). The reaction was started by the addition of 5 mM ATP and stopped by the addition of ice-cold 5% trichloroacetic acid. The ATPase activity was evaluated by measuring the release of inorganic phosphate as described earlier (Fiske and Subbarow, 1925) at 700 nm.

Binding of dinoseb to the mitochondria was measured at 37 °C in 1.5 mL incubation medium containing 2 mg mitochondrial protein, 260 mM mannitol, 1 mM EGTA, 10 mM Tris-HCl (pH 7.4) and variable dinoseb concentrations in the range 10–100 µM. After 7 min of incubation, the samples were rapidly centrifuged for 5 min at 10000g in a refrigerated centrifuge (2 °C). Dinoseb in the supernatant, representing free dinoseb, was measured spectro-

photometrically at 370 nm ($\epsilon = 1.27 \times 10^4 \text{ M}^{-1} \text{ cm}^{-1}$). The bound dinoseb was calculated by difference (added dinoseb - free dinoseb) and expressed as nmol/mg protein.

Protein content of the mitochondrial suspensions was measured using the Folin-phenol reagent and bovine serum albumin as standard (Lowry et al., 1951).

Calculation of the potential of mean force (PMF) across the lipid bilayer

The dinoseb molecule was built using the Avogadro software (Hanwell et al., 2012) and the antechamber tools within the Amber16 (Case et al., 2016) molecular simulation package were used to generate the input parameter files for the molecular dynamics simulation. The atom types followed the general Amber force field (GAFF) conventions (Wang et al., 2004). The charges for dinoseb were generated using the RESP ESP charge Derive Server (REDS) using the RESP-A1 method (Vanquelef et al., 2011). The original charges generated by the antechamber tool were then substituted and the force field parameters obtained from GAFF were used to build the membrane/dinoseb system.

For the lipid bilayer construction the choice was the 1-palmitoyl-2-oleoyl-sn-glycero-3-phosphocholine (POPC) model. This choice was based on the general popularity of this model in the literature and the proximity of its dynamical behavior to experiment data for a range of properties (Dickson et al., 2014). The hydrated bilayer structure was obtained from the CHARMM-GUI server from the membrane builder tool (Jo et al., 2008). The dinoseb was manually inserted in the water solvated lipid box in substitution to 5 water molecules. The water-solvated lipid box was then minimized using a mixed scheme with steepest-descent and conjugate gradient with 5000 steps of each (Vanquelef et al., 2011). The system was then heated for 150 ps using the Langevin thermostat (Grest and Kremer, 1986) with a collision frequency of 1 ps^{-1} at constant volume. The time step used was 2 fs with a cutoff for non-bonded interactions of 10 \AA . The temperature was gradually increased to its final value of 310.15 K. During the heating process, all lipid molecules were held fixed with a harmonic force constant of $10 \text{ kcal/mol} \cdot \text{\AA}^2$. During the last 100 ps, the system was simulated with anisotropic Berendsen weak coupling barostat with a pressure relaxation time of 2 ps (Berendsen et al., 1984). To equilibrate the dimensions of the periodic boundary conditions, another 5000 ps were simulated using the same parameters as the last step but without the position restraints. At

last, a long production run of 250 ns was run to equilibrate the lipid bilayer and the dinoseb molecule.

For calculating the potential of mean force (PMF) for crossing the membrane with the dinoseb molecule, the umbrella sampling method was used, followed by a weighted histogram analysis of the resulting distance distributions (Kumar et al., 1992). The reaction path for the PMF was chosen as the distance between the centers of mass (COM) between the dinoseb and the lipid bilayer. The COM of the lipid bilayer was defined as the COM of the nitrogen atoms of each choline group. The starting structure was incremented in 0.5 Å steps, giving a total of 152 simulation windows and 75.5 Å of total mean path, which corresponded to the complete path between one side of the periodic box to the other, perpendicular to the plane formed by the lipid bilayer surface.

The dinoseb molecule was restrained in each window to its corresponding distance value by a harmonic potential with a force constant of 5 kcal/mol · Å. The restraint was applied to the dinoseb's COM only in the Z Cartesian coordinate. Each window was simulated for 10 ns, giving a total of 1.52 μs. The simulation parameters used were the same as those ones used in the production run described above. The distribution histograms for the distances obtained in each window were checked for overlap and then submitted to the Weighted Histogram Analysis Method (WHAM) procedure (Kumar et al., 1992), giving the resulting PMF values. Convergence was checked using different sample sizes and auto correlation times from the resulting distance files as inputs for the WHAM procedure.

Analysis of the liver response to a dinoseb step input

The liver response to the dinoseb step input (constant infusion) was analyzed using the model of space-distributed and variable transit times adapted to the isolated perfused rat liver (Goresky et al., 1970; Bracht et al., 1980). This model describes the exchange of substances between the extracellular space and cell and the possible metabolic transformation in the liver. For a substance whose distribution into the cellular space is flow-limited and which undergoes irreversible metabolic transformation in the cellular environment the following equation applies (Kelmer-Bracht et al., 1993):

$$S(t) = \int_0^t \left[\frac{1}{1 + \Phi} \right] \cdot S'_{\text{water}} \left(\frac{(t - t_0)}{(1 + \Phi)} + t_0 \right) \cdot e^{-k_{\text{met}}(t - t_0)} dt \quad (1)$$

In Eq. (1), $S(t)$ is the experimental outflowing dinoseb curve resulting from a constant infusion into the portal vein, t is the infusion time, $(1 + \Phi)$ is the ratio of the apparent distribution space of the infused substance to the distribution space of labeled water, k_{met} the coefficient for metabolic transformation and t_0 the uniform transit time in the large vessels. From the definition of $(1 + \Phi)$ it can be deduced that Φ represents the ratio of extra apparent space occupied by the substance to the water space; $\Phi = 0$ if the distribution space of the substance coincides with the aqueous distribution space. The term $S'_{\text{water}} \left(\frac{(t - t_0)}{(1 + \Phi)} + t_0 \right)$ is the first derivative of the liver response to a step input (constant infusion) of [^3H]water at time $[(t - t_0)/(1 + \Phi) + t_0]$.

The intracellular concentration of dinoseb (C_i) was calculated according to a previously derived formula (Kelmer-Bracht et al., 1993):

$$C_i = (1 + \Phi + \Phi / \theta) C_e \quad (2)$$

In Eq. (2) C_e is the extracellular concentration and θ the ratio of the intra- to the extracellular water space.

Eqs. (1) was fitted to the experimental curves of dinoseb using an iterative, nonlinear least-squares procedure (Björck and Dahlquist, 1972). The calculations were done using a specially designed structured computer program written in the Turbo-Basic language. Preliminary estimates of the parameters were introduced before initiating the iterative procedures. Numerical interpolation between the experimental points was accomplished by means of spline functions (Björck and Dahlquist, 1972). Romberg's algorithm was used for the numerical integration (Björck and Dahlquist, 1972).

Statistical analysis

The error parameters presented in the graphs are standard errors of the mean. Statistical analysis was done by means of the GraphPadPrism software (version 5.0). Variance analysis was done with post-hoc testing according to Student-Newman-Keuls ($p \leq 0.05$). Computation of the IC_{50} and EC_{50} values was done by numerical interpolation using Stineman's formula (Wagon, 1999). The software used was the *Scientist* program from MicroMath Scientific Software (Salt Lake City, UT, USA).

Results

Theoretical approach to the interactions of dinoseb with the cellular membranes

Molecular dynamics simulations were done in order to get a description of the theoretical interactions of dinoseb with the lipid bilayers. The potential mean force (PMF) graph in Fig. 1A shows the energy profile for moving the dinoseb molecule across a phospholipid bilayer. The graph shows a 2-fold symmetry to its center, as it would be expected due to the symmetry of the bilayer. The highest energy values for the mean free path are centered at the membrane/water interface and the lowest one within the hydrophobic region of the bilayer. Fig. 1B shows the partial exposure of the hydrophobic butan-2-yl group of the dinoseb molecule to the highly polar environment of the phosphatidylcholine groups and to the solvent, while one of the nitro groups still interacts with the oleoyl and palmitoyl chains. The energy difference between the lowest and the highest energy configuration is 6.5 kcal/mol, while the difference between the averages of the lowest and highest energies is 5.9 kcal/mol. Equilibrium constants (K_{eq}) for the distribution of dinoseb between the non-polar lipid phase and the polar phases can be calculated by the well known relationship $K_{eq} = e^{PMF/RT}$ in which T and R represent the absolute temperature and the universal gas constant (1.98 cal Kelvin⁻¹ mol⁻¹), respectively. At 37 °C the K_{eq} values are equal to 3.75×10^4 and 1.42×10^4 , respectively, for the highest and lowest energy configurations.

Experimental approaches to the interactions of dinoseb with the cellular membranes

The high affinity of dinoseb for the cellular lipid bilayer presented in the preceding section generates the hypothesis that the compound will probably permeate the cell membrane at high rates and that extensive binding to the cellular membranes can be expected. These questions were approached in the present work by mathematical analysis of the liver responses to a step input of dinoseb. The compound was infused in the perfused liver during a period of 54 minutes at a portal concentration of 10 μM and the outflowing perfusate was monitored for the presence of dinoseb and possible transformation products. Fig. 2 shows representative results of the chromatographic assays that were run. The appearance of dinoseb was monitored at 370 nm. The liver did not release any

component absorbing at 370 nm when perfused with Krebs/Henseleit bicarbonate buffer alone. Dinoseb at the concentration of 10 μM in the portal perfusate generated a single peak with a retention time of 5 minutes. At 8 minutes after starting infusion, dinoseb in the outflowing perfusate still appeared as a single component, though at a lower concentration when compared to the portal one. At 54 minutes perfusion time the dinoseb peak of the outflowing perfusate sample was almost as intense as that of the portal sample, but the presence of at least one additional component at 5.9 minutes was apparent. This could be a metabolite which, however, represents less than 1% of the infused dinoseb. Several perfusate samples taken at different times (13 times) were chromatographed to confirm the observations in Fig. 2. They allow to conclude that the single pass transformation of dinoseb (perfusion was done in an open system without recirculation) is not significant and, consequently, the concentration of the compound can be monitored more easily by measuring absorbance at 370 nm without interference by the presence of metabolites. Fig. 3 shows the mean results that were obtained by measuring the dinoseb concentration in the outflowing perfusate as a function of time. The concentration of dinoseb in the outflowing perfusate was represented as a fraction of the inflowing concentration. The response of the liver to a step input of [^3H]water is also shown. The latter, which undergoes flow-limited distribution into the whole aqueous space of the liver (Bracht et al., 1980), provides the indispensable reference curve. As expected from previous reports, [^3H]water appeared rapidly after starting infusion with only a few seconds delay and the venous/portal ratio tended rapidly to unity. The appearance of dinoseb was substantially delayed (approximately 1 minute) and tended very slowly to unity. As shown elsewhere by theoretical and experimental analyses the difference in the behavior of both [^3H]water and dinoseb reflects basically differences in their apparent or real distribution spaces. The outflow profile indicates that the apparent distribution space of dinoseb greatly exceeds that of [^3H]water (Bracht et al., 1980; Eler et al., 2013). Both curves tend to unity, however, a consequence of the fact that single pass transformation is not significant for both substances. When the infusion was stopped at 50 minutes perfusion time dinoseb returned slowly to the perfusion fluid and after 26 minutes, time at which the perfusion was definitively interrupted, 75% of the infused dinoseb had been recovered (not shown). This is consistent with reversible binding to the cellular membranes as suggested by the

molecular dynamics simulations described above. The position of the dinoseb curve relative to the water curve, besides indicating great differences in the apparent distribution spaces, indicates that dinoseb permeates the cell membrane at very high rates (flow-limited distribution) (Goresky et al., 1970; Bracht et al., 1980; Kelmer-Bracht et al., 1993). In such cases equation (1) can be used to determine the relative distribution space (Φ) and the metabolic transformation coefficient (k_{met}). For this purpose, equation (1) was fitted to the experimental dinoseb curve by means of a least-squares procedure, using the liver response to the [^3H]water step input as the reference curve. As the dinoseb curve tends to unity, k_{met} could not be determined. For this reason k_{met} was put equal to zero during the fitting procedure that allowed to determine Φ . Fitting converged rapidly and the optimized values of Φ and t_0 (the delay in the large vessels and tubing system before and after the liver) and the statistical parameters of the fitting procedure are given in the legend to Fig. 3. The goodness of fit can also be visually evaluated by comparing the trajectory of the experimental points with the calculated curve. The theoretical curve runs fairly equidistant from the irregularities of the experimental curve that reflect, most probably, hemodynamic changes that occurred during the long perfusion time. The optimized Φ value allows to calculate the intracellular concentration (C_i) under equilibrium conditions (when the normalized outflow curve approaches unity) by means of equation (2) that was derived on the assumption of a very fast permeation of the cell membrane (Kelmer-Bracht et al., 1993). With θ (intra- to the extracellular water space) equal to 1.71 (Eler et al., 2013) and C_e equal to 10 μM , C_i turns out to be equal to 438.7 μM . This means a C_i/C_e ratio as high as 43.9, denoting a quite pronounced concentration gradient between extracellular space and cellular environment at equilibrium. C_i calculated using equation (2) is referred to the cellular water space even though most dinoseb is certainly not to be found in the cellular water but rather in the lipid bilayers.

The results of the indicator dilution experiments just described above are consistent with the molecular dynamics calculations that predict extensive binding to cellular membranes. A suitable way of measuring binding to an intracellular component rich in membranes is to use isolated mitochondria. This was done by incubating isolated mitochondria with various concentrations of dinoseb during fixed times. Precipitation of the organelles allowed to measure the free dinoseb in the supernatant, from which the bound fraction can be computed

by difference. Fig. 4 shows the results of these experiments with dinoseb up to 100 μM . Binding was confirmed and the concentration dependence shows a linear relationship, i.e., saturation was not achieved in the range up to 100 μM , which is a very high concentration in biological terms. The mean binding degree in the experiments shown in Fig. 4, in which the mitochondrial protein concentration was equal to 1 mg/mL, was equal to $31.7 \pm 2.8\%$. The linear regression coefficient of 0.218 given in the legend to Fig. 4 has the dimensions (nmol/mg protein) per μM concentration unit. It can be used for calculating the amount of dinoseb that will bind to the mitochondria for any concentration increment ($\Delta\mu\text{M}$).

Quantification of the uncoupling effect of dinoseb in isolated mitochondria

A limited number of experiments was done with isolated mitochondria in order to quantify the uncoupling effect of dinoseb under our conditions. Two parameters were measured: the ATPase activity and the respiratory activity. The latter can also be measured in the perfused liver. The results are shown in Fig. 5. As expected, the ATPase activity (ATP hydrolysis) of intact mitochondria was low in the absence of dinoseb (Katyare et al., 1971). It was increased by dinoseb in a saturable manner in the range up to 5 μM . Half-maximal stimulation (EC_{50}), evaluated by numeral interpolation, occurred at the concentration of 0.775 μM . Oxygen uptake was measured using succinate as the electron donor and in the presence of oligomycin. Under these conditions acceleration of oxygen uptake is only possible if the proton gradient is dissipated by a mechanism independent of ATP-synthase (Lou et al., 2007). Dinoseb increased oxygen uptake at concentrations up to 1 μM (4.5-fold). After this concentration oxygen uptake began to decrease again, but there was still stimulation at the concentration of 5 μM (2.2-fold). Half-maximal stimulation can be expected at the concentration of 0.29 μM .

Glycogen catabolism and oxygen uptake in the perfused liver

Glycogen catabolism is intimately connected to energy metabolism especially because part of the released glucose enters the glycolytic pathway. To see how dinoseb affects glycogen catabolism and related parameters, livers from fed rats were perfused with substrate-free medium. Under these conditions the liver cells survive at the expense of glycogen degradation via glycolysis and oxidation of endogenous fatty acids that can be evaluated by measuring oxygen

uptake (Scholz and Bücher, 1965). Under these conditions, also, the liver releases glucose, lactate and pyruvate as a result of glycogen catabolism. The results of experiments in which the actions of four dinoseb concentrations (2.5, 5, 10 and 15 μM) were investigated are illustrated by Fig. 6. This range of concentrations was derived from preliminary experiments with dinoseb concentrations near to the concentration producing half-maximal oxygen uptake in isolated mitochondria (0.29 μM , see Fig. 5). These experiments revealed that such low concentrations would not be effective in the perfused liver. Fig. 6A illustrates the time course of the action of 15 μM dinoseb, but the same experimental protocol was used with all other concentrations. After a pre-perfusion period of 10 minutes, dinoseb was infused during 20 minutes, followed by additional 10 minutes of drug-free perfusion. Four parameters were measured: glucose output, lactate and pyruvate productions and oxygen consumption. Dinoseb modified all parameters: lactate production, and glucose output and oxygen uptake were increased and pyruvate production was diminished. The onset of the effects was fast. Oxygen uptake was already at the new steady-state 2 minutes after starting the infusion. The same occurred with glucose output. Lactate production was somewhat delayed in relative terms, but steady-state was achieved at 4 minutes after starting infusion. The decrease in pyruvate production, however, demanded more time. The simultaneous decrease in pyruvate production and increase in lactate production caused a marked increase in the lactate/pyruvate ratio, which under these conditions reflects the cytosolic NADH/NAD⁺ ratio (Sies, 1982). Cessation of the infusion of dinoseb progressively abolished all effects. The actions of dinoseb are, thus, reversible. Panel B in Fig. 6 shows the concentration dependences of the various effects. Oxygen uptake and lactate production started to increase at the concentration of 2.5 μM ; glucose output started to increase at 5 μM and pyruvate production started to decrease also at 5 μM . Oxygen uptake was a saturable function of the concentration and half-maximal stimulation (EC_{50}) can be expected at 2.83 μM ; this is approximately one order of magnitude above the same effect in isolated mitochondria. Glucose output and lactate production experienced a small decrease in the passage from 10 to 15 μM . The EC_{50} 's for glucose output and lactate production stimulations were, respectively, 5.97 and 3.90 μM ; the IC_{50} for pyruvate production inhibition was 6.77 μM .

Lactate gluconeogenesis and related parameters

Gluconeogenesis from lactate in the liver is strictly dependent on an efficient energy transduction in the mitochondria. As an inhibitor of energy metabolism, dinoseb should affect this biosynthetic route as do other inhibitors (Moreira et al., 2013). The experiments that were done with 2 mM lactate as the gluconeogenic precursor are illustrated by Fig. 7. Livers from 18 hours fasted rats were perfused in order to ensure low glycogen levels. Under such conditions the rate of glucose output reflects mainly the rate of gluconeogenesis and respiration occurs mainly at the expense of endogenous fatty acids (Comar et al., 2016). As expected, lactate infusion progressively raised glucose production, oxygen uptake and pyruvate release (Fig. 7A). The infusion of 15 μ M dinoseb at 36 minutes perfusion time caused an immediate increase in oxygen uptake, accompanied by rapid drops in glucose and pyruvate productions. At this concentration the effect of dinoseb on glucose production developed rapidly and was almost complete, i.e., in approximately 4 minutes glucose production was completely abolished. The diminution of pyruvate production ceased after 8 minutes infusion. The effects on oxygen uptake and pyruvate production were fully reversed when the infusion of dinoseb was ceased. Glucose production was only 45% reversed at the concentration of 15 μ M, but recovery was almost complete at lower concentrations (not shown). Fig. 7B shows the concentration dependences of the dinoseb effects. The IC_{50} for glucose production was 6.88 μ M and the EC_{50} for oxygen uptake 5.0 μ M. The diminution of pyruvate production occurred only at the highest concentrations, namely 10 and 15 μ M.

Effects of dinoseb on fructose metabolism

Lactate generates predominantly anabolic reactions, but fructose generates both anabolic and catabolic reactions (Moreira et al., 2013). Fructose as substrate can, thus, be used for investigating simultaneously the action of dinoseb on both catabolic and anabolic pathways. The results obtained in the experiments with fructose and dinoseb are shown in Fig. 8. Here again livers from fasted rats were used in order to minimize interference by the metabolic fluxes derived from endogenous glycogen. As expected from previous reports (Moreira et al., 2013), the infusion of fructose greatly accelerates glucose output, but also lactate and pyruvate productions. The the latter two reflect the catabolic glycolytic pathway (Fig. 8A). The effects of 15 μ M dinoseb were complex,

excepting perhaps glucose production, which was rapid and completely inhibited in 4 minutes. This effect was almost 100% reversible. Its concentration dependence was similar to that found with lactate and the IC_{50} was equal to 5.34 μM (Fig. 8B). Oxygen uptake suffered a rapid increase upon 15 μM dinoseb infusion (Fig. 8A). This increase was transient and inhibition developed progressively, reaching levels well below those seen before fructose infusion. With 15 μM dinoseb lactate and pyruvate productions behaved similarly to oxygen uptake, rapid stimulations were followed by inhibition. With lower concentrations of dinoseb, on the other hand, stimulation tended to predominate (time courses not shown), what generated the more complex effect versus concentration relationships shown in Fig. 8B. Plotted in Fig. 8B were always the rates found at 20 minutes dinoseb infusion, i.e., the final rates, even when there was no clear tendency for reaching a steady-state. Oxygen uptake was stimulated at concentrations up to 10 μM ; inhibition was found only at the concentration of 15 μM . The concentration for half-maximal stimulation (EC_{50}) was 2.85 μM . Pyruvate production was stimulated only at the concentration of 2.5 μM while inhibition was significant at the concentration of 10 and 15 μM . Lactate production, finally, was stimulated at concentrations up to 5 μM and inhibition was significant at the concentration of 15 μM .

Alanine-derived carbon and nitrogen fluxes

The purpose of the experiments that were done with alanine was to analyse the simultaneous action of dinoseb on carbon and nitrogen fluxes that are driven by this substrate. As illustrated by Fig. 9A 6 parameters were quantified and alanine infusion increased all of them. The infusion of 15 μM dinoseb at 36 minutes perfusion time affected all parameters. Here again glucose production was completely abolished. Reversibility was equal to 70% at the concentration of 15 μM , but tended to completion at lower concentrations. Urea production was also strongly inhibited, an expected phenomenon if one considers the energy-dependence of ureagenesis. The concentration dependences of the actions of dinoseb on these two energy-dependent routes is shown in the bottom of Fig. 9B. The IC_{50} 's were 3.04 and 5.15 μM for glucose and urea production, respectively. Contrary to what happened when fructose was the substrate, oxygen uptake was stimulated over the whole concentration range (Fig. 9B). The fluctuation in the curve makes an EC_{50} determination uncertain. Ammonia

production was increased by dinoseb, an observation that is consistent with the simultaneous inhibition of urea production. The concentration dependence presented a maximum at the concentration of 10 μM ; half-maximal stimulation can be expected at 5.28 μM . The decline in ammonia production in the passage from 10 to 15 μM dinoseb is, in principle at least, consistent with the kinetics of lactate and pyruvate production. The production of these two metabolites requires the transfer of the amine group, which eventually appears as ammonia. And, lactate and pyruvate productions were stimulated at low dinoseb concentrations, but experienced a decline at the highest ones, especially pyruvate.

Cellular adenine mononucleotide levels

The mononucleotide levels (AMP, ADP and ATP) were measured under two different conditions: in livers from fed rats being perfused with substrate-free perfusion medium (Fig. 10A) and in livers from fasted rats being perfused with perfusion medium containing 2 mM lactate (Fig. 10B). A diminution in the ATP levels is expected to occur in consequence of the uncoupling action of dinoseb (Saling et al., 2011; Moreira et al., 2013). In livers from fed rats the ATP levels were 62% diminished by 15 μM dinoseb (Fig. 10A); in livers from fasted rats the diminution was 79.5% with 10 μM dinoseb (Fig. 10B). Livers from fasted rats are, thus, more sensitive to dinoseb in this respect. Other modifications were also dissimilar between the fed and fasted state. In the fed state the ADP content was increased; in the fasted state it was decreased. In both states, fed and fasted, the AMP content was increased. However, the total mononucleotide content (AMP + ADP + ATP) was strongly diminished in the fasted state and not significantly decreased in the fed state. These differences may bear relation to the fact that, energetically, livers from fed rats were still producing ATP via glycolysis (see Fig. 6), whereas livers in the fasted state, under our perfusion conditions, relied entirely on the respiratory chain as the source of ATP.

Discussion

Markers of the uncoupling effect of dinoseb in the liver

The set of data obtained in the present work shows that dinoseb acts on liver metabolism and is able to affect several metabolic routes which are linked in some way to energy metabolism. The modifications in the metabolic fluxes are, in general, attributable to its reported uncoupling action (Palmeira et al., 1994a). A particularly revealing observation in the present work is the stimulation of oxygen uptake in isolated mitochondria caused by dinoseb in the presence of oligomycin, which blocks the ATP-synthase. This can only occur if phosphorylation and electron flow are disconnected from each other. In the perfused liver, however, the most important observations, which have also been traditionally reported for other uncouplers of oxidative phosphorylation, are (Soboll et al., 1978; Acco et al., 2004; Saling et al., 2011; Moreira et al., 2013): a) stimulation of oxygen consumption at low concentrations; b) diminution of the ATP content combined with diminutions in the ATP/ADP and ATP/AMP ratios; c) increase in the cytosolic NADH/NAD⁺ ratio, as indicated by the lactate/pyruvate ratio; d) inhibition of gluconeogenesis from three different substrates, namely lactate, fructose and alanine; e) stimulation of glycolysis and fructolysis as a cytosolic compensatory phenomenon for the diminished mitochondrial ATP production; f) stimulation of glycogenolysis as a means of providing glucose 6-phosphate for the increased glycolytic flux; g) impairment of ammonia detoxification. In general all these effects were reversible, i.e., when the infusion of dinoseb was stopped the alterations in the metabolic fluxes tended to return to the levels found before starting infusion. In spite of these general characteristics that are common to compounds that interfere with energy metabolism by uncoupling oxidative phosphorylation, dinoseb also presents peculiarities when compared to other uncouplers that are worth to be discussed in detail.

Interactions of dinoseb with the cellular membranes

The behaviour of dinoseb in the perfused liver could be described by a space-distributed and variable transit times model (Goresky et al., 1970; Bracht et al., 1980). This model takes into account convection along the sinusoidal beds and steady infusion of the solute. Whereas in isolated cell models the extracellular concentration varies with time (Makino et al., 1990), in the model

used in the present work the extracellular concentration facing all cells becomes equal to the inflowing concentration once equilibrium is reached. Uptake of dinoseb into the cell is extremely rapid, as its outflow profile conforms to an equation presupposing flow-limited distribution (Goresky et al., 1970; Bracht et al., 1980). Furthermore, it is also highly concentrative, as revealed by the equilibrium intra- to extracellular concentration ratio (C_i/C_e) of 43.9. Basically, the formation of concentration gradients can be generated by an active transport system or by binding to intracellular components. Active transport is ultimately dependent on the energy charge of the cell, i.e., from the ATP concentration. Considering that dinoseb actually depletes the cellular ATP, an energy-dependent concentration gradient of dinoseb is unlikely. Moreover, the high C_i/C_e ratio also implies in a very high intracellular concentration, $C_i = 439 \mu\text{M}$ for $C_e = 10 \mu\text{M}$ when expressed in terms of the cellular aqueous space. Interactions of dinoseb at such a high concentration with the mitochondria in the cell would produce irreversible damage, in contrast to the reversible action of dinoseb in the perfused liver. The $C_i = 439 \mu\text{M}$ is, thus, unlikely to represent a free concentration in the aqueous cellular environment. On the contrary, binding to cellular structures is more likely, corroborated especially by the molecular dynamics simulations that revealed a high affinity of dinoseb for the hydrophobic regions of the lipid bilayer. This high affinity of dinoseb for the lipid bilayer is likely to generate extensive binding to membranes in general and to other hydrophobic structures within the cell. This includes, evidently, the mitochondrial membranes, as indeed demonstrated experimentally in this work.

It should be remarked that the membrane model that was chosen for the molecular dynamics simulations was a general one that takes not into account the different compositions of the various intracellular membranes (mitochondria, endoplasmic reticulum, etc.). The main characteristics of the membrane system however, meaning a hydrophobic region separated by a polar region from the bulk solvent, are correctly reproduced. Since all models reproduce, to some level of tolerance, the same free energy profile for crossing the lipid bilayer, this seemed to us the correct choice (Neale and Pomès, 2016). Also, since the exact membrane composition at the interaction sites with the dinoseb molecule are virtually impossible to know, any model of choice would be an arbitrary one. The effects of a pH difference across the membrane (which is likely to exist in the case of mitochondria) has not been examined. Although this situation may

indeed affect the nominal values of the free energy profiles (Lähdesmäki et al., 2010), it would be difficult to predict the combined effect of both the water and lipid phases on the final values, especially because dinoseb by itself, as a protonophor, is expected to modify the pH gradient. Such a study would require a much more detailed and specific study.

The molecular dynamics simulations predict a membranous hydrophobic lipid phase/aqueous phase concentration ratio in the order of 10^4 or more. Since the volume of the membranous hydrophobic lipid phase is not known, however, it is also impossible to calculate the absolute concentration of dinoseb in this space. It is possible and of interest, however, to calculate the molar dinoseb/phospholipid ratio in the liver. An answer to this question will indicate at least if there is enough room to accommodate the great amounts of dinoseb that are taken up during a constant infusion at the concentration of $10 \mu\text{M}$, for example. Calculations in this respect can be done using our concentration data and those available in the literature on the chemical composition of the liver. If the liver being perfused with $10 \mu\text{M}$ dinoseb contains 439 nmol of the compound per mL cellular water ($439 \mu\text{M}$), this corresponds to 351.2 nmol per gram liver. The latter can be calculated using the information that 0.8 mL cellular water per g liver are accessible via the portal vein (Fernandes et al., 2002). Furthermore, the phospholipid content of the liver of male rats is 28 mg/g (Davidson, 1957). This corresponds to $37 \mu\text{mol/g}$ if one assumes a mean molecular mass of 750 g/mol . The molar ratio of dinoseb to phospholipids would, thus, be around 0.0095 . This is certainly not enough for disrupting the membranes, though it may eventually modify their properties to a certain degree. There is, however, enough room within the lipid bilayers of the liver to accommodate the amounts of dinoseb that are taken up when the vascular concentration is $10 \mu\text{M}$. Furthermore, the liver also contains approximately 14 mg/g neutral lipids, which are likely to be able to accommodate at least a fraction of the uncoupler. And, finally, binding can also occur to ligand proteins, especially to the fatty acid binding proteins, a superfamily of intracellular lipid binding proteins which exert the general function of lipid trafficking (Goresky et al., 1978; Córscico, 2006).

Summing up all the possibilities listed above only a fraction of the cellularly incorporated dinoseb will be present in the mitochondrial membranes, where the compound will presumably act as an uncoupler. It is very difficult to quantify the amount of dinoseb that is bound to the mitochondria inside the cells.

A binding curve was produced experimentally (Fig. 4), but the parameter derived from it can only be used if the free (unbound) dinoseb concentration is known. The latter is very difficult to estimate because it depends on several unknown factors including the possibility of an asymmetric distribution of the free form across the plasma membrane. The binding curve in Fig. 4, however, can be used to evaluate if the absence of saturation in the concentration range of up to 100 μM surpasses the binding capacity of the mitochondrial membranes. For the extra mitochondrial concentration of 100 μM application of the linear regression coefficient of 0.218 results in 21.8 nmol bound dinoseb per mg protein. Since in mitochondria the protein/lipid ratio is 3.2 (Goldhor, 1968), this would correspond to 69.8 nmol/mg phospholipid, or to a molar dinoseb/phospholipid ratio of 0.0519. In molar terms and in the particular conditions of the incubation system used for obtaining the data in Fig. 4, dinoseb corresponded to 5% of the total phospholipids in the mitochondrial membranes, still considerably far from a saturation point. The fact that the energy level of dinoseb is practically the same over the whole hydrophobic phase of the lipid bilayer (see Fig. 1) is consistent with this interpretation. It should be remarked that binding of dinoseb to the thylacoid membranes (chloroplasts) is pH dependent and is more pronounced at lower pH values (for example, when pH is decreased from 8 to 6; Oettmeier and Masson, 1980). This could mean that highly acidic environments within the cell, such as those surrounding mitochondria, should favor dinoseb binding and its related effects at least at the initial stages of the infusion. This line of thought opens the way for the possibility that the concentrations of dinoseb in the various cellular environments are not necessarily uniform, but dependent on specific local conditions.

Peculiarities of the uncoupling action of dinoseb

One of the peculiarities of the action of dinoseb is the concentration range at which it acts in the whole liver in comparison with the concentration range in isolated mitochondria. In general terms, for example, the concentrations of dinoseb that generate half-maximal stimulation of oxygen uptake are at least ten times higher in the perfused liver when compared to isolated mitochondria, 2.83-5.80 μM when compared to 0.17-0.29 μM (Palmeira et al., 1994a). This reflects also in the concentrations for half-maximal inhibition of gluconeogenesis which are comparable to the concentrations that produce half-maximal stimulation of

oxygen uptake (3.04-6.88 μM). It also reflects in the concentrations necessary to affect the ATP levels in the perfused liver, as found in the present work, and in isolated hepatocytes (Palmeira et al., 1994b). It is true that effects caused by respiratory inhibitors in isolated mitochondria tend to occur usually at higher concentrations in the intact cell when compared to isolated mitochondria. In the case of dinoseb, however, the difference seems to be more pronounced compared to other uncouplers. 2,4-Dinitrophenol, for example, stimulates half-maximally oxygen uptake in isolated mitochondria in the vicinity of 15-20 μM (Chappell et al., 1964; Hanstein and Hatefi, 1974) or even 50 μM (Abo-Khatwa et al., 1996) and causes 50% inhibition of gluconeogenesis from alanine in the perfused liver at a concentration of 17.9 μM (Saling et al., 2011). At the concentration of 30 μM 2,4-dinitrophenol increases oxygen consumption of the perfused liver by 83% and glycolysis by 156% (Soboll et al., 1978). There are other examples of uncouplers presenting relatively small differences between their active concentrations in isolated mitochondria and perfused liver (Saling et al., 2011; Abo-Khatwa et al., 1996; Moreira et al., 2013). Differences of one order of magnitude or more between the concentrations required in isolated mitochondria and perfused liver for an effective uncoupling activity seem, thus, not to be the general rule. Pronounced differences in the active concentrations of inhibitors of energy metabolism between mitochondria and intact cells can be expected when the inhibitor permeates the cell membrane at low rates or when its transformation into an inert substance occurs at very high rates. The latter possibility does not apply to dinoseb because its transformation occurs at such low rates that it is hardly detectable after a single passage through the liver. On the other hand, although the compound has evidently rapid and free access to the cellular space its distribution is strongly constrained by its high affinity to the various lipid environments. This could be limiting in some way its interactions with the mitochondria within the cellular environment.

Concluding remarks

This work presents for the first time a comprehensive investigation on how dinoseb affects the various metabolic pathways in the liver that are linked to energy transduction. At low concentrations (up to 2.5 μM) the compound can be considered a metabolic agent that modifies metabolic fluxes. After levels of contamination that lead to concentrations above 2.5 μM , however, toxicity is

enormously increased. The present work was also the first demonstration that dinoseb has full access to the whole liver space in a flow-limited manner, probably because the compound is efficiently dissolved by the hydrophobic portion of the cellular membranes. The latter finding is in contrast to a previous suggestion that permeation of the cell membrane could be a limiting factor in the accessibility of dinoseb and related compounds to the intracellular environment (Palmeira et al., 1994b).

In spite of the difference of at least one order of magnitude in the dinoseb concentrations that effectively uncouple phosphorylation between isolated mitochondria and intact liver cells, the compound can still be regarded as a highly efficient metabolic agent. All its actions are significant at concentrations well below 10 μM and the active concentration range falls within one order of magnitude. It is, thus, a short range uncoupler, generally dangerous for humans and animals (Lou et al., 2007). Its actions are also more dangerous because it depresses much more the ATP levels than uncouplers like 2,4-dinitrophenol and juglone, for example, at concentrations producing similar increments in oxygen uptake as these two substances (Soboll et al., 1978; Saling et al., 2011). Furthermore, its effects in the perfused liver are all exerted within similar concentration ranges. For example, the analogue 2,4-dinitrophenol, still used and even inadequately recommended for weight loss purposes, inhibits half-maximally alanine gluconeogenesis at the concentration of 17.9 μM , but stimulates half-maximally urea production at the concentration of 4.76 μM (Saling et al., 2011). A similar behaviour was found for juglone, the uncoupler found in the wall nut (Saling et al., 2011). Inhibition of urea production by 2,4-dinitrophenol and juglone occurs only at concentrations considerably higher than those producing gluconeogenesis inhibition. Dinoseb, however, did not stimulate urea production, and its inhibitory action on this parameter (meaning ammonia detoxification) occurred at concentrations similar to those producing gluconeogenesis inhibition. These and similar phenomena are consistent with the higher toxicity of dinoseb when compared to several other natural or synthetic uncouplers.

Funding

This work was funded by grants from the Conselho Nacional de Desenvolvimento Científico e Tecnológico (CNPq; grant number 302615/2011-3).

Conflict of interest

The authors state that they have no conflict of interest concerning the present article.

Appendix a. supplementary data

Supplementary data to this article can be found online at <http://dx.doi.org/10.1016/j.taap.2017.06.013>.

References

- Abo-Khatwa, N.A., Al-Robal, A.A., Jahwari, D.A., 1996. Lichen acids as uncouplers of oxidative phosphorylation of mouse-liver mitochondria. *Nat. Toxins* 4, 96-102.
- Acco, A., Comar, J.F., Bracht, A., 2004. Metabolic effects of propofol in the isolated perfused rat liver. *Basic Clin. Pharmacol. Toxicol.* 95, 166-174.
- Berendsen, H.J.C., Postma, J.P.M., van Gunsteren, W.F., DiNola, A., Haak, J.R., 1984. Molecular dynamics with coupling to an external bath. *J. Chem. Phys.* 81, 3684. doi: 10.1063/1.448118
- Bergmeyer, H.U., 1974. *Methods of Enzymatic Analysis*. Verlag Chemie-Academic Press, Weinheim-London.
- Björck, A., Dahlquist, G., 1972. *Numerische Methoden*. Oldenburg Verlag, München.
- Bracht, A., Schwab, A.J., Scholz, R., 1980. Studies of flow-rates in the isolated perfused rat liver by pulse labelling with radioactive substrates and mathematical analysis of the wash-out kinetics. *Hoppe Seyler's Z. Physiol. Chem.* 361, 357-377.
- Bracht, A., Ishii-Iwamoto, E.L., Salgueiro-Pagadigoria, C.L., 2003. O estudo do metabolismo energético em mitocôndrias isoladas de tecido animal. In: Bracht, A., Ishii-Iwamoto, E.L. (Eds.), *Métodos de Laboratório em Bioquímica*. Editora Manole, São Paulo, pp. 227-247.
- Case, D.A., Betz, R.M., Botello-Smith, W., Cerutti, D.S., Cheatham, T.E., Darden, T.A., Duke, R.E., Giese, T.J., Gohlke, H., Goetz, A.W., Homeyer, N., Izadi, S., Janowski, P., Kaus, J., Kovalenko, A., Lee, T.S., LeGrand, S., Li, P., Lin, C., Luchko, T., Luo, R., Madej, B., Mermelstein, D., Merz, K.M., Monard, G., Nguyen, H., Nguyen, H.T., Omelyan, I., Onufriev, A., Roe, D.R., Roitberg, A., Sagui, C., Simmerling, C.L., Swails, J., Walker, R.C., Wang, J., Wolf, R.M., Wu, X., Xiao, L., York, D.M., Kollman, P.A., 2016. *AMBER 2016*. University of California, San Francisco.
- Chappell, J.B., 1964. The effects of 2,4-dinitrophenol on mitochondrial oxidations. *Biochem. J.* 90, 237-248.
- Comar, J.F., de Oliveira, D.S., Bracht, L., Kemmelmeier, F.S., Peralta, R.M., Bracht, A., 2016. The metabolic responses to L-glutamine of livers from rats with diabetes types 1 and 2. *PLoS ONE* 11(8), e0160067. doi: 10.1371/journal.pone.0160067.
- Córsico, B., 2006. Intracellular lipid transport: structure-function relationships in fatty acid binding proteins. *Future Lipidol.* 1, 615-622.
- Davidson, M.D., 1957. Chemistry of the liver cell. *Brit. Med. Bull.* 13, 77-81.

Dickson, C.J., Madej, B.D., Skjevik, Å.A., Betz, R.M., Teigen, K., Gould, I.R., Walker, R.C., 2014. Lipid14: the amber lipid force field. *J. Chem. Theory Comput.* 10, 865–879.

Eler, G.J., Santos, I.S., de Moraes, A.C., Mito, M.S., Comar, J.F., Peralta, R.M., Bracht, A., 2013. Kinetics of the transformation of n-propyl gallate and structural analogs in the perfused rat liver. *Toxicol. Appl. Pharmacol.* 273, 35-46.

Fernandez, T.R.L., Suzuki-Kemmelmeier, F., de Oliveira, D.S., Bracht, A., 2002. Changes in distribution spaces and cell permeability caused by ATP in the rat liver. *Liver* 22, 35-42.

Fiske, C.H., Subbarow, Y., 1925. The colorimetric determination of phosphorus. *J. Biol. Chem.* 66, 375-400.

Goldhor S., 1968. Protein : lipid ratios of liver mitochondria during development. *J. Cell. Biol.* 37, 823-825.

Goresky, C.A., Ziegler, W.H., Bach, G.G., 1970. Capillary exchange modelling. Barrier-limited and flow-limited distribution. *Circ. Res.* 27, 739–764.

Goresky, C.A., Daly, D.S., Mishkin, S., Arias I.M., 1978. Uptake of labeled palmitate by the intact liver: role of intracellular binding sites. *Am. J. Physiol.* 234, E542–E553.

Grest, G.S., Kremer, K., 1986. Molecular dynamics simulation for polymers in the presence of a heat bath. *Phys. Ver. A* 33, 3628-3631.

Guan, Y., Wei, J., Zhang, D., Zu, M., Zhang, L., 2013. To identify the important soil properties affecting dinoseb adsorption with statistical analysis. *SCI World J.* Article ID 362854, 7 pages.

Hanstein, W., Hatefi, Y., 1974. Characterization and localization of mitochondrial binding sites with an uncoupler capable of photoaffinity labeling. *J. Biol. Chem.* 249, 1356-1362.

Hanwell, M.D., Curtis, D.E., Lonie, D.C., Vandermeersch, T., Zurek, E., Hutchison, G.R., 2012. Avogadro: an advanced semantic chemical editor, visualization, and analysis platform. *J. Cheminform.* 4, 17. Doi:10.1186/1758-2946-4-17

Heusinkveld, H.J., van Vliet, A.C., Nijssen, P.C.G., Westerink, R.H.S., 2016. In vitro neurotoxic hazard characterization of dinitrophenolic herbicides. *Toxicol. Lett.* 252, 62-69.

Jo, S., Kim, T., Iyer, V.G., Im, W., 2008. CHARMM-GUI: a web-based graphical user interface for CHARMM. *Comput. Chem.* 29, 1859–1865.

Katyare, S.S., Fatterpaker, P., Sreesivasan, A., 1971. Effect of 2,4-dinitrophenol (DNP) on oxidative phosphorylation in rat liver mitochondria. *Arch. Biochem. Biophys.* 144, 209-215.

Kelmer-Bracht, A.M., Ishii, E.L., Andrade, P.V.M., Bracht, A., 1984. Construction of a liver perfusion apparatus for studies on metabolic regulation and mechanisms of drug action. *Braz. Arch. Biol. Technol.* 27, 419–438.

Kelmer-Bracht, A.M., Ishii-Iwamoto, A.L., Bracht, A., 1993. Transport and distribution space of the anti-inflammatory drug niflumic acid in the perfused rat liver. *Biochem. Pharmacol.* 45, 1863–1871.

Kumar, S., Bouzida, D., Swendsen, R.H., Kollman, P.A., Rosenberg, J.M., 1992. The weighted histogram analysis method for free-energy calculations on biomolecules. i. The method. *J. Comput. Chem.* 13, 1011-1021.

Lähdesmäki, K., Ollila, O.H.S., Koivuniemi, A., Kovanen, P.T., Hyvönen, M.T., 2010. Membrane simulations mimicking acidic pH reveal increased thickness and negative curvature in a bilayer consisting of lysophosphatidylcholines and free fatty acids. *Biochim. Biophys. Acta - Biomembr.* 1798, 938–946.

Lou, P.H., Hansen, B.S., Olsen, P.H., Tullin, S., Murphy, M.P., Brand, M.D., 2007. Mitochondrial uncouplers with an extraordinary dynamic range. *Biochem. J.* 407, 129–140.

Lowry, O., Rosebrough, N.J., Farr, A.C., Randall, R.J., 1951. Protein measurement with the Folin phenol reagent. *J. Biol. Chem.* 193, 265–275.

Makino, K., Ohshima, H., Kondo, T. 1990. Kinetic model for membrane transport. 1. Effects of the membrane volume and partitioning kinetics. *Biophys. Chem.* 35, 95-95.

McBean, C., 2012. *The Pesticide Manual*. BCPC Publications, Hampshire.

Mito, M.S., Castro, C.V., Peralta, R.M., Bracht, R.M., 2014. Effects of ranolazine on carbohydrate metabolism in the isolated perfused rat liver. *Open J. Med. Chem.* 4, 87-95.

Moreira, C.T., Oliveira, A.J., Comar, J.F., Peralta, R.M., Bracht, A., 2013. Harmful effects of usnic acid on hepatic metabolism. *Chem. Biol. Int.* 203, 502-511.

Neale, C., Pomès, R., 2016. Sampling errors in free energy simulations of small molecules in lipid bilayers. *Biochim. Biophys. Acta - Biomembr.* 1858, 2539–2548.

Oettmeier, W., Masson, K., 1980. Synthesis and thylakoid membrane binding of the radioactively labeled herbicide dinoseb. *Pesticide Biochem. Physiol.* 14, 86-97.

Palmeira, C.M., Moreno, A.J., Madeira, V.M., 1994a. Interactions of herbicides 2,4-D and dinoseb with mitochondrial bioenergetics. *Toxicol. Appl. Pharmacol.* 127, 50-57.

Palmeira, C.M., Moreno, A.J., Madeira, V.M., 1994b. Metabolic alterations in hepatocytes promoted by the herbicides paraquat, dinoseb and 2,4-D. *Arch. Toxicol.* 68, 24-31.

Preiss, U., Wallnöfer, P.R., Engelhardt, G., 1988. Partial purification and properties of an esterase from tomato cell suspension cultures hydrolysing pyrethroid insecticide cyfluthrin. *Pestic. Sci.* 23, 13-24.

ProfResearch Reports, 2014. Global and Chinese dinoseb-acetate industry, 2009-2019 market research report. <http://www.profresearchreports.com/global-and-chinese-dinoseb-acetate-industry-2009-2019-research-report-market> (accessed 23.03.2017)

Saling, S.C., Comar, J.F., Mito, M.S., Peralta, R.M., Bracht, A., 2011. Actions of juglone on energy metabolism in the rat liver. *Toxicol. Appl. Pharmacol.* 257, 319-327.

Scholz, R., Bücher, T., 1965. Hemoglobin-free perfusion of rat liver. In: Chance, B., Estabrook, R.W., Williamson, J.R. (Eds.), *Control of Energy Metabolism*. Academic Press, New York, pp. 393-414.

Sies, H., 1982. Nicotinamide nucleotide compartmentation. In: Sies, H. (Ed.), *Metabolic Compartmentation*. Academic Press, London, pp. 205-231.

Soboll, S., Scholz, R., Heldt, H.W., 1978. Subcellular metabolite concentrations. Dependence of mitochondrial and cytosolic ATP systems in the metabolic state of perfused rat liver. *Eur. J. Biochem.* 87, 377-390.

Vanquelef, E., Simon, S., Marquant, G., Garcia, E., Klimerak, G., Delepine, J.C., Cieplak, P., Dupradeau, F. Y., 2011. R.E.D. server: a web service for deriving RESP and ESP charges and building force field libraries for new molecules and molecular fragments. *Nucleic Acids Res.* 39, Web Server issue W511-W517 doi:10.1093/nar/gkr288

Voss, D.O., Campello, A.P., Bacila, M., 1961. The respiratory chain and the oxidative phosphorylation of rat brain mitochondria. *Biochem. Biophys. Res. Comm.* 4, 48-51.

Wagon, S., 1999. *Mathematica in Action*. Springer-Verlag, New York.

Wang, J., Wolf, R.M., Caldwell, J.W., Kollman, P.A., Case, D.A., 2004. Development and testing of a general amber force field. *J. Comput. Chem.* 25, 1157-1174.

Zaharia, M., Tudorachi, L., Pintilie, O., Gradinaru, R., Murariu, M., 2016. Banned dinitrophenols still trigger both legal and forensic issues. *Environ. Forensics* 17, 120-130.

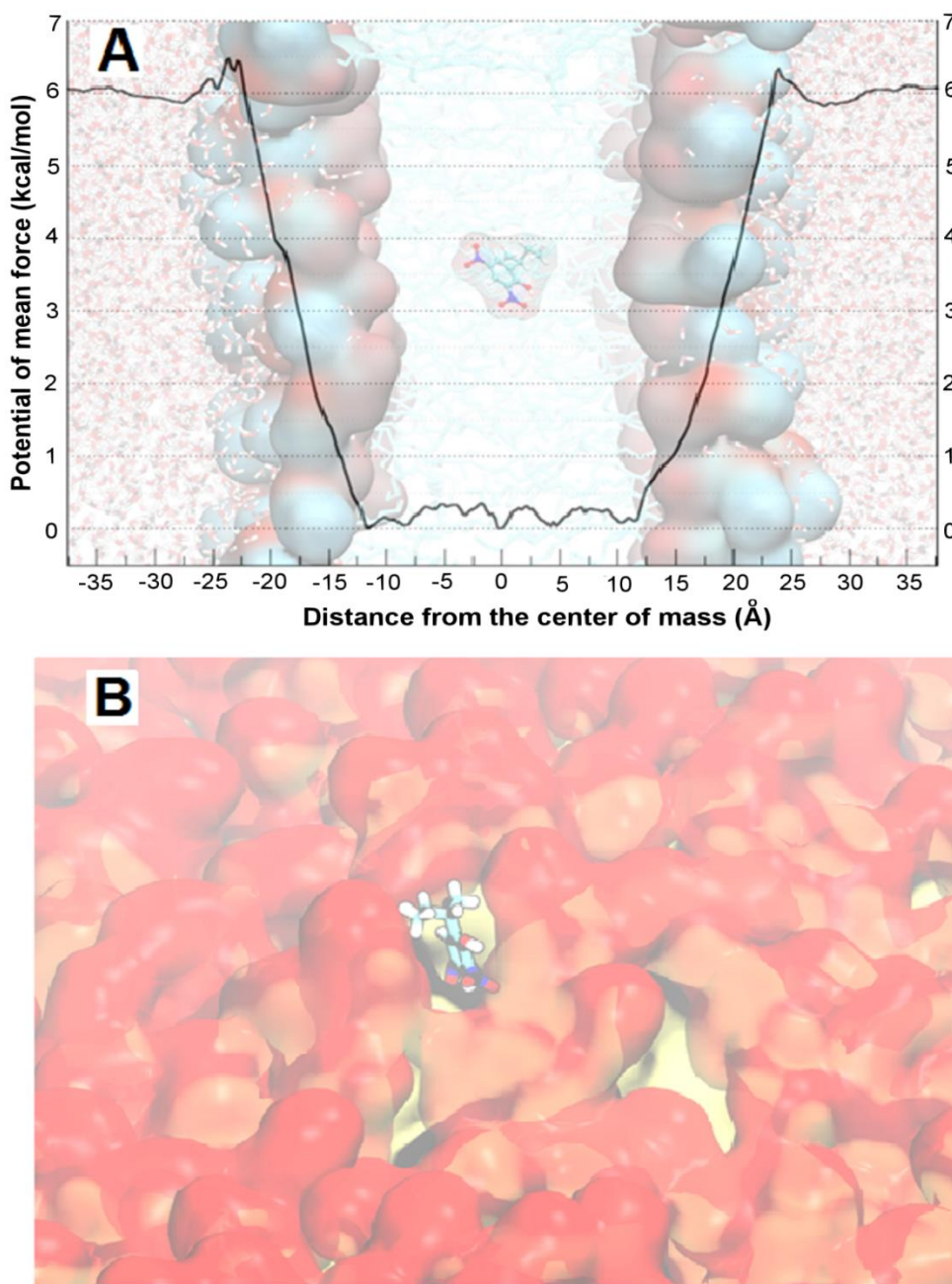


Figure 1. **Selected views of the molecular dynamics simulation of the behaviour of dinoseb in a phospholipid bilayer.** Panel (A) shows the calculated potential of mean force (PMF) profile for the transfer of the dinoseb across the phospholipid bilayer. Panel B represents a snapshot of a frame from the membrane/water interface. The membrane nonpolar and polar groups are represented in orange and red, respectively. In the center is the dinoseb molecule. (For interpretation of the references to colour in this figure legend, the reader is referred to the web version of this article).

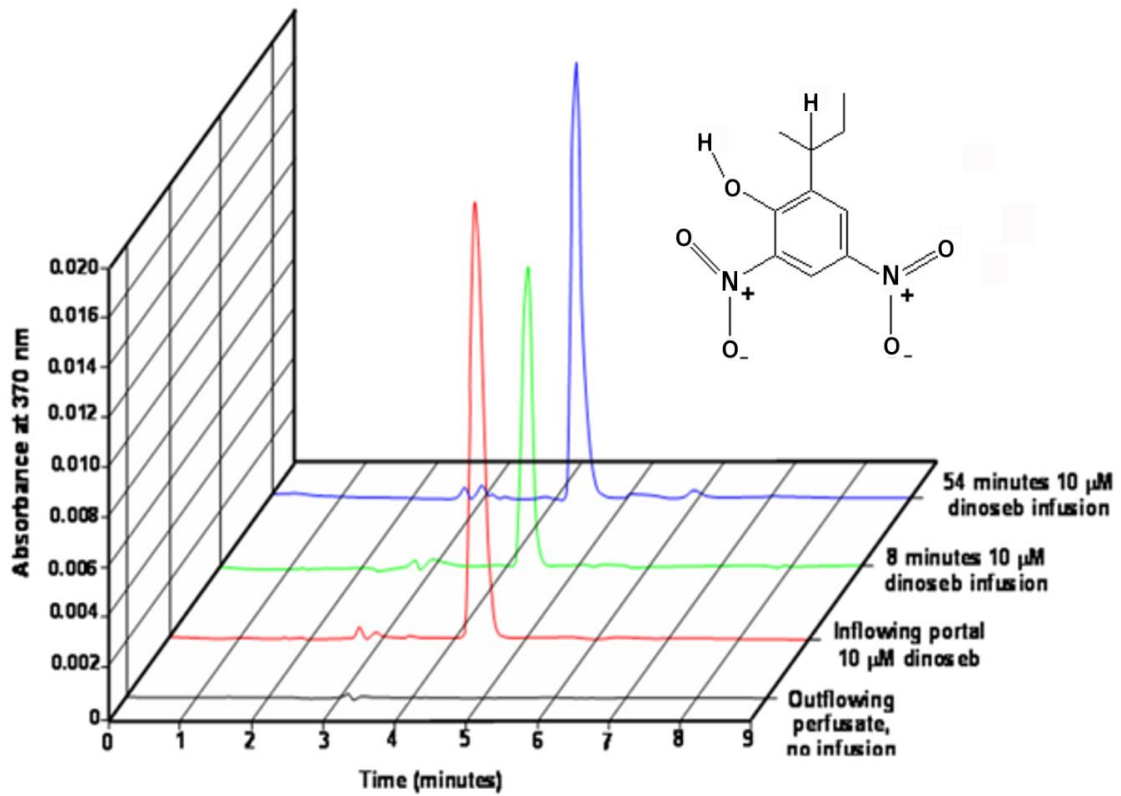


Figure 2. **Portal dinoseb infusion in the perfused liver: selected chromatographic profiles of in- and outflowing perfusate samples.** Livers of fed or fasted rats were perfused with Krebs/Henseleit-bicarbonate buffer (pH 7.4) as described in materials and methods. Samples were collected before and at different times after the onset of the infusion. These samples were fractionated by HPLC with spectrophotometric detection as described in the Materials and Methods section. The conditions of the sample are given in the right of side of the chromatograms.

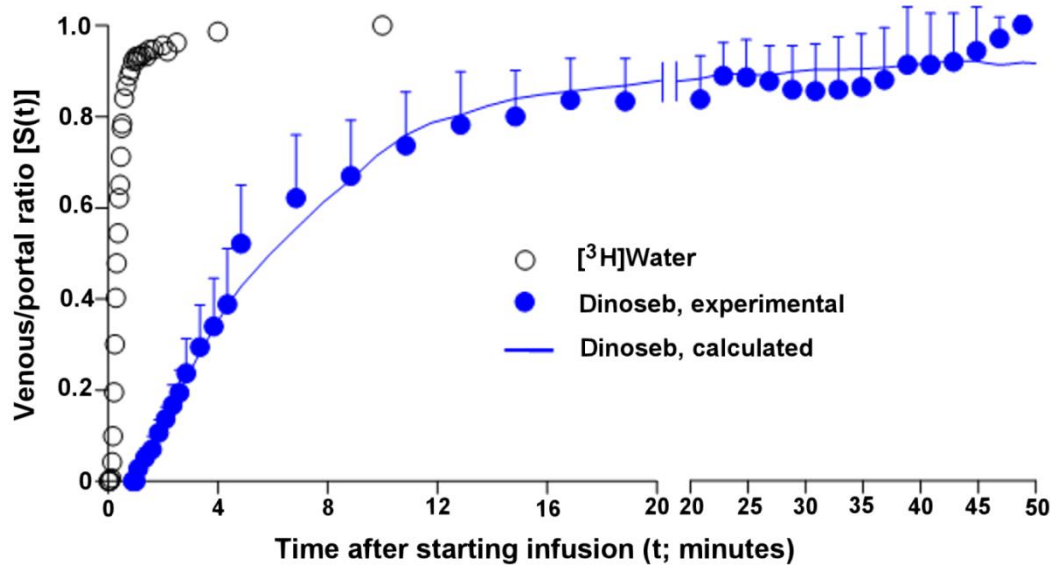


Figure 3. **Experimental and computed fractional outflow profiles of dinoseb.** Dinoseb ($10 \mu\text{M}$) and $[^3\text{H}]$ water were infused at constant rates. Samples of the effluent perfusate were collected for ^3H counting and for the spectrophotometric determination of dinoseb. The results were expressed as fractions of the inflowing concentration (venous portal ratio). Equations (1) and (2) were fitted simultaneously to the experimental data using a non-linear least squares procedure. The continuous line, corresponding to $S(t)$ in equation (1), was calculated using the optimized parameters: $\Phi = 27.048 \pm 4.895$; $t_0 = 0.141 \pm 0.026$ minutes; $k_{\text{met}} = 0$. The standard error of the estimate was equal to 3.82×10^{-2} and the coefficient of determination equal to 0.988 ($r = 0.994$).

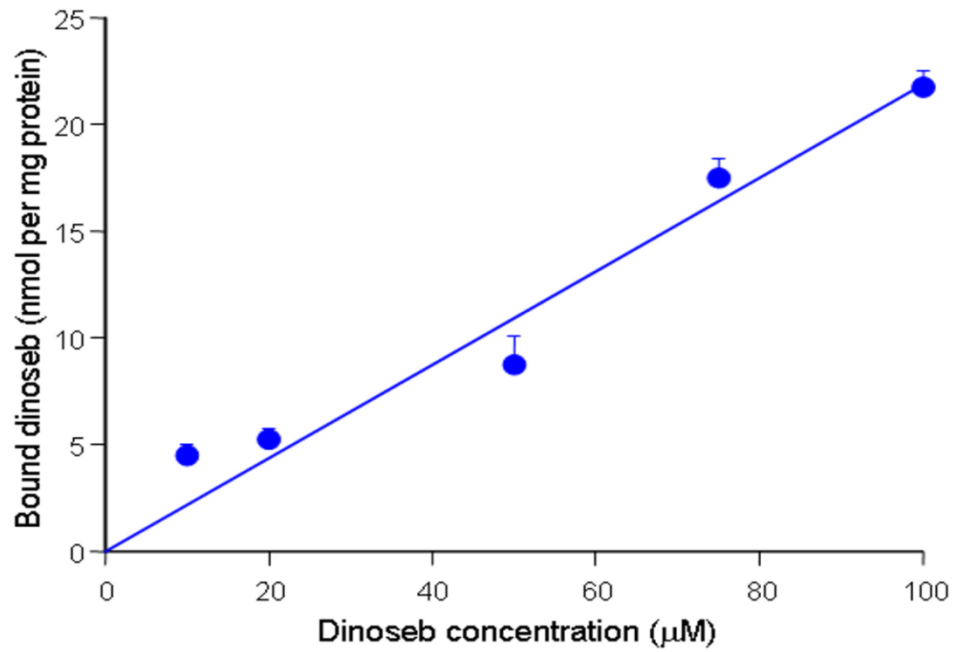


Figure 4. **Binding of dinoseb to isolated rat liver mitochondria.** Binding was measured as described in the materials and methods. The data points represent means of four experiments. Bars represent mean standard errors. The continuous line represents the optimized linear regression curve ($y = 0.218 \pm 0.012x$). The correlation coefficient was equal to 0.985.

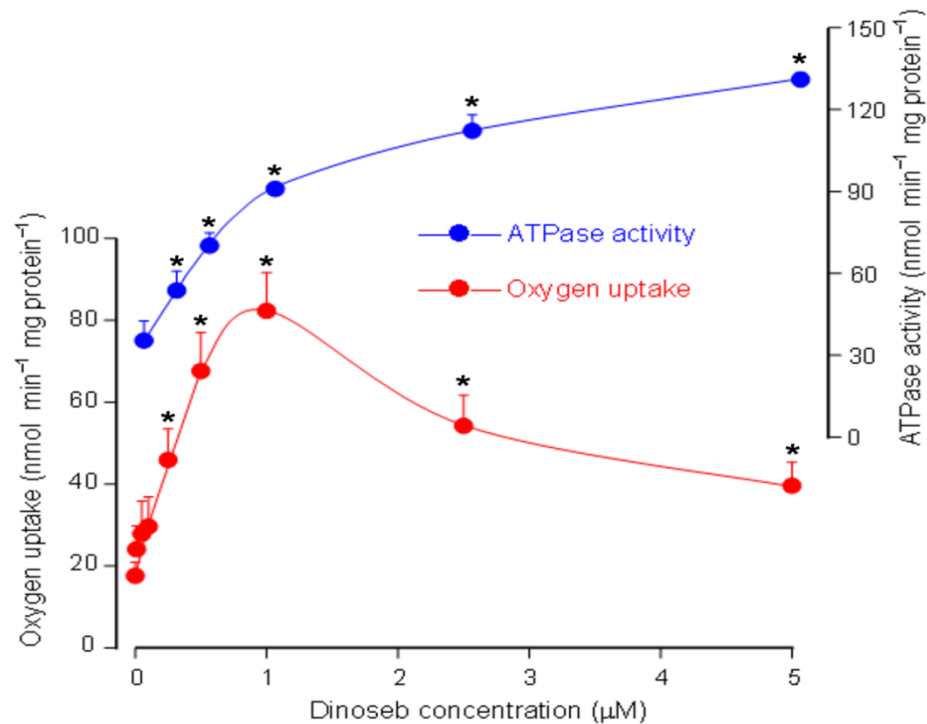


Figure 5. **Effects of dinoseb on mitochondrial respiration and ATPase activity.** Freshly prepared intact mitochondria were incubated at 37 °C as described in the materials and methods section. Oxygen uptake was measured polarographically and the ATPase activity was quantified as phosphate released from ATP. Details about the incubation media and concentrations are given in the Materials and Methods section. Each datum point is the mean \pm SEM of 4 (oxygen uptake measurements) or 3 (ATPase activity) independent experiments. Asterisks (*) indicate statistical significance in comparison with the control condition ($p \leq 0.05$), i.e., absence of dinoseb.

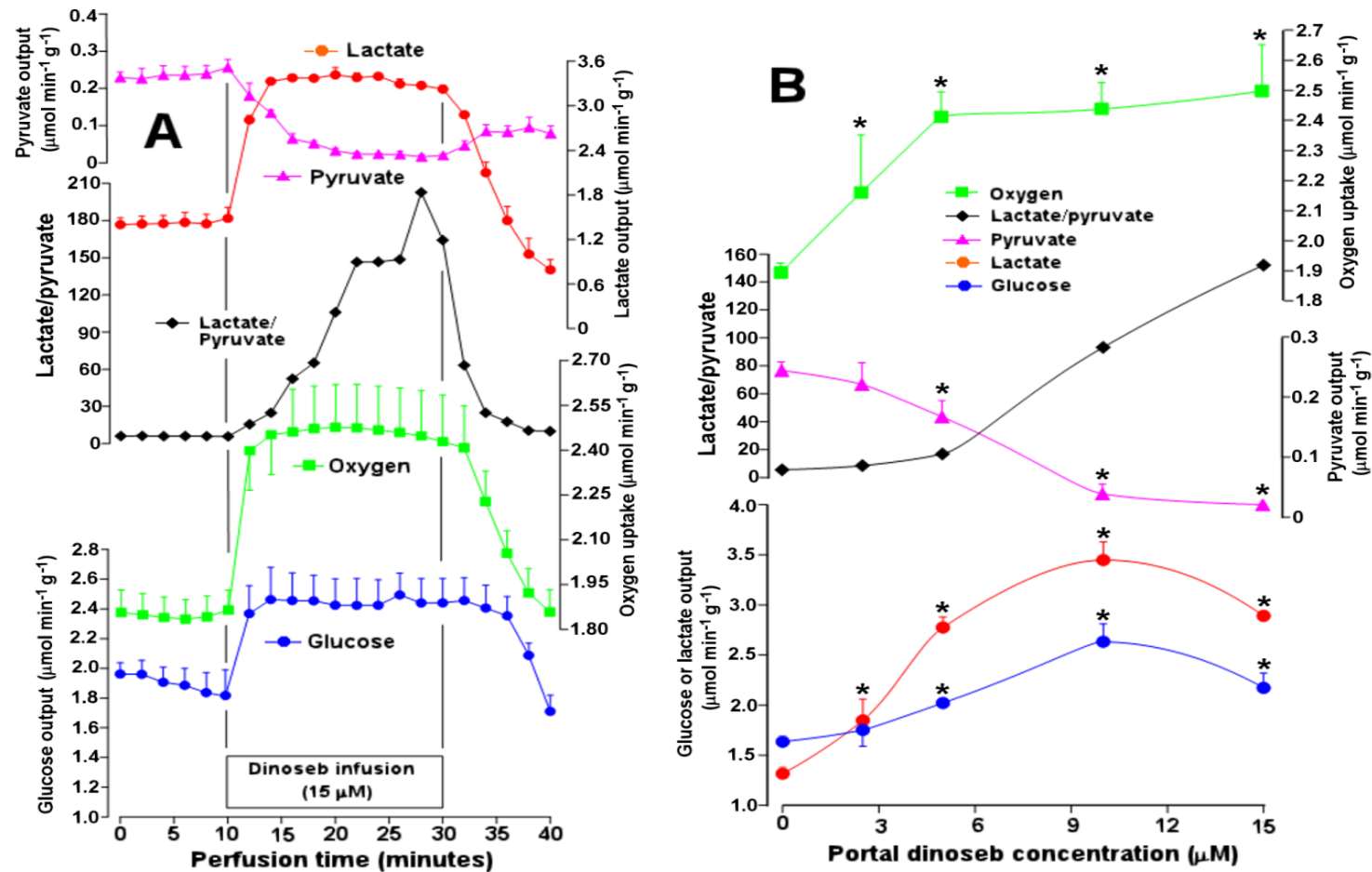


Figure 6. **Time courses and concentration dependences of the actions of dinoseb on glycogen catabolism and oxygen uptake.** Livers from fed rats were perfused as described in the materials and methods section. Panel A shows the time courses of the changes caused by 15 μM dinoseb. The effluent perfusate was sampled in 2 min intervals and analyzed for its glucose, lactate, and pyruvate contents. Oxygen consumption was followed polarographically. Panel B summarizes the results of similar experiments in which dinoseb was infused in the range between 2.5 and 15 μM . Each datum point represents the mean of 3 liver perfusion experiments. Bars are standard errors of the mean. Asterisks (*) indicate statistical significance in comparison with the control condition ($p \leq 0.05$), i.e., absence of dinoseb.

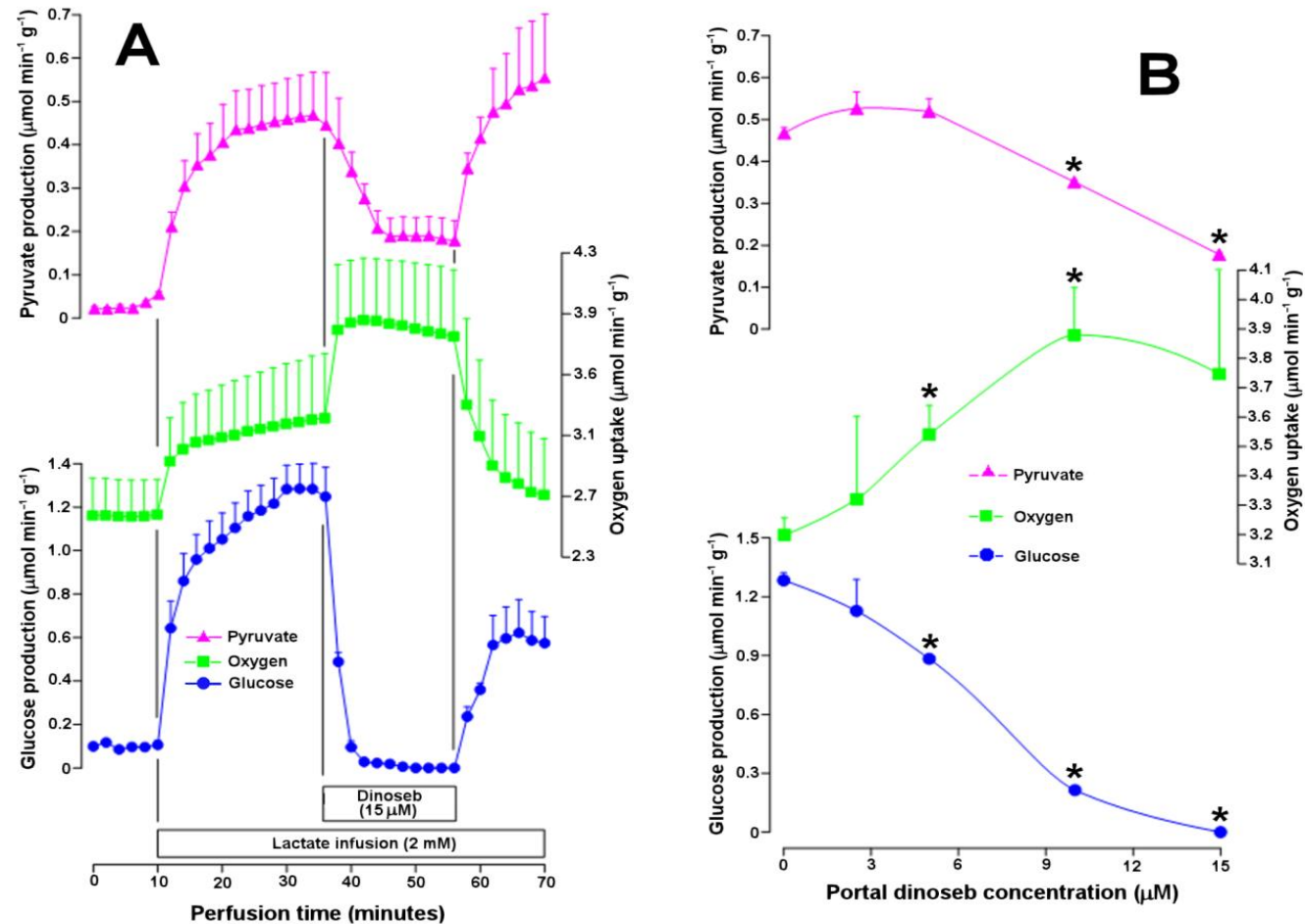


Figure 7. **Time courses and concentration dependences of the actions of dinoseb on lactate gluconeogenesis and related parameters.** Livers from fasted rats were perfused as described in the materials and methods section. Panel A shows the time courses of the changes caused by 15 μM dinoseb. Lactate (2 mM) was infused as indicated. The effluent perfusate was sampled in 2 min intervals and analyzed for its glucose and pyruvate contents. Oxygen consumption was followed polarographically. Panel B summarizes the results of similar experiments in which dinoseb was infused in the range between 2.5 and 15 μM . Each datum point represents the mean of 3 liver perfusion experiments. Bars are standard errors of the mean. Asterisks (*) indicate statistical significance in comparison with the control condition ($p \leq 0.05$), i.e., absence of dinoseb.

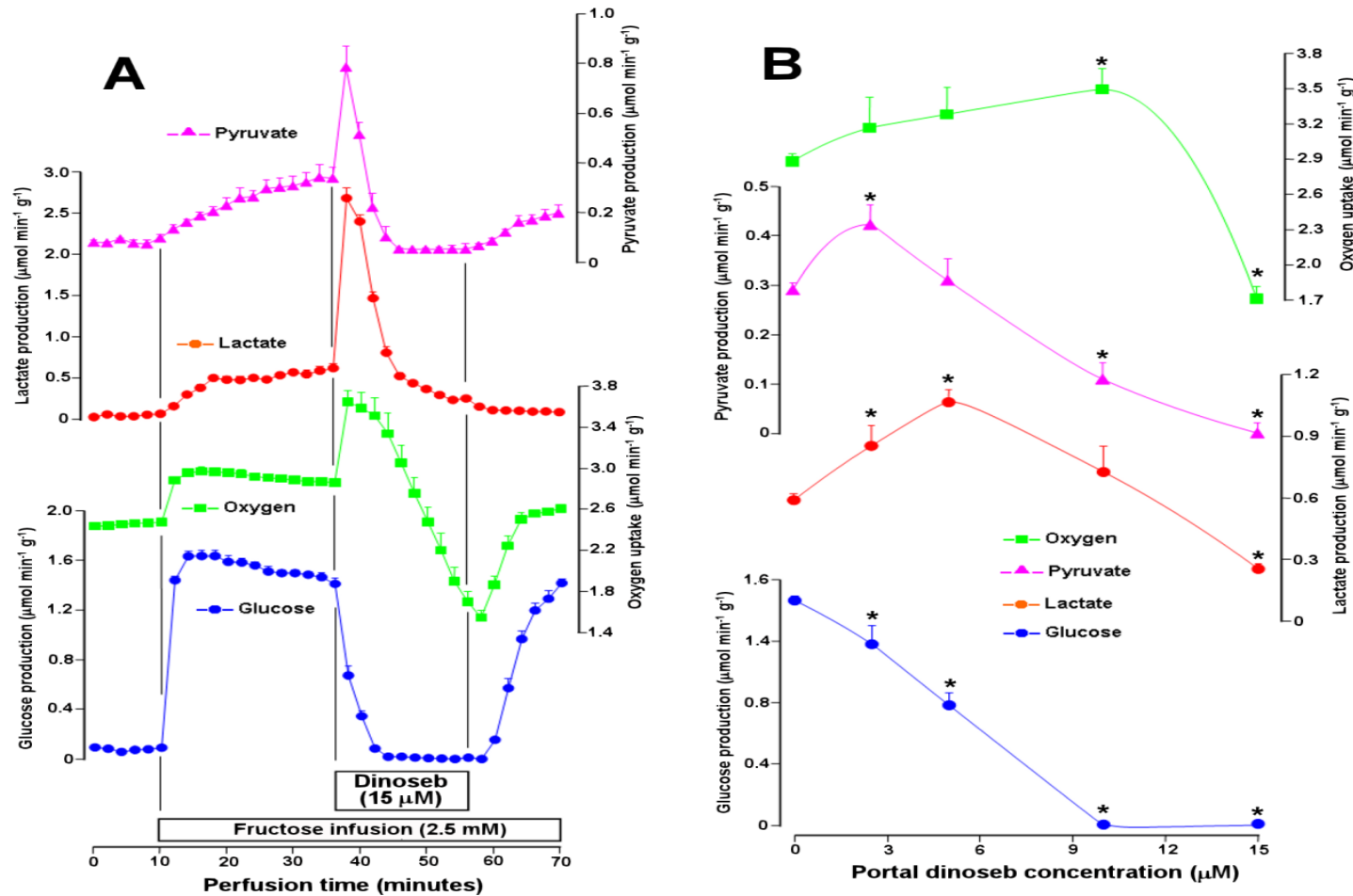


Figure 8. Time courses and concentration dependences of the actions of dinoseb on fructose metabolism. Livers from fasted rats were perfused as described in the materials and methods section. Panel A shows the time courses of the changes caused by 15 μM dinoseb. Fructose (2.5 mM) was infused as indicated. The effluent perfusate was sampled in 2 min intervals and analyzed for its glucose, lactate and pyruvate contents. Oxygen consumption was followed polarographically. Panel B summarizes the results of similar experiments in which dinoseb was infused in the range between 2.5 and 15 μM . Each datum point represents the mean of 3 liver perfusion experiments. Bars are standard errors of the mean. Asterisks (*) indicate statistical significance in comparison with the control condition ($p \leq 0.05$), i.e., absence of dinoseb.

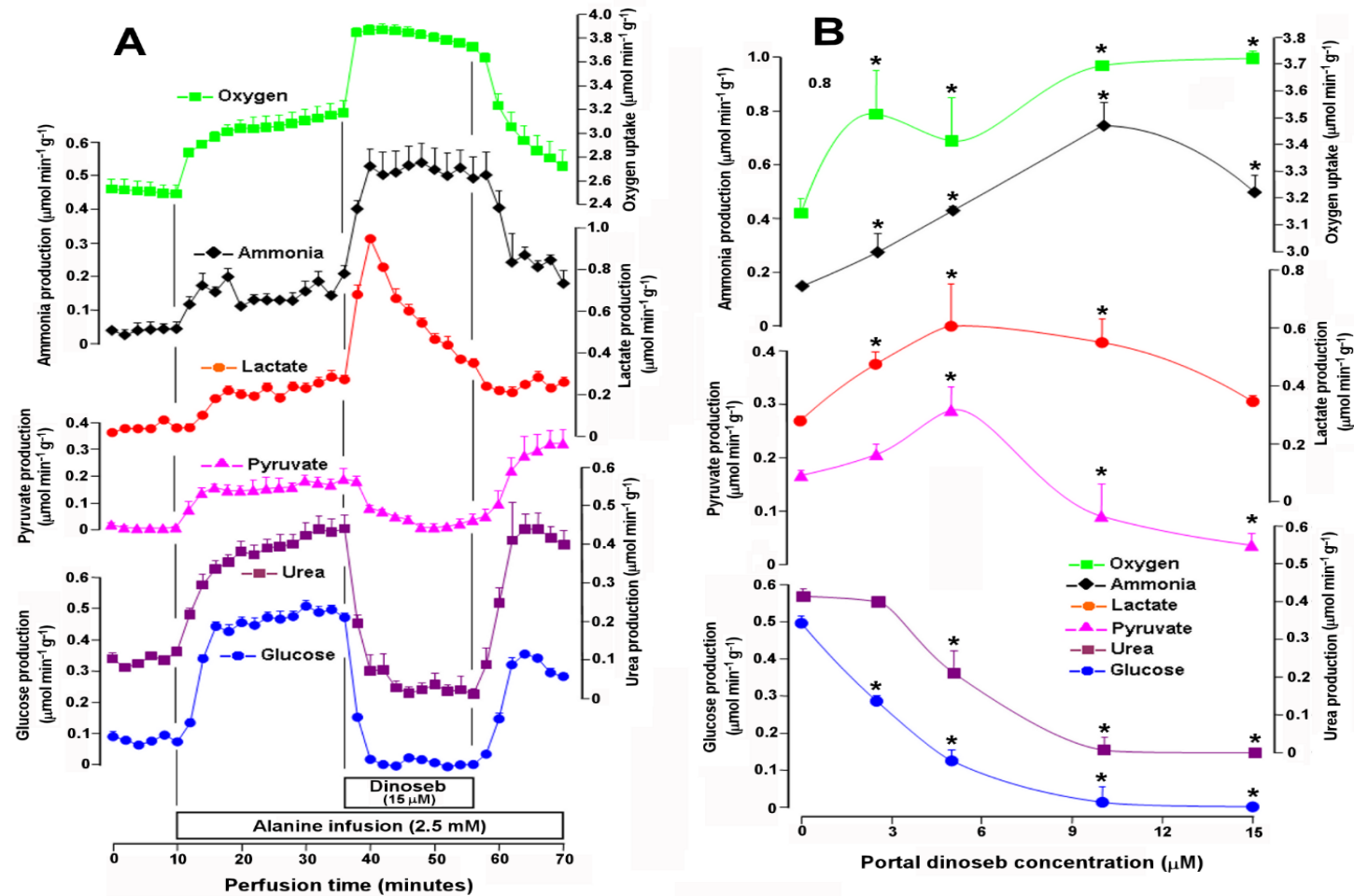


Figure 9. **Time courses and concentration dependences of the actions of dinoseb on alanine-derived metabolic fluxes of carbon and nitrogen.** Livers from fasted rats were perfused as described in the materials and methods section. Panel A shows the time courses of the changes caused by 15 μM dinoseb. Alanine (2.5 mM) was infused as indicated. The effluent perfusate was sampled in 2 min intervals and analyzed for its glucose, lactate, pyruvate, ammonia and urea contents. Oxygen consumption was followed polarographically. Panel B summarizes the results of similar experiments in which dinoseb was infused in the range between 2.5 and 15 μM . Each datum point represents the mean of 3 liver perfusion experiments. Bars are standard errors of the mean. Asterisks (*) indicate statistical significance in comparison with the control condition ($p \leq 0.05$), i.e., absence of dinoseb.

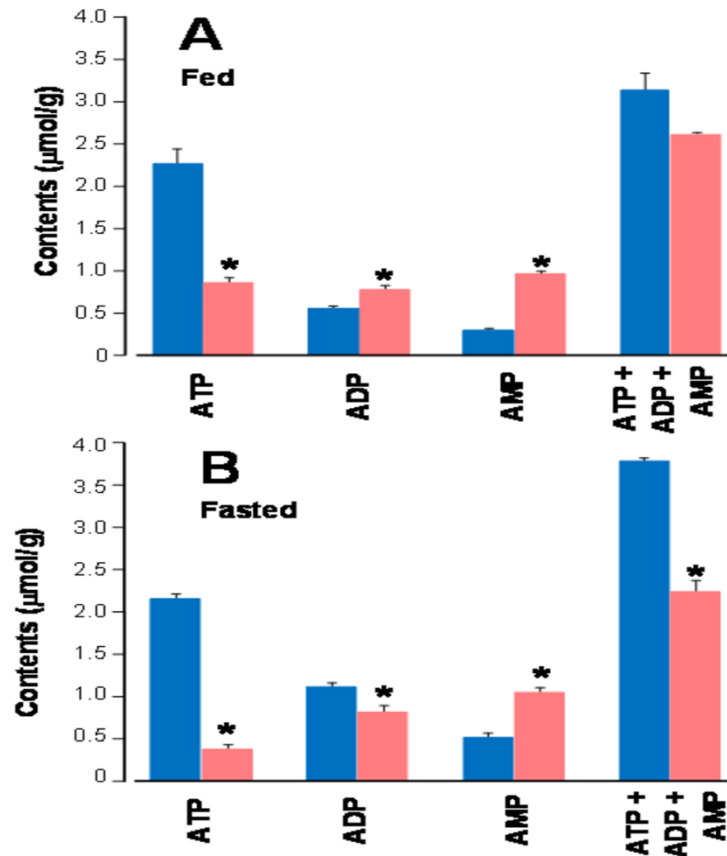


Figure 10. **Influence of dinoseb on the hepatic contents of adenine mononucleotides in the fed and fasted state.** Livers were perfused in an open system as described in the materials and methods section. Livers from fed rats were pre-perfused with Krebs/Henseleit-bicarbonate buffer for 10 min and, after that, dinoseb (15 μM) was infused for 20 min. For the experiments with livers from fasted rats, L-lactate (2 mM) was infused at 10 min and dinoseb (10 μM) was infused 26 min after L-lactate infusion for 20 min. The livers were freeze-clamped in liquid nitrogen and the adenine nucleotides were extracted with cold perchloric acid. Control determinations were done with livers that were freeze-clamped at the same perfusion time in the absence of substrate (fed condition) or in the presence of L-lactate but without dinoseb infusion. Values are means \pm SEM. Asterisks indicate statistical significance in comparison with the corresponding controls.

SUPPLEMENTARY MATERIAL

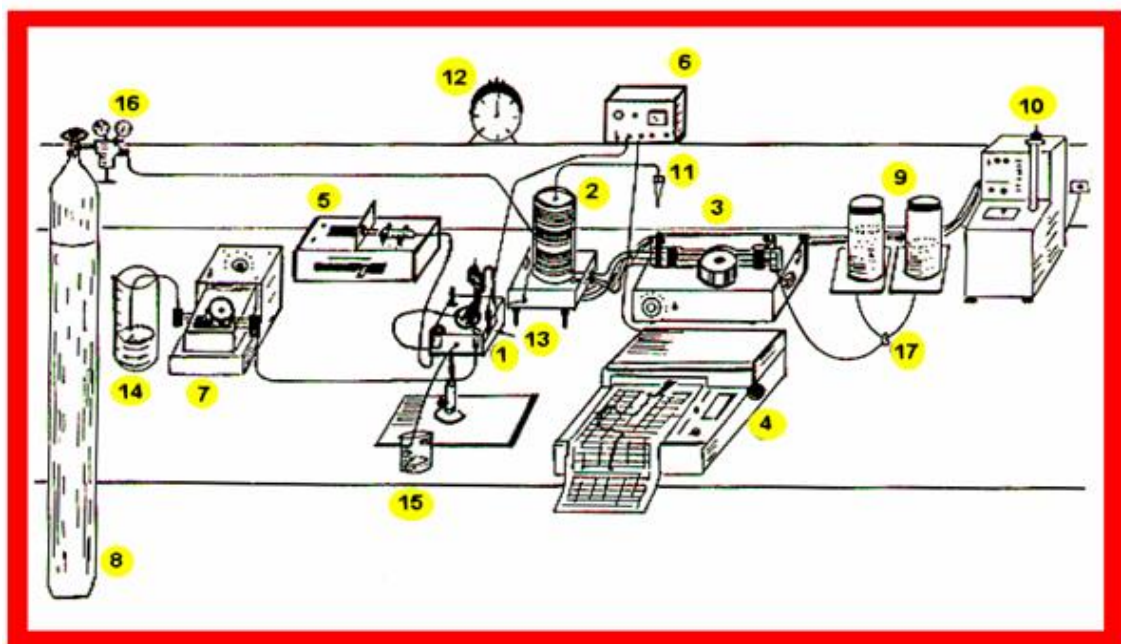


Figure S1. Schematic representation of the perfusion apparatus. Legends: (1) liver chamber showing the position of the liver under perfusion; (2) membrane oxygenator with simultaneous heating and gas exchange; (3) peristaltic pump for the inflowing perfusion liquid; (4) potentiometric recorder; (5) infusion pump connected to the liver chamber; (6) polarograph connected to the recorder; (7) peristaltic pump for removing the effluent perfusate; (8) carbogenic mixture reservoir; (9) perfusion fluid reservoirs; (10) thermostated bath with recirculation pump for heating the oxygenator; (11) gas flow detector; (12) chronometer; (13) combined platinum and silver electrodes ("oxygen electrode") connected to the polarograph; (14) reservoir for the outflowing perfusate (to be discarded) (15) para-flow and bilis collection; (16) gas flow regulator; (17) switch for changing the perfusion fluid reservoir.

Actions of two organo-chlorinated herbicides, 2,4-dichlorophenoxyacetic acid and picloram, on liver metabolism

Gabriela Bueno Franco Salla, Lívia Bracht, Angela Valderrama Parizotto, Rosane Marina Peralta, Fabrício Bracht and Adelar Bracht

Department of Biochemistry, University of Maringá, 87020900 Maringá, Brazil

Corresponding author:

Adelar Bracht

Department of Biochemistry

University of Maringá

5790 Avenida Colombo

87020900 Maringá, Brazil

Email: adebracht@uol.com.br; abracht@uem.br

Abstract

Tordon[®] is the commercial name of a mixture of two organo-chlorinated herbicides, 2,4-D and picloram. Both compounds affect energy transduction in isolated mitochondria, especially 2,4-D, which acts as an uncoupler. These effects were characterized in isolated mitochondria, but there have been only limited efforts in characterizing the consequences for the cellular metabolism. For this reason, the present study aimed at characterizing the actions of these two compounds on liver biochemistry and their cellular distribution using mainly the isolated perfused rat liver. 2,4-D increased glycolysis in the range from 10 to 400 μM . Picloram did not increase glycolysis in the range up to 1 mM. The lactate to pyruvate ratio, indicative of the redox potential of the cytosolic NAD^+ -NADH couple was also increased by 2,4-D. Both compounds inhibited lactate gluconeogenesis. Inhibitions by 2,4-D and picloram were incomplete, reaching maximally 46% and 23%, respectively. No synergism between 2,4-D and picloram was detected with reference to gluconeogenesis inhibition. Both compounds diminished the cellular ATP levels. Biotransformations of 2,4-D and picloram were slow, but their distribution was flow-limited, i.e., occurred at high rates. For extracellular concentrations of 10 μM , the equilibrium cellular concentrations of 2,4-D and picloram were 94.62 and 27.79 μM , respectively, when expressed in terms of the physical aqueous space. Molecular dynamics simulations revealed that 2,4-D presented a very low affinity for the hydrophobic lipid bilayers. The membrane/aqueous phase partition coefficients were 6.27×10^{-14} and 1.25×10^{-9} for the anionic and protonated forms, respectively. This suggests that the relatively high cellular concentration of 2,4-D does not reflect binding to lipids but rather to other structures such as proteins, for example. It can be concluded that inhibition of energy metabolism is possibly a relevant component of the toxicity of 2,4-D and of the commercial product Tordon[®] that contains the compound in addition to picloram.

Key-words: organo-chlorinated herbicides; hepatic metabolism; 2,4-D; picloram.

Introduction

Tordon[®] is the commercial name given to a mixture of two herbicides, 4-amino-3,5,6-trichloro-2-pyridinecarboxylic acid and 2,4-dichlorophenoxyacetic acid. The former is widely known as picloram and the latter is currently called 2,4-D (see chemical structures in Figure 1). The formulation is recommended and amply used as a postemergent herbicide for the control of a variety of annual and deep-rooted perennial broadleaf weeds. Several combinations are used, but the molar ratio of 4 parts of 2,4-D and 1 part of picloram seems to be the most frequent formulation (Pereira et al., 1994).

As most pesticides in general, both compounds are toxic to mammals and humans when ingested at high doses. The acute toxicity of phenoxyacetic acid derivatives varies substantially from species to species and, in fact, LD₅₀ doses between 100 and 1200 mg/kg have been reported (Hartig, 1992; Bukowska, 2006). Due to the widespread use of 2,4-D and other phenoxyacetic acid derivatives, exposure of humans and animals is relatively high in rural areas. Several deleterious actions are well documented for 2,4-D and the list includes teratogenic, neurotoxic, immuno-suppressive, cytotoxic and hepatotoxic effects (Garabrant and Philbert, 2002; Bukowska, 2006; Oghabian et al., 2014; Qurratu and Reehan, 2016). It is generally accepted that picloram is less toxic than 2,4-D. The acute oral LD₅₀ in rats is approximately 8200 mg/kg (Ben-Dyke et al., 1970). However, salts of picloram seem to be more toxic as for the potassium salt (which is water soluble) LD₅₀ values of 954 and 686 mg/kg were reported for male and female rats, respectively (Hayes et al., 1986). The liver seems to be the primary target of picloram toxicity. Hypertrophy of centrilobular hepatocytes has been found, for example, in addition to increased infiltration of mononuclear infiltrates (Hayes et al., 1986).

Liver toxicity has been investigated in both cellular and subcellular systems. For the latter there are several studies using isolated mitochondria. An early study with isolated rat liver mitochondria proposed an uncoupling action for 2,4-D and other related herbicides (Zychlinski and Zolnierowicz, 1990). In a more detailed study with rat liver mitochondria Palmeira et al. (1994a) demonstrated that 2,4-D does not act solely as an uncoupler but also that it depresses coupled respiration, decreases the mitochondrial membrane potential

and inhibits succinate dehydrogenase and the cytochrome c reductase complex. These effects were observed in the range between 0.1 and 1 mM. A subsequent attempt was made by Palmeira et al. (1994b) at verifying if the consequences of these effects on the energy status of isolated hepatocytes are significant. It was found that 2,4-D in fact decreases the ATP levels of isolated hepatocytes, but only at concentrations above 1 mM. The action of picloram on isolated liver mitochondria was investigated using the commercial preparation Tordon[®] (Pereira et al., 1994). In this work approximately the same effects found by Palmeira et al. (1994a) for pure 2,4-D were described, but it is difficult to evaluate precisely the role of picloram because Pereira et al. (1994) expressed concentration in terms of nmol per mg protein in their incubations and it is not always clear what was the protein concentration in each incubation. A gross evaluation, however, suggests that the effects of Tordon[®] on rat liver mitochondria might have some contribution of both compounds, picloram and 2,4-D. This conclusion is corroborated by observations in plant mitochondria. It has been shown, for example, that picloram inhibits oxidation of succinate and α -ketoglutarate in cucumber mitochondria (Foy et al., 1965), and inhibits ATP induced swelling and stimulates ATPase in barley and safflower mitochondria (Chang and Foy, 1971).

All these studies have been done decades ago and, surprisingly, they have been only occasionally complemented by studies using intact cell systems. An exception is the histochemical study of Heene (1966) suggesting that 2,4-D might be acting as an inhibitor of muscle glycogen phosphorylase. There are also studies indicating that 2,4-D might affect energy metabolism in the muscle of rats (Kuhn and Stein, 1964). In these studies, metabolic fluxes were not measured. Systematic studies on how 2,4-D affects hepatic metabolic fluxes and how it interacts with the liver membranes have not yet been done. For this reason we decided to undertake a systematic study using the isolated perfused rat liver for investigating the possible actions of 2,4-D on energy metabolism and energy metabolism-dependent parameters. Parallel experiments were also done with picloram, as the latter compound is frequently used in association with 2,4-D in the herbicide formulation Tordon[®].

Materials and methods

Materials

The liver perfusion apparatus was built in the workshops of the University of Maringá. Picloram and 2,4-dichloropheoxyacetic acid (2,4-D) were purchased from Sigma Chemical Co. (St Louis, USA). Tritiated water ($[^3\text{H}]\text{H}_2\text{O}$) was purchased from Amersham Pharmacia Biotech. All enzymes and coenzymes used in the enzymatic assays were purchased from Sigma Chemical Co. (St Louis, USA). All standard chemicals were from the best available grade (98-99.8 % purity).

Animals

Male Wistar rats, weighing 240–260 g, were used in the experiments. The animals were housed in individual cages, maintained on a regulated light–dark cycle and fed *ad libitum* with a standard laboratory diet (Nuvilab[®], Colombo, Brazil). The rats were starved for 18 h prior to the experiments, when required. Sodium thiopental anesthesia was applied before preparation of the liver for perfusion. The anesthetic was injected intraperitoneally (50 mg/kg). The criterion of anesthesia was the absence of body or limb movement in response to a standardized tail clamping stimulus. Experiments were done in accordance with the worldwide accepted ethical guidelines for animal experimentation and were previously approved by the Ethics Committee of Animal Experimentation of the University of Maringá (protocol number 8172271015).

Liver perfusion

Hemoglobin-free, non-recirculating perfusion was done (Scholz and Bücher, 1965; Kelmer-Bracht et al., 1984). After cannulation of the portal and cava veins the liver was installed in a plexiglass chamber. Constant flow perfusion was done with a peristaltic pump (Minipuls 3, Gilson, France). The flow rate was adjusted between 30 and 32 mL/min, according to the liver weight (Scholz and Bücher, 1965; Kelmer-Bracht et al., 1984). The perfusion fluid was Krebs/Henseleit-bicarbonate buffer (pH 7.4) containing 25 mg/100 mL bovine-serum albumin, saturated with a mixture of oxygen and carbon dioxide (95:5) by means of a membrane oxygenator with simultaneous temperature adjustment (37 °C). The composition of the Krebs/Henseleit-bicarbonate buffer is the

following: 116 mM NaCl, 25 mM NaHCO₃, 5.9 mM KCl, 1.2 mM Na₂SO₄, 1.18 mM MgCl₂, 1.24 mM NaH₂PO₄ and 2.5 mM CaCl₂. The perfusion fluid enters the liver via a cannula inserted into the portal vein and leaves the organ via a cannula inserted into the cava vein. Samples of the effluent perfusion fluid were collected and analyzed for their metabolite contents. Substrates and picloram or 2,4-D were added to the perfusion fluid according to the experimental protocols and at the desired concentrations.

Metabolite assays

Samples of the effluent perfusion fluid were collected according to the experimental protocol and analyzed for their metabolite contents. The following compounds were assayed by means of standard enzymatic procedures: glucose, lactate and pyruvate (Bergmeyer, 1974). The oxygen concentration in the outflowing perfusate was monitored continuously, employing a teflon-shielded platinum electrode adequately positioned in a plexiglass chamber at the exit of the perfusate (Kelmer-Bracht et al., 1984). Metabolic rates were calculated from input-output differences and the total flow rates and were referred to the wet weight of the liver.

The hepatic contents of the adenine nucleotides were measured by HPLC after freeze-clamping the perfused liver with liquid nitrogen (Mito et al., 2014). Two gram of the freeze-clamped liver were macerated in liquid nitrogen until homogeneity. To the powdered liver 6 mL of 0.6 M perchloric acid was added and the suspension was homogenized in a van Potter-Elvehjem homogenizer. The resulting homogenate was centrifuged at 4000g for 10 minutes and the resulting homogenate neutralized with fixed volumes of potassium carbonate (0.5 M). The precipitated potassium perchlorate was eliminated by filtration and the filtrate used for the adenine nucleotides determinations. The HPLC system (Shimadzu, Japan) consisted of a system controller (SCL-10AVP), two pumps (model LC10ADVP), a column oven (model CTO-10AVP) and an UV-Vis detector (model SPD-10AV). A reversed-phase C18 CLC-ODS column (5 µm, 250 × 4.6 mm i.d., Shimadzu) protected with a CLC-ODS precolumn (5 µm, 4 × 3 mm i.d., Phenomenex) was used with a gradient from reversed-phase 0.044 mol/L phosphate buffer solution, pH 6.0, to 0.044 mol/L phosphate buffer solution plus methanol (1:1), pH 7.0. In percent methanol, the gradient was the following: at 0 min, 0%; at 2.5 min, 0.5%; at 5 min, 3%; at 7 min, 5%; at 8 min, 12%; at 10

min, 15%; at 12 min, 20%; at 20 min, 30%. The temperature was kept at 35 °C, and the injection volume was 20 µL with a flow rate of 0.8 mL/min. Monitoring was performed spectrophotometrically at 254 nm. Identification of the peaks of the investigated compounds was carried out by a comparison of their retention times with those obtained by injecting standards under the same conditions. The concentrations of the compounds were calculated by means of the regression parameters obtained from the calibration curves. The calibration curves were constructed by separating chromatographically standard solutions of the compounds. Linear relationships were obtained between the concentrations and the areas under the elution curves.

Picloram, 2,4-D and ³H assays

The quantification of picloram and 2,4-D in the perfusate was done by HPLC. The same apparatus and column systems described in the preceding subsection was used.

For picloram the mobile phase was 80% acetonitrile and 20% water. Monitoring was done spectrophotometrically at 228 nm, with a flow rate of 0.5 mL/min at a temperature of 35 °C. For 2,4-D the mobile phase was 58% methanol, 40% water and 2% acetic acid. The wavelength for the spectrophotometric detection was 280 nm, the flow rate 0.6 mL/min and the temperature 35 °C. Identification of the picloram and 2,4-D peaks was done by comparison of their retention times with those observed by injecting the corresponding standards under identical conditions. The concentrations were calculated by means of the regression parameters obtained from a calibration curve.

Quantification of ³H present in the perfusate samples as [³H]H₂O was done by liquid scintillation counting (TriCarb 2810 TR International model from Perkin Elmer Health science). A commercial scintillation liquid formed by an aqueous biodegradable emulsion (BCS®, Biodegradable Counting scintillant, Amersham) was used.

Calculation of the potential of mean force (PMF) across the lipid bilayer

The 2,4-D⁻ (anionic) and 2,4-DH (protonated) molecules were build using the Avogadro software in two different protonation states (Hanwell et al., 2012) and the antechamber tools within the Amber16 (Case et al., 2016) molecular

simulation package were used to generate the input parameter files for the molecular dynamics simulations. For both protonation states, the atom types followed the general Amber force field (GAFF) conventions (Wang et al., 2004). The charges for 2,4-D⁻ and 2,4-DH were generated using the RESP ESP charge Derive Server (REDS) using the RESP-A1 method (Vanquelef et al., 2011). The original charges generated by the antechamber tool were then substituted and the force field parameters obtained from GAFF were used to build the membrane/2,4-D system. Since the same system construction procedure was used for both the anionic and protonated form, the following section is valid for both protonation states.

For the lipid bilayer construction the choice was the 1-palmitoyl-2-oleoyl-sn-glycero-3-phosphocholine (POPC) model. This choice was based on the general popularity of this model in the literature and the proximity of its dynamical behavior to experiment data for a range of properties (Dickson et al., 2014). The hydrated bilayer structure was obtained from the CHARMM-GUI server from the membrane builder tool (Jo et al., 2008). The 2,4-D⁻/H was manually inserted in the water solvated lipid box in substitution to 5 water molecules. The water-solvated lipid box was then minimized using a mixed scheme with steepest-descent and conjugate gradient with 5000 steps of each (Vanquelef et al., 2011). The system was then heated for 150 ps using the Langevin thermostat (Grest and Kremer, 1986) with a collision frequency of 1 ps⁻¹ at constant volume. The time step used was 2 fs with a cutoff for non-bonded interactions of 10 Å. The temperature was gradually increased to its final value of 310.15 K. During the heating process, all lipid molecules were held fixed with an harmonic force constant of 10 kcal/mol · Å². During the last 100 ps, the system was simulated with anisotropic Berendsen weak coupling barostat with a pressure relaxation time of 2 ps (Berendsen et al., 1984). To equilibrate the dimensions of the periodic boundary conditions, another 5000 ps were simulated using the same parameters as the last step but without the position restraints. At last, a long production run of 250 ns was run to equilibrate the lipid bilayer and the 2,4-D⁻/H molecule.

For calculating the potential of mean force (PMF) for crossing the membrane with the 2,4-D⁻/H molecules, the umbrella sampling method was used, followed by a weighted histogram analysis of the resulting distance distributions (Kumar et al., 1992). The reaction path for the PMF was chosen as

the distance between the centers of mass (COM) between the 2,4-D and the lipid bilayer. The COM of the lipid bilayer was defined as the COM of the nitrogen atoms of each choline group. The starting position for each of the umbrella sampling simulations was set starting at -31 Å from the COM of the lipid bilayer and then, for each subsequent window, incremented in 0.42 Å steps, giving a total of 150 simulation windows and 62 Å of total mean path, which corresponded to the path between one side of the periodic box to the other, perpendicular to the plane formed by the lipid bilayer surface.

The 2,4-D⁻/H molecules were restrained in each window to their corresponding distance value by an harmonic potential with a force constant of 5 kcal/mol · Å. The restraint was applied to the 2,4-D's COM only in the Z Cartesian coordinate. Each window was pre-equilibrated with a 50 ns simulation using the same parameters used in the equilibration step. Each equilibrated window was then simulated for 10 ns, giving a total of 1.5 μs. The distribution histograms for the distances obtained in each window were checked for overlap and then submitted to the Weighted Histogram Analysis Method (WHAM) procedure (Kumar et al., 1992), giving the resulting PMF values. Convergence was checked using different sample sizes and auto correlation times from the resulting distance files as inputs for the WHAM procedure.

Analysis of the liver response to step inputs of picloram and 2,4-D

The liver responses to step inputs of picloram and 2,4-D (constant infusion) were analyzed using the model of space-distributed and variable transit times adapted to the isolated perfused rat liver (Goresky et al., 1970; Bracht et al., 1980). This model describes the exchange of substances between the extracellular space and cell and the possible metabolic transformation in the liver. For a substance whose distribution into the cellular space is flow-limited and which undergoes irreversible metabolic transformation in the cellular environment the following equation applies (Kelmer-Bracht et al., 1993):

$$S(t) = \int_0^t \left[\frac{1}{1 + \Phi} \right] \cdot S'_{\text{water}} \left(\frac{(t - t_0)}{(1 + \Phi)} + t_0 \right) \cdot e^{-k_{\text{met}}(t - t_0)} dt \quad (1)$$

In Eq. (1), $S(t)$ is the experimental outflowing picloram or 2,4-D curves resulting from a constant infusion into the portal vein, t is the infusion time, $(1 + \Phi)$ is the ratio of the apparent distribution space of the infused substance to the distribution space of labeled water, k_{met} the coefficient for metabolic

transformation and t_0 the uniform transit time in the large vessels. From the definition of $(1+\Phi)$ it can be deduced that Φ represents the ratio of extra apparent space occupied by the substance to the water space; $\Phi = 0$ if the distribution space of the substance coincides with the aqueous distribution space. The term $S'_{\text{water}} \left(\frac{(t - t_0)}{(1 + \Phi)} + t_0 \right)$ is the first derivative of the liver response to a step input (constant infusion) of [^3H]water at time $[(t - t_0)/(1 + \Phi) + t_0]$.

The intracellular concentrations of picloram and 2,4-D (C_i) were calculated according to a previously derived formula (Kelmer-Bracht et al., 1993):

$$C_i = (1 + \Phi + \Phi/\theta)C_e \quad (2)$$

In equation (2) C_e is the extracellular concentration and θ the ratio of the intra- to the extracellular water space.

Eq. (1) was fitted to the experimental curves of picloram and 2,4-D using an iterative, nonlinear least-squares procedure (Björck and Dahlquist, 1972). The calculations were done using a specially designed structured computer program written in the Turbo-Basic language. Preliminary estimates of the parameters were introduced before initiating the iterative procedures. Numerical interpolation between the experimental points was accomplished by means of spline functions (Björck and Dahlquist, 1972). Romberg's algorithm was used for the numerical integration (Björck and Dahlquist, 1972).

Statistical analysis

The error parameters presented in the graphs are standard errors of the mean. Statistical analysis was done by means of the GraphPadPrism software (version 5.0). Variance analysis was done with post-hoc testing according to Student-Newman-Keuls ($p \leq 0.05$).

Results

Glycogen catabolism and oxygen uptake in the perfused liver

As a first approach experiments were planned in order to test possible effects of 2,4-D and picloram on glycogen catabolism, glycolysis and oxygen uptake. Livers from fed rats when perfused with substrate-free medium survive at the expense of glycogen degradation via glycolysis and oxidation of endogenous fatty acids (Scholz and Bücher, 1965; Kelmer-Bracht et al., 1984). Under these conditions the livers release glucose, lactate and pyruvate as a result of glycogen catabolism. Figure 2A illustrates the time course of the effects of 200 μM 2,4-D which was introduced at 10 minutes perfusion time. The introduction of 2,4-D was followed by progressive increases in lactate production and oxygen uptake. Oxygen uptake reached a maximum at 22 minutes perfusion time (12 min 2,4-D infusion). After this maximum it tended to decline, but there was still stimulation at 40 minutes when the infusion of 2,4-D was stopped. Lactate production raised progressively and reached more or less stable values during the period of 25 to 40 minutes perfusion time. Cessation of the 2,4-D infusion was followed by a decline in both oxygen uptake and lactate production, meaning a relatively fast reversion of the effects. Pyruvate production declined upon 2,4-D infusion without returning to its original level after infusion cessation. The effect of 2,4-D on glucose output was poorly defined, with a decreasing tendency during the infusion with an apparent recovery before its cessation. The stimulating effects of 2,4-D on oxygen uptake and lactate production also occurred at other concentrations in the range between 10 to 400 μM , though the intensities were different. This is illustrated by Figure 2B which shows the concentration dependences of the effects of 2,4-D. The increases of lactate production and oxygen uptake present clear concentration dependences. For both parameters maximal stimulation was found at the concentration of 200 μM . The stimulations at the concentration of 10 μM were small, but statistically significant. Pyruvate production tended to increase at concentrations up to 100 μM but statistical significance was lacking. The parameter was inhibited at the concentration of 200 μM , as already shown in Figure 2A, with a recovery at the concentration of 400 μM . These modifications of the lactate and pyruvate productions also resulted in increases in the lactate to pyruvate ratio, which reflects the cytosolic NADH to NAD⁺ to ratio (Sies, 1982). In this case the

calculations revealed a sharp peak at the concentration of 200 μM . For glucose output, the fluctuations during the 2,4-D infusion, similar to those shown in Figure 2A, did not allow to establish any reasonable effect versus concentration relationship.

Experiments similar to those described above for 2,4-D were done with picloram. The results of the experiments, that were done with the concentration of 200 μM , are shown in Figure 3. Although some minor fluctuations are apparent, the conclusion is that picloram did not significantly affect any of the parameters related to glycogen catabolism that were measured. The same is valid for oxygen uptake.

Lactate gluconeogenesis and related parameters

Gluconeogenesis from lactate in the liver is usually regarded as a sensitive indicator for the energy status of the cell because it is strictly dependent on an efficient energy transduction in the mitochondria. If 2,4-D and picloram affect energy metabolism in the hepatocytes they should equally inhibit lactate gluconeogenesis (Moreira et al., 2013; Salla et al., 2017). The results of the experiments in which the possible effects of 2,4-D were investigated are summarized in Figure 4. Panel A shows the time course of the actions of 200 μM 2,4-D on glucose production, pyruvate production and oxygen uptake in the presence of 2 mM lactate. Lactate infusion, started at 10 min perfusion time, produced the usual increases in all monitored parameters (Moreira et al., 2013; Salla et al., 2017). The introduction of 200 μM 2,4-D caused a progressive diminution in glucose production. The decrease seemed to have almost stabilized after 30 minutes of 2,4-D infusion. Upon cessation of the infusion glucose production was progressively restored to values close to the basal ones. The infusion of 2,4-D also tended to decrease pyruvate production and to increase oxygen uptake, but with considerable fluctuations from experiment to experiment, as indicated by the pronounced standard errors. The experiments with 200 μM 2,4-D were repeated with other concentrations in the range between 20 and 400 μM . The results are shown in Figure 4B, in which the final values after 30 min 2,4-D infusion were represented against the concentration. Figure 4B shows that inhibition of gluconeogenesis was already significant at the concentration of 20 μM . It increased when the 2,4-D concentration was increased, but was already maximal at the concentration of 200 μM (46%). The

other parameters, oxygen uptake and pyruvate production, showed only fluctuations that were not significant at the 5% level.

The effects of picloram on lactate gluconeogenesis were measured using the same protocol as for 2,4-D. Figure 5 shows the results. Panel A shows the time course of the effects of 100 μM . Picloram inhibited glucose production to a small extent, an effect that was reversible, though the reversion took a considerable time. Picloram also tended to decrease pyruvate production. The reversion was unusual in that at the end of the perfusion experiment pyruvate production had reached levels well above those observed just after starting picloram infusion. Finally, picloram also tended to decrease oxygen uptake, with considerable fluctuations from experiment to experiment. These effects of picloram were explored further in the concentration range from 50 to 1000 μM and the results are shown in panel B of Figure 5. Gluconeogenesis inhibition did not increase in the range between 100 and 1000 μM (approximately 23%). Inhibition of pyruvate production was also significant in statistical terms, but did not increase with picloram concentrations above 200 μM . Finally, oxygen uptake presented small fluctuations, without statistical significance.

As already mentioned in the Introduction, the commercial formulation Tordon[®] is a mixture containing 4 parts of 2,4-D and 1 part of picloram. A synergistic action of both compounds as been frequently suggested, though never confirmed (Oakes and Pollak, 1999). A test of this hypothesis with reference to gluconeogenesis inhibition was done in the present work and the results are shown in Figure 6. The effects of the combination 200 μM 2,4-D plus 50 μM picloram were similar to those found when 2,4-D was infused alone (Figure 2A). Inhibition of glucose production was equal to 36.5%, actually less than what was found with 200 μM 2,4-D alone, which inhibited by 46%. This observation rules out any synergistic effects of 2,4-D and picloram with respect to the inhibition of gluconeogenesis although it may be reflecting another kind of concerted interaction.

Cellular adenine mononucleotide levels

If the diminution of gluconeogenesis and the increase in lactate production are at least in part consequences of actions on mitochondrial energy metabolism, the cellular levels of ATP should be decreased by 2,4-D or picloram (Saling et al., 2011; Salla et al., 2017). This hypothesis was tested and the levels of AMP, ADP

and ATP were measured after freeze-clamping perfused livers with liquid nitrogen. The results are shown in Figure 7. The conditions of these measurements correspond to those of the experiments shown in Figures 4A and 5A, i.e., the livers were under gluconeogenic conditions. Figure 7A shows that 200 μM 2,4-D diminished the ATP content by 41%. The levels of AMP and ADP were also decreased, but to a lesser extent, so that the ATP/ADP ratio was also decreased. However, there was also a diminution in the total content of the adenine mononucleotides.

Picloram also decreased the ATP content, to lesser extent than 2,4-D, more precisely by 31%. Differently to 2,4-D, however picloram did not decrease the ATP/ADP ratio, which generally exerts a regulatory role. Picloram, however, also decreased the total content of the adenine mononucleotides.

Outflow profiles of 2,4-D and picloram

The distribution spaces of 2,4-D and picloram were investigated by analyzing the liver responses to step inputs (constant infusions) of these substances, followed by a mathematical analysis of the outflow profiles. Picloram and 2,4-D were infused in separate experiments for up to 30 minutes at the concentration of 10 μM and the effluent perfusate was sampled at intervals of 15 sec to 5 min. The concentration of 10 μM was chosen for facilitating comparison with previous similar experiments that were done with the herbicide dinoseb (Salla et al., 2017). Both picloram and 2,4-D were assayed by HPLC, as described in the experimental section. The results are shown in Figure 8 in which the outflowing fractions (outflowing/portal concentrations) of both compounds were represented against the time after the onset of the infusion. Figure 8 also shows the corresponding outflow profile of [^3H]water and dinoseb. The latter was included for comparative purposes and reproduced from a previous report (Salla et al., 2017). Tritiated water, which undergoes flow-limited distribution into the whole aqueous space of the liver (Bracht et al., 1980), provides the indispensable reference curve. Tritiated water appeared rapidly after starting infusion with only a few seconds delay and the venous/portal ratio tended rapidly to unity. In respect to the [^3H]water curve, the 2,4-D and picloram curves were delayed, the former considerably more than the latter. With time, however, both curves tended to unity. This reflects the fact that the single pass transformation of both compounds is minimal under steady-state conditions, a conclusion that is

consistent with the low rates of metabolic transformation reported for these two compounds (Khana and Yang, 1966). The delay of the 2,4-D and picloram curves was much less pronounced than that of the dinoseb curve, a fact that reflects differences in the apparent distribution spaces (Bracht et al., 1980; Eler et al., 2013). However, the position of the 2,4-D and picloram curves, totally shifted to the right of the [³H]water curve, also indicates that both molecules distribute into their corresponding spaces at very high rates (flow-limited distribution) (Goresky et al., 1970; Bracht et al., 1980; Kelmer-Bracht et al., 1993). In such cases Eq. (1) can be used to determine the relative distribution space (Φ) and the metabolic transformation coefficient (k_{met}). For this purpose, Eq. (1) was fitted to the experimental 2,4-D and picloram curves by means of a least-squares procedure, using the liver response to the [³H]water step input as the reference curve. As both curves tend to unity, k_{met} is too small for being determined from the single pass outflow profiles. For this reason k_{met} was put equal to zero during the fitting procedures that allowed to determine Φ . Fitting converged rapidly and the mean optimized values of Φ are listed in Table 1. Remembering that $1 + \Phi$ is the ratio of the apparent distribution space of the infused substance to the distribution space of labeled water (see Materials and Methods section), the values of 2,4-D and picloram indicate that their apparent distribution spaces exceed that of the cellular water space by factors of 6.34 and 2.69, respectively. These apparent distribution spaces are, notwithstanding, much smaller than the distribution space of dinoseb (Salla et al., 2017), as shown in Table 1. The optimized Φ value allows to calculate the cellular content (C_i) under equilibrium conditions (when the normalized outflow curve approaches unity) by means of Eq. (2) that was derived on the assumption of a very fast permeation of the cell membrane (Kelmer-Bracht et al., 1993). The values in Table 1 were calculated assuming θ (intra- to the extracellular water space) equal to 1.71 (Eler et al., 2013) and are valid for the extracellular concentration (C_e) employed in the experiments, i.e., 10 μM . The value of θ was determined using labeled sucrose as the extracellular reference. The C_i values calculated according to Eq. (2) represent, thus, the intracellular contents referred to the hepatic aqueous space to which sucrose has no access. It does not imply that the compound is present solely in the aqueous phase. The cellular contents of 2,4-D and picloram are substantially higher compared to the extracellular ones, but much smaller than those of dinoseb for the same extracellular concentration.

Interactions of 2,4-D with membranes

Both picloram and 2,4-D present distribution spaces in excess to the aqueous space, a phenomenon that frequently denotes binding to cellular structures such as membranes or macromolecules. Interactions of a given substance with a typical membrane can be analyzed by means of molecular dynamics simulations, which allow to predict the energy profile of the trajectory of a molecule traversing a typical membrane from one side to the other. This kind of analysis was done for 2,4-D, which is more active on energy metabolism. Figure 9 illustrates the results of the simulations that were done with the protonated and anionic forms of 2,4-D. In this graph the energy levels (potential mean force, PMF) for the 2,4-D molecules moving across a typical cell membrane were represented. The energy in the aqueous environment was taken as the zero level. In the background, the structure of the lipid bilayer was drawn in addition to the water molecules at both sides. A 2,4-D molecule at the center of the bilayer, moving from left to right, is represented. It can be seen that when 2,4-D moves within the membrane the latter invaginates slightly towards the carboxylic group. This deformation is accompanied by the penetration of water molecules, amidst the hydrocarbon chains and the bent lipid headgroups, around the solute. Besides this, the interaction of 2,4-D with the polar groups of the membrane is strong enough for deforming the membrane to a considerable degree. It can be seen that there are phosphatidylcholine groups extending themselves almost to the center of the membrane.

The resulting PMF changes for the anionic and protonated forms present curves with the minima located in the bulk water and the maxima at the bilayer center. The highest energy levels for the mean path are clearly located within the hydrophobic region of the lipid bilayer. For the purposes of the present work it is more useful to convert the potential mean force difference (PMF) in Figure 9 into the equilibrium distribution between two phases, which can be regarded as an equilibrium constant (K_{eq}). This can be done by means of the well known formula

$$K_{eq} = e^{-PMF/RT} \quad [3]$$

in which T and R represent the absolute temperature and the universal gas constant ($1.98 \text{ cal Kelvin}^{-1} \text{ mol}^{-1}$), respectively. The negative sign in the exponential in combination with the positive PMF values result in the membrane/aqueous phase partition coefficient (K_{eq}) for a given form. At 37 °C the K_{eq} values for the partition between the polar groups of the membrane at 20

Å from the mass center and the aqueous environment are both equal to 0.99. This means a roughly similar solubility in the aqueous environment and in the polar region of the membrane. Dislocation to the membrane interior leads to progressive and finally drastic changes in the K_{eq} values. At 10 Å from the mass center, for example, the equilibrium distributions between the lipid phase of the membrane and the aqueous environment are 1.29×10^{-3} and 6.55×10^{-5} for the protonated and anionic forms, respectively. And, finally, at the center of mass the K_{eq} are equal to 1.29×10^{-9} and 6.29×10^{-14} for the protonated and anionic forms, respectively. The overall meaning of these data is that the solubility in water or in the polar groups of both forms of 2,4-D greatly exceeds their solubility in the hydrophobic region.

Discussion

Effects on metabolism

The results obtained in this work reveal that both 2,4-D and picloram are active on energy metabolism in the intact liver. In principle the modifications caused by these compounds conform to those usually expected from inhibitors of energy metabolism at the mitochondrial level. At least the following effects can be classified as pertaining to the category of effects that are expected from inhibitors of energy metabolism: (a) inhibition of gluconeogenesis, (b) increase in lactate production (at least for 2,4-D) and (c) diminution of the ATP levels (Saling et al., 2011; Moreira et al., 2013; Salla et al., 2017; Simões et al., 2017). Furthermore, stimulation of oxygen uptake under glycogenolytic conditions by 2,4-D can be regarded as a sign of uncoupling (Salla et al., 2017) whereas inhibition of oxygen uptake by picloram under gluconeogenic conditions could be indicating inhibition of the electron flow in the respiratory chain (Simões et al., 2017). The absence of oxygen uptake stimulation by 2,4-D under gluconeogenic conditions can be regarded as reflecting the fact that oxygen uptake was already accelerated by the oxidation of lactate, which was used as the gluconeogenic precursor. Although all these results, especially when taken in combination, are expected for both compounds based on what is known about their actions on isolated mitochondria, there are several details that cannot be explained very easily and that deserve to be discussed here.

First of all it is necessary to mention that the present study was designed to examine the actions of the two herbicides as components of Tordon[®], with total exclusion of the possible effects of the proprietary surfactant or other components of the formulation. The latter has been shown not to be inactive on isolated mitochondria (Oakes and Pollak, 1999). Following this reasoning, data obtained in experiments in which mitochondria were exposed to the commercial formulation will not be considered in the discussion (Pereira et al., 1994). Concerning the experiments with the perfused liver it is noteworthy that all inhibitory effects of 2,4-D on gluconeogenesis and of picloram on gluconeogenesis and oxygen uptake were incomplete, i.e., after attaining a certain degree (more pronounced for 2,4-D in the case of gluconeogenesis) further increases in concentration did not produce any increases in the inhibition degrees. The most simple explanation would be that the effects on mitochondria are also

incomplete, so that the observations in intact cells merely reflect the actions on mitochondria. This might be partly true, as in fact several inhibitory effects of 2,4-D in isolated mitochondria seem to be incomplete, as described in the study of Palmeira et al. (1994). For example, inhibition of state 3 by 2,4-D reached 35% at the concentration of 400 μM whereas the inhibition of ADP depolarization was only 44.5% at the same concentration. The concentration of 400 μM was the highest one used in the present work. However, further increases of the 2,4-D concentrations in the experiments with isolated mitochondria to values up to 800 μM still resulted in additional inhibitory responses (Palmeira et al., 1994), whereas in the present study the perfused liver ceased to respond to increases above 200 μM in the case of 2,4-D. More surprising than the lack of response to concentrations above 200 μM is the response of the liver to low concentrations of 2,4-D. It should be recalled that lactate stimulation began at the concentration of 10 μM and gluconeogenesis inhibition was already significant at the concentration of 20 μM . The lowest concentration used by Palmeira et al. (1994) was 100 μM , and it is clear from their effect versus concentration relationships that effects at concentrations below the latter could hardly be detected. The same seems to be true for picloram, whose actions on plant mitochondria require concentrations as high as 1 mM (Foy et al., 1965; Chang and Foy, 1971). In the perfused liver, however, inhibition of gluconeogenesis began at the concentration of 50 μM . It should be stressed that, in general, the effects of respiratory inhibitors in intact cells occur at concentrations higher than those that are active in isolated mitochondria. Dinoseb is a good example, its effects in the liver occur at concentrations (2.5-10 μM) that are one order of magnitude above those active in isolated mitochondria (0.2-1 μM ; Salla et al., 2017). In the case of dinoseb the whole cellular environment in the perfused liver seems to work as a protective shield for the mitochondria. For 2,4-D and even picloram, the opposite seems to occur. An explanation for this phenomenon is difficult to devise. It could be related to the kind of molecules that bind 2,4-D and which are not present in preparations of isolated mitochondria, as will be discussed below. It should be further remarked that the experiments of the present work do not indicate any synergistic effect that enhances the action on mitochondria when both components, 2,4-D and picloram, are simultaneously present, confirming a previous proposition (Oakes and Pollak, 1999). If some kind of cooperative action of 2,4-D and picloram occurs, it would be much more in the direction of a

diminished inhibition of gluconeogenesis as, in fact, the simultaneous presence of both compounds resulted in a slight tendency toward a less pronounced inhibition.

Transformation and interactions with the hepatic tissue

The single pass extraction under steady-state conditions of both 2,4-D and picloram was minimal. The meaning of this finding is that the rates of transformation of both substances are low and that many passages through the liver are needed to attain a substantial degree of transformation. Under such circumstances, excretion may be faster than transformation as indeed revealed by studies in which excretion of these compounds was investigated. Experiments in sheep with [¹⁴C]2,4-D revealed that 95.8% of the radioactivity was excreted in the urine and 1.4 % in the faeces within 72 hours as unchanged 2,4-D (Clark et al., 1964). In analogous studies with rats, 75.5%–94.2%, depending on the dose, was excreted unchanged in the urine and faeces within 144 hours (Khana and Yang, 1966). Picloram is also rapidly absorbed in the gastrointestinal tract and excreted almost unchanged in urine and faeces of rats in 48 hours (Nolan et al., 1980). The urinary excretion was 80 to 84%, faecal of 15% and biliar less than 0.5% (Nolan et al., 1984). Similar results were obtained with human volunteers (Nolan et al., 1984).

Studies on the distribution of 2,4-D in the rat revealed the highest concentrations in tissues like liver, kidney, lungs and spleen. The lowest concentrations were found in the adipose tissue and central nervous system (Erne, 1966). These earlier observations can be reconciled with the findings of the present work. The lowest concentrations found in the adipose tissue and nervous system agree with our simulations of the interactions of 2,4-D with the membrane lipid bilayer. From these simulations it is clear that even the undissociated form of 2,4-D is less soluble in lipidic structures than in the aqueous phase. These conclusions agree well with the low concentrations found in tissues that are rich in lipids such as the adipose tissue. On the other hand, the high concentrations of 2,4-D found in the liver in this early study (Erne, 1966) are consistent with our finding of a relatively high cellular concentration in the perfused liver, greatly exceeding the concentration in the extracellular space when expressed in terms of the cellular water content. It is important to note that expressing the cellular concentration in terms of the water content does not

imply that the substance is solely restricted to the cellular aqueous phase, interactions with structural components being highly probable.

Binding to structural components can promote effective sequestration of a given compound, a phenomenon that leads to an apparent concentrative uptake. This phenomenon was indeed much more pronounced for dinoseb, as shown in a previous work (Salla et al., 2017), than for 2,4-D and picloram. Dinoseb, however, revealed to be much more soluble in the lipid bilayers, whereas exactly the opposite occurred with 2,4-D. As shown by our calculations, even the protonated (nonanionic) form of 2,4-D shows little affinity for the hydrophobic regions of a typical membrane. This is clearly revealed by the various partition coefficients, calculated using the computed PMF values. The PMF spike in the center of the membrane, which presents the least affinity for 2,4-D, was already described in the literature for other compounds, as for example aminoacids, especially for those possessing a polar side chain (e.g., histidine and aspartate; Johansson and Lindahl, 2009; Li et al., 2013). This spike has been interpreted as resulting from solute reorientation and solvation as the molecule gets farther from the proximal bilayer leaf and closer to the distal leaf. The deformation of the bilayer caused by 2,4-D implies that the desolvation of the charged species presents an energetic cost that exceeds that of the bilayer deformation and is, thus, influenced by the bilayer thickness and chemical composition (Li et al., 2013).

The low affinity of the lipid bilayer for 2,4-D raises two important questions: (a) how does the compound permeate the cell membrane, and (b), to what cellular components does the compound bind for justifying its high apparent distribution space that exceeds the water space by a factor of 6.36. With respect to the cell membrane permeation, it is true that a thermodynamic parameter such as the PMF does not, in principle at least, inform about rates of diffusion. However, since the absolute mass transfer rates depend on the local concentrations, it seems reasonable to conclude that passage of even the protonated form through the membrane will occur at rates that are not compatible with the development of the intracellular metabolic effects and, especially, are not compatible with the flow-limited distribution suggested by the experimental outflow profiles following a step input. Furthermore, although the energy level of the protonated form in the membrane is more favourable, it should be mentioned that the anionic form of 2,4-D largely predominates in the

aqueous environment, as the pK_a of its carboxyl has been reported to be equal to 2.6. This means, that at pH 7.4 the 2,4-D⁻/2,4-DH ratio is equal to 6.3×10^4 . Free diffusion even of the protonated form seems, thus, a not very likely mechanism for a rapid cell membrane permeation. It is true that solvation into the polar upper layer of the membrane can be fast and eventually contribute to the distribution space of 2,4-D, but this is probably a minor component. For these reasons it looks much likely that access of 2,4-D to the whole cellular space is facilitated by one or more transport systems. The liver cell membranes possess several carboxylic acid transport systems, including at least one that presents a wide specificity, so that mediated transport of 2,4-D can be regarded as a real possibility (Roelofsen et al. 1997; Geier et al., 2007). With respect to the second question raised above, the structures that bind 2,4-D for justifying its great intracellular concentration, the most likely ones are proteins, because these are the main macromolecular components that must be considered after the exclusion of the supramolecular structures represented by the several systems of lipid bilayers within the cell (mitochondria, endoplasmic reticulum, etc.). It is impossible to devise, however, if specific or general binding occurs. Or even, if binding of 2,4-D to protein-membrane interfaces represents an important factor. These are clearly open questions worth of being investigated in both experimental and computational terms.

Concluding remarks

In summary, it can be concluded that both compounds, 2,4-D and picloram, affect energy metabolism in the intact liver cells, the former being more active than the latter. Inhibition of energy metabolism is possibly a relevant component of the toxicity of 2,4-D and of the commercial product Tordon[®] that contains the compound in addition to picloram. In spite of having been intensely investigated in the past for their properties and pharmacologic/toxicologic effects, this is the first study in which data on the metabolic effects of 2,4-D and picloram in intact cell systems are displayed. Furthermore, the present work also suggests that much more can still be done in order to bring to light details about the interactions of both 2,4-D and picloram with the animal tissues in general. Although the hepatic cells are able to retain considerable amounts of 2,4-D, interactions with the lipophilic structures are energetically unfavourable. Interactions with other structures are likely to occur

and are a field still open to investigations not only with respect to 2,4-D and picloram, but also for other types of organo-chlorinated pesticides.

Funding

This work was funded by a grant from the Conselho Nacional de Desenvolvimento Científico e Tecnológico (CNPq; proc. n. 302615/2011-3). Gabriela Bueno Franco Salla was a scholarship recipient from the (CNPq). Adelar Bracht is a Senior Professor, financed by the Fundação Araucaria (UEM-Fundação Araucaria agreement n. 276/2015).

Conflict of interest

The authors state that they have no conflict of interest concerning the present article.

References

- Ben-Dyke, R., Sanderson, D.M., Noakes, D. N. 1970. Acute toxicity data for pesticides. *World Ver. Pest. Control* 9, 119-127.
- Berendsen, H.J.C., Postma, J.P.M., van Gunsteren, W.F., DiNola, A., Haak, J.R., 1984. Molecular dynamics with coupling to an external bath. *J. Chem. Phys.* 81, 3684. doi: 10.1063/1.448118
- Bergmeyer, H.U., 1974. *Methods of Enzymatic Analysis*. Verlag Chemie-Academic Press, Weinheim-London.
- Björck, A., Dahlquist, G., 1972. *Numerische Methoden*. Oldenburg Verlag, München.
- Bukowska, B. 2006. Toxicity of 2,4-dichlorophenoxyacetic acid – molecular mechanisms. *Polish J. Environ. Strud.* 15,365-374.
- Bracht, A., Schwab, A.J., Scholz, R., 1980. Studies of flow-rates in the isolated perfused rat liver by pulse labelling with radioactive substrates and mathematical analysis of the wash-out kinetics. *Hoppe Seyler's Z. Physiol. Chem.* 361, 357–377.
- Case, D.A., Betz, R.M., Botello-Smith, W., Cerutti, D.S., Cheatham, T.E., Darden, T.A., Duke, R.E., Giese, T.J., Gohlke, H., Goetz, A.W., Homeyer, N., Izadi, S., Janowski, P., Kaus, J., Kovalenko, A., Lee, T.S., LeGrand, S., Li, P., Lin, C., Luchko, T., Luo, R., Madej, B., Mermelstein, D., Merz, K.M., Monard, G., Nguyen, H., Nguyen, H.T., Omelyan, I., Onufriev, A., Roe, D.R., Roitberg, A., Sagui, C., Simmerling, C.L., Swails, J., Walker, R.C., Wang, J., Wolf, R.M., Wu, X., Xiao, L., York, D.M., Kollman, P.A., 2016. *AMBER 2016*. University of California, San Francisco.
- Chang, E. K., Foy, C. L., 1971. Effects of picloram on mitochondrial swelling and ATPase. *Weed Sci.* 19, 54-58.
- Clark, D. E., Young, J. E., Younger, R. L., Hunt, L. M., McLaran, J. K., 1964. Animal metabolism of herbicides, fate of 2,4-dichlorophenoxyacetic acid in sheep. *J. Agric. Food Chem.* 12, 43-45.
- Dickson, C.J., Madej, B.D., Skjevik, Å.A., Betz, R.M., Teigen, K., Gould, I.R., Walker, R.C., 2014. Lipid14: the amber lipid force field. *J. Chem. Theory Comput.* 10, 865–879.
- Eler, G.J., Santos, I.S., de Moraes, A.C., Mito, M.S., Comar, J.F., Peralta, R.M., Bracht, A., 2013. Kinetics of the transformation of n-propyl gallate and structural analogs in the perfused rat liver. *Toxicol. Appl. Pharmacol.* 273, 35–46.
- Erne, K., 1966. Distribution and elimination of chlorinated phenoxyacetic acids in animals. *Acta Vet. Scand.* 7, 240-256.

- Foy, C.L., Penner, D. 1965. Effect of inhibitors and herbicides on tricarboxylic acid cycle substrate oxidation by isolated cucumber mitochondria. *Weeds* 13, 226-231.
- Garabrant, D.H., Philbert, M.A. 2002. Review of 2,4-dichlorophenoxyacetic acid (2,4-D) epidemiology and toxicology. *Crit. Rev. Toxicol.* 32, 233-257.
- Geier, A., Wagner, M., Dietrich, C. G., Trauner, M., 2007. Principles of hepatic organic anion transporter regulation during cholestasis, inflammation and liver regeneration. *Biochem. Biophys. Acta* 1773, 283-308.
- Goresky, C.A., Ziegler, W.H., Bach, G.G., 1970. Capillary exchange modelling. Barrier-limited and flow-limited distribution. *Circ. Res.* 27, 739-764.
- Grest, G.S., Kremer, K., 1986. Molecular dynamics simulation for polymers in the presence of a heat bath. *Phys. Ver. A* 33, 3628-3631.
- Hanwell, M.D., Curtis, D.E., Lonie, D.C., Vandermeersch, T., Zurek, E., Hutchison, G.R., 2012. Avogadro: an advanced semantic chemical editor, visualization, and analysis platform. *J. Cheminform.* 4, 17. Doi:10.1186/1758-2946-4-17
- Hartig, K. (Program Director), 1992. 2,4-Dichlorophenoxyacetic acid (2,4-D). In.: *The MAK-Collection for Occupational Health and Safety, Occupational Toxicants*, vol. 4. Wiley Online Library, <https://doi.org/10.1002/3527600418.mb9475vere0004>.
- Hayes, J.R., Condie, L.W., Borzelleca, J.F. 1986. Acute, 14-day repeated dosing, and 90-day subchronic toxicity studies of potassium picloram. *Fund. Appl. Toxicol.* 7, 464-470.
- Heene, R. 1966. Hemmung glycogenbildender Enzyme durch 2,4-Dichlorphenoxyazetat (2,4-D) an Kryostatschnitten des Wamrblüterskelettmuskels. *Histochemie* 8, 45-53.
- Jo, S., Kim, T., Iyer, V.G., Im, W., 2008. CHARMM-GUI: a web-based graphical user interface for CHARMM. *Comput. Chem.* 29, 1859-1865.
- Johansson, A.C.V., Lindahl, E., 2009. Titratable amino acid solvation in lipid membranes as a function of protonation state; *J. Phys. Chem. B* 113, 245-253.
- Kelmer-Bracht, A.M., Ishii, E.L., Andrade, P.V.M., Bracht, A., 1984. Construction of a liver perfusion apparatus for studies on metabolic regulation and mechanisms of drug action. *Braz. Arch. Biol. Technol.* 27, 419-438.
- Kelmer-Bracht, A.M., Ishii-Iwamoto, A.L., Bracht, A., 1993. Transport and distribution space of the anti-inflammatory drug niflumic acid in the perfused rat liver. *Biochem. Pharmacol.* 45, 1863-1871.
- Khana, S.S., Yang, C., 1966. Metabolism of ¹⁴C-labeled 2,4-D in rats. *J. Agric. Food Chem.* 14, 500-503.

Kuhn, E., Stein, W. 1964. Modell-Myotonie nach 2,4-Dichlorphenoxyazetat bei der Ratte. In vitro- und in vivo-Untersuchungen über den Einfluß von 2,4-D auf den Energiestoffwechsel des Muskels. *Klin. Wschrif.* 42, 1215-1216.

Kumar, S., Bouzida, D., Swendsen, R.H., Kollman, P.A., Rosenberg, J.M., 1992. The weighted histogram analysis method for free-energy calculations on biomolecules. i. The method. *J. Comput. Chem.* 13, 1011-1021.

Li, L., Vorobyov, I., Allen, T.W., 2013. The different interactions of lysine and arginine side chains with lipid membranes. *J. Phys. Chem. B* 117, 11906–11920.

Mito, M.S., Castro, C.V., Peralta, R.M., Bracht, R.M., 2014. Effects of ranolazine on carbohydrate metabolism in the isolated perfused rat liver. *Open J. Med. Chem.* 4, 87-95.

Moreira, C.T., Oliveira, A.J., Comar, J.F., Peralta, R.M., Bracht, A., 2013. Harmful effects of usnic acid on hepatic metabolism. *Chem. Biol. Int.* 203, 502-511.

Nolan, R.J., Smith, F.A., Muller, C.J., Curl, T.C., 1980. Kinetics of ¹⁴C-labeled picloram in male Fischer 344 rats. Midland, Mich.: Toxicology Research Laboratory, Health and Environmental Science, Dow Chemical Co., U.S.A. (unpublished) 34 pp.

Nolan, R.I., Freshour, N.L., Kastl, P.E., Saunders, J.H., 1984. Pharmacokinetics of picloram in male volunteers. *Toxicol. Appl. Pharmacol.* 76, 264-269

Oghabian, Z., Ghanbarzede, N., Sharifi, M. D., Mehrpour, O., 2014. Treatment of 2,4-dichlorophenoxyacetic acid (2,4-D) poisoning; a case study. *Int. J. Med. Toxicol. Foren. Med.* 4, 104-107.

Oakes, D.J., Pollak, J. K. 1999. Effects of a hepbicide formulation, Tordon 7D[®], and its individual components on the oxidative functions of mitochondria. *Toxicology* 136, 41-52.

Palmeira, C.M., Moreno, A. J., Madeira, V. M. 1994a. Interactions of herbicides 2,4-D and inoseb with liver mitochondrial bioenergetics. *Toxicol. Appl. Pharmacol.* 127, 50-57.

Palmeira, C.M., Moreno, A. J., Madeira, V. M. 1994b. Metabolic alterations in hepatocytes promoted by the herbicides paraquat, dinoseb and 2,4-D. *Arch. Toxicol.* 68, 24-31.

Pereira, L.F., Campello, A.P., Silveira, O. 1994. Effect of Tordon 2,4-D 64/240 triethanolamine BR on energy metabolism of rat liver mitochondria. *J Appl. Toxicol.* 14, 21-26.

Qurratu, A., Reehan, A. 2016. A review of 2,4-dichlorophenoxyacetic acid (2,4-D) derivatives: 2,4-D dimethylamine salt and 2,4-D butyl ester. *Int. J. Appl. Eng. Res.* 11, 9946-9955.

Roelofsen, H., Müller, M., Jansen, P. L. M. 1997. Regulation of organic anion transport in the liver. *Yale J. Biol. Med.* 70, 435-445.

Saling, S.C., Comar, J.F., Mito, M.S., Peralta, R.M., Bracht, A., 2011. Actions of juglone on energy metabolism in the rat liver. *Toxicol. Appl. Pharmacol.* 257, 319-327.

Salla, G. B. F., Bracht, L., Sá-Nakanishi, A.B., Parizotto, A. V., Bracht, F., Peralta, R. M., Bracht, A., 2017. Distribution, lipid-bilayer affinity and kinetics of the metabolic effects of dinoseb in the liver. *Toxicol. Appl. Pharmacol.* 329, 259-271.

Scholz, R., Bücher, T., 1965. Hemoglobin-free perfusion of rat liver. In: Chance, B., Estabrook, R.W., Williamson, J.R. (Eds.), *Control of Energy Metabolism*. Academic Press, New York, pp. 393-414.

Sies, H., 1982. Nicotinamide nucleotide compartmentation. In: Sies, H. (Ed.), *Metabolic Compartmentation*. Academic Press, London, pp. 205-231.

Simões, M. S., Bracht, A., Parizotto, A.V., Comar, J. F., Peralta, R. M., Bracht, A., 2017. The metabolic effects of diuron in the rat liver. *Env. Toxicol. Pharmacol.* 54, 53-61.

Vanquelef, E., Simon, S., Marquant, G., Garcia, E., Klimerak, G., Delepine, J.C., Cieplak, P., Dupradeau, F. Y., 2011. R.E.D. server: a web service for deriving RESP and ESP charges and building force field libraries for new molecules and molecular fragments. *Nucleic Acids Res.* 39, Web Server issue W511-W517 doi:10.1093/nar/gkr288

Wang, J., Wolf, R.M., Caldwell, J.W., Kollman, P.A., Case, D.A., 2004. Development and testing of a general amber force field. *J. Comput. Chem.* 25, 1157-1174.

Zychlinski, L., Zolnierowicz, S. 1990. Comparison of uncoupling activities of chlorophenoxy herbicides in rat liver mitochondria. *Toxicol. Lett.* 52, 25-34.

Table 1

Parameters reflecting the distribution spaces of three herbicides in the liver. The parameter Φ , the extra apparent space of each herbicide divided by the water space, was determined by fitting Equation (1) to the corresponding experimental outflow profiles. Examples are illustrated by Figure 8. The mean t_0 value (transit time in the large vessels and tubing system) was equal to 0.199 ± 0.014 min. The mean standard errors of the estimate were 0.0706 ± 0.003 and 0.0509 ± 0.002 for the picloram and 2,4-D outflow profiles, respectively. The intracellular concentration, C_i , was calculated using equation (2). The inflowing extracellular concentration (C_e) of each herbicide was equal to $10 \mu\text{M}$.

Herbicide	Φ	C_i/C_e	C_i (μM)
Picloram	1.69 ± 0.20	2.67	26.79
2,4-D	5.34 ± 0.82	9.46	94.62
Dinoseb*	27.05 ± 4.90	43.86	438.7

*Data from Salla et al. (2017).

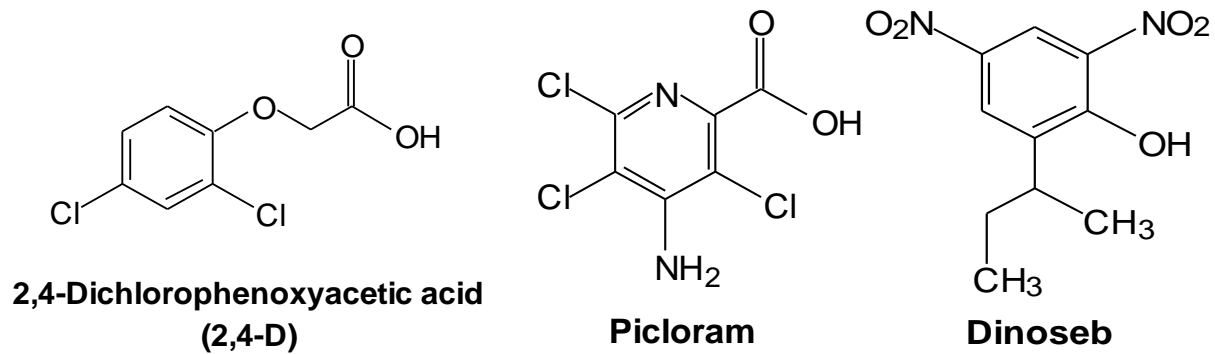


Figure 1. **Structural formulae of 2,4-D, picloram and dinoseb.**

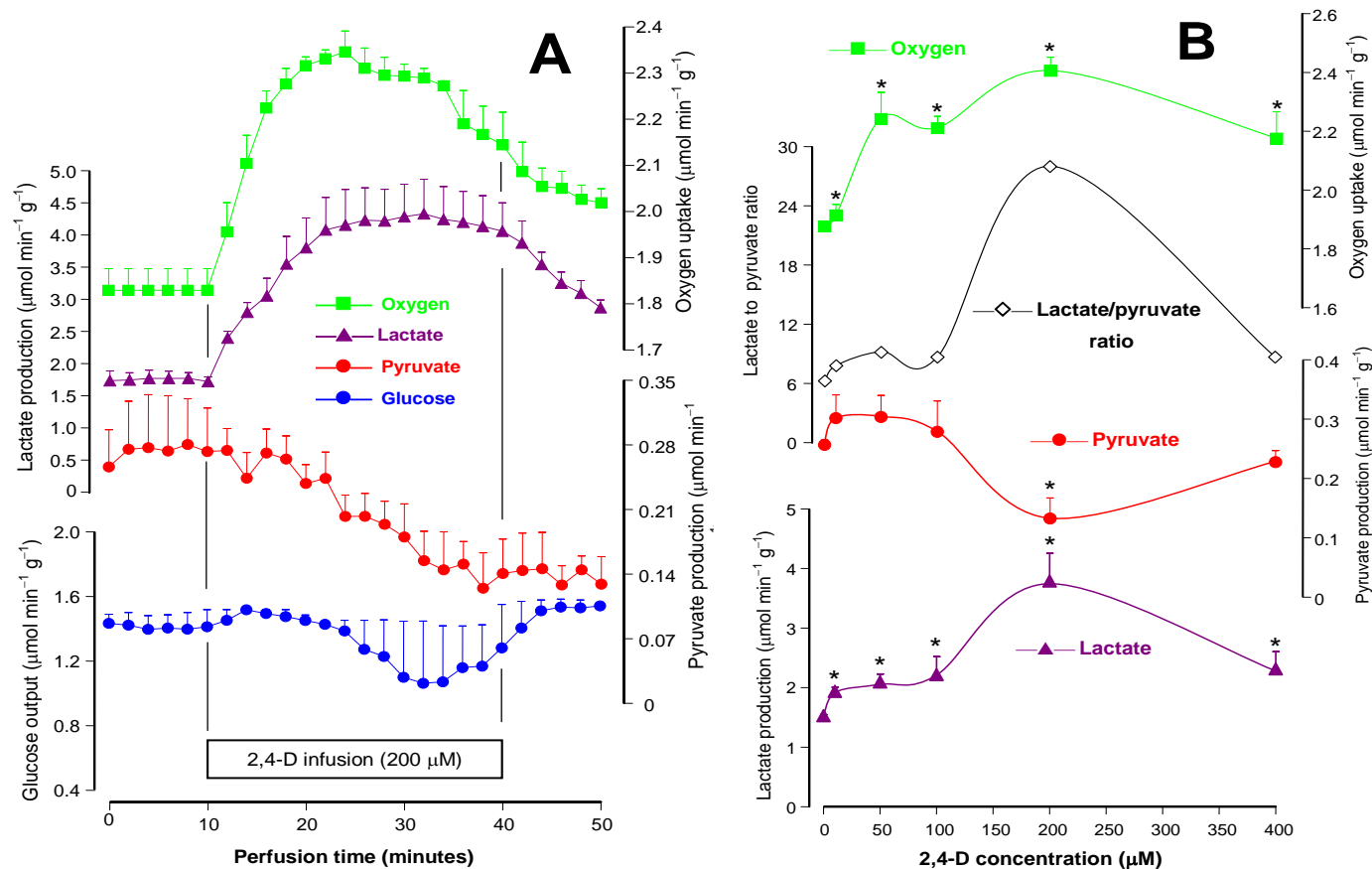


Figure 2. Time courses and concentration dependences of the actions of 2,4-D on glycogen catabolism and oxygen uptake. Livers from fed rats were perfused as described in the materials and methods section. Panel A shows the time courses of the changes caused by 200 μM 2,4-D. The effluent perfusate was sampled in 2 min intervals and analyzed for its glucose, lactate, and pyruvate contents. Oxygen consumption was followed polarographically. Panel B summarizes the results of similar experiments in which 2,4-D was infused in the range between 10 and 400 μM . Each datum point represents the mean of 3 liver perfusion experiments. Bars are standard errors of the mean. Asterisks (*) indicate statistical significance in comparison with the control condition ($p \leq 0.05$), i.e., absence of 2,4-D.

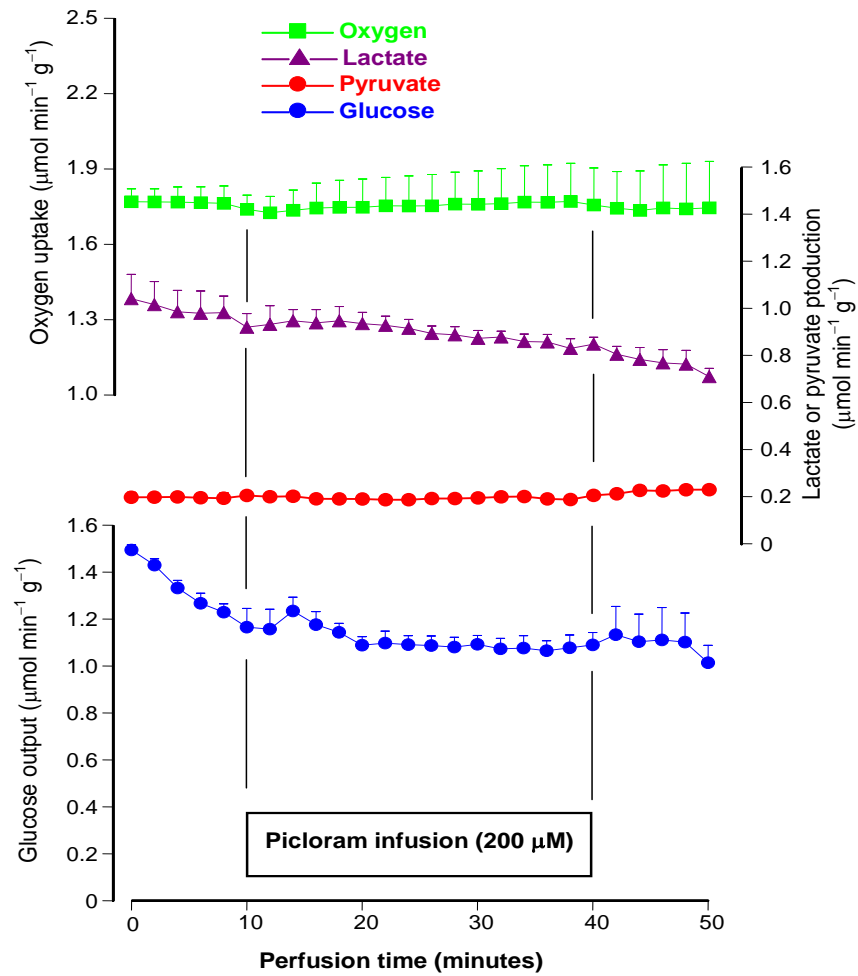


Figure 3. **Time courses of the actions of 200 μM picloram on glycogen catabolism and oxygen uptake.** Livers from fed rats were perfused as described in the materials and methods section. The effluent perfusate was sampled in 2 min intervals and analyzed for its glucose, lactate, and pyruvate contents. Oxygen consumption was followed polarographically. Each datum point represents the mean of 3 liver perfusion experiments. Bars are standard errors of the mean.

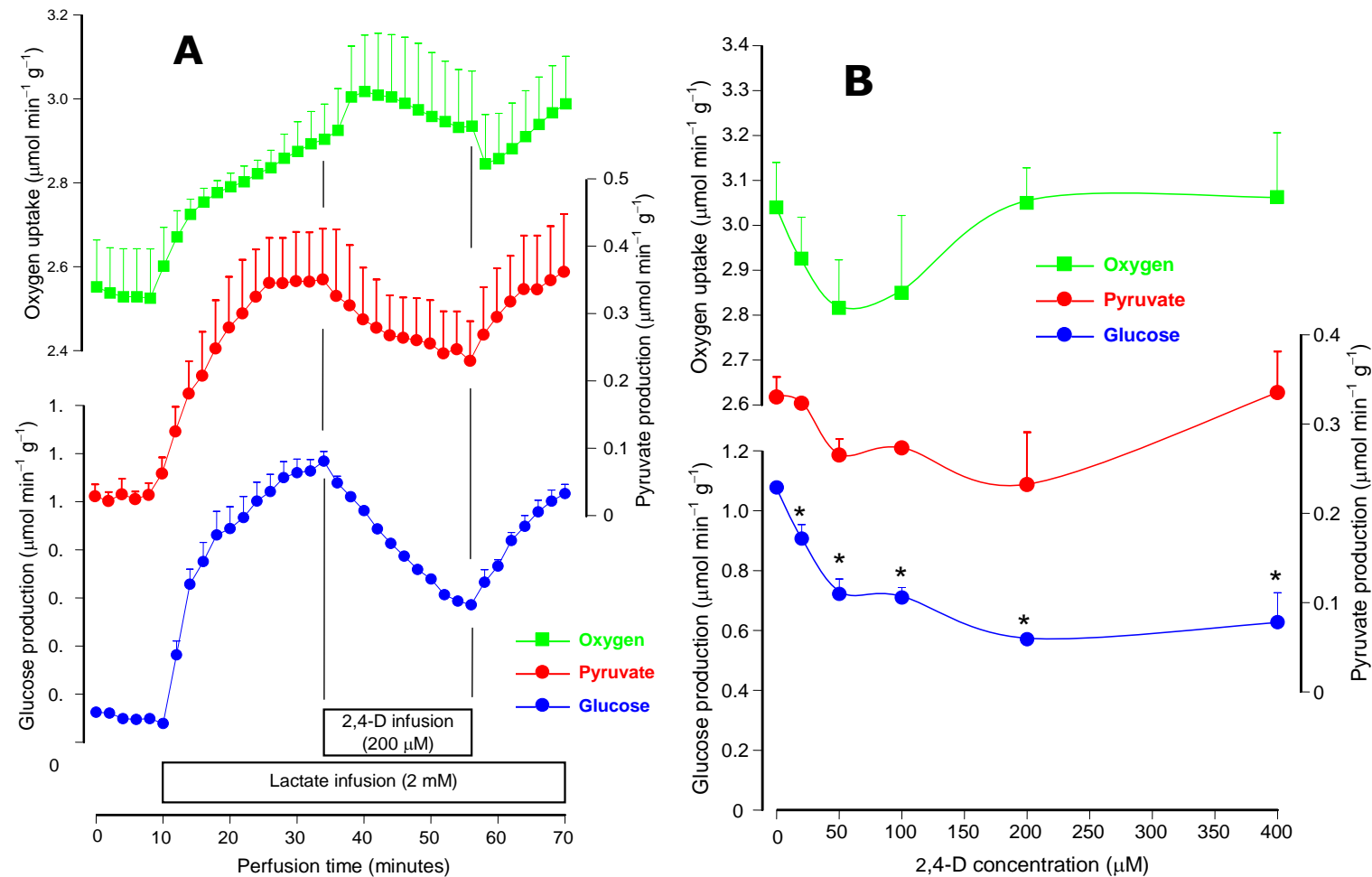


Figure 4. Time courses and concentration dependences of the actions of 2,4-D on lactate gluconeogenesis and related parameters. Livers from fasted rats were perfused as described in the materials and methods section. Panel A shows the time courses of the changes caused by 200 μM 2,4-D. Lactate (2 mM) was infused as indicated. The effluent perfusate was sampled in 2 min intervals and analyzed for its glucose and pyruvate contents. Oxygen consumption was followed polarographically. Panel B summarizes the results of similar experiments in which 2,4-D was infused in the range between 10 and 400 μM . Each datum point represents the mean of 3 liver perfusion experiments. Bars are standard errors of the mean. Asterisks (*) indicate statistical significance in comparison with the control condition ($p \leq 0.05$), i.e., absence of 2,4-D.

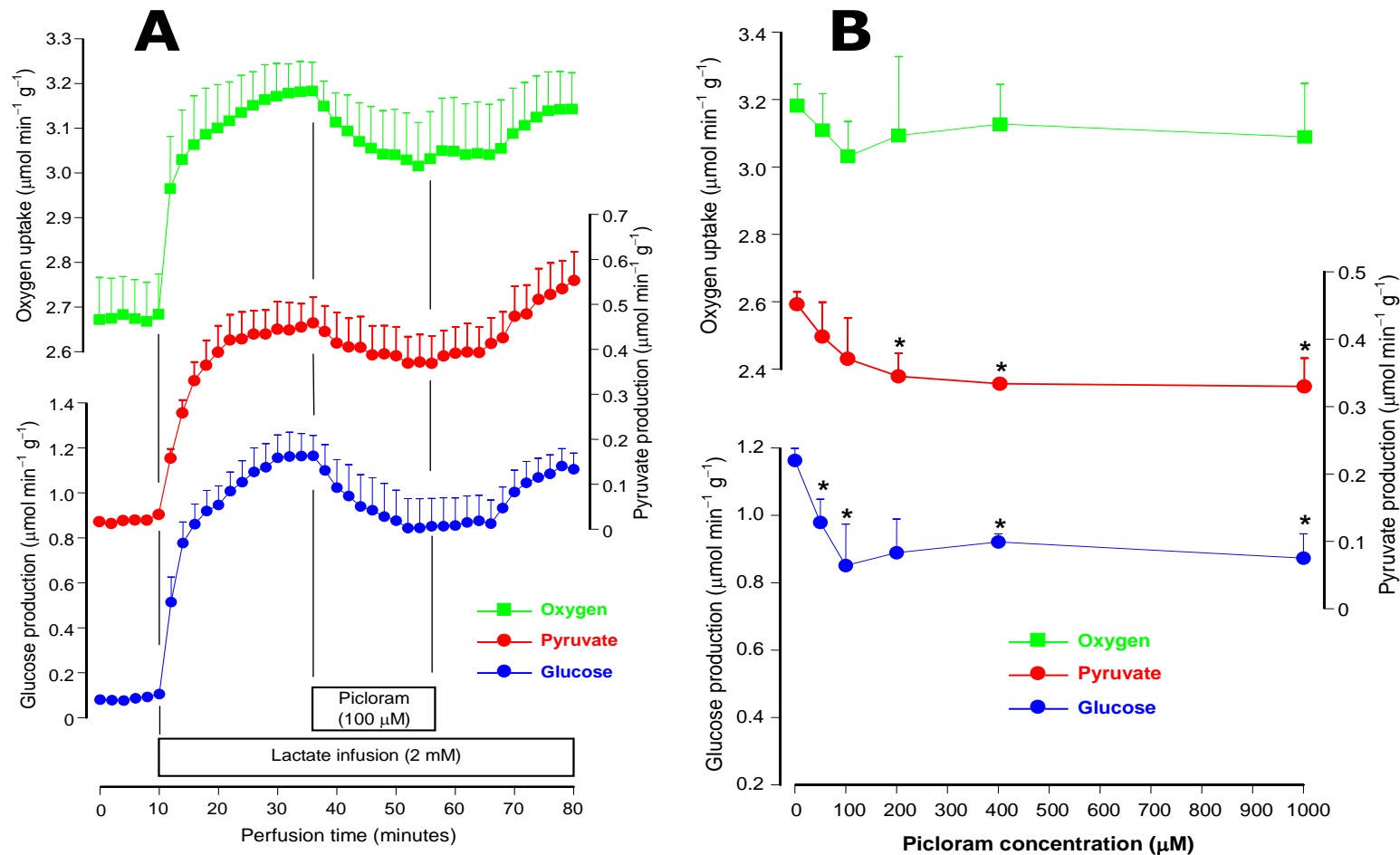


Figure 5. **Time courses and concentration dependences of the actions of picloram on lactate gluconeogenesis and related parameters.** Livers from fasted rats were perfused as described in the materials and methods section. Panel A shows the time courses of the changes caused by 100 μM picloram. Lactate (2 mM) was infused as indicated. The effluent perfusate was sampled in 2 min intervals and analyzed for its glucose and pyruvate contents. Oxygen consumption was followed polarographically. Panel B summarizes the results of similar experiments in which picloram was infused in the range between 50 and 1000 μM . Each datum point represents the mean of 3 liver perfusion experiments. Bars are standard errors of the mean. Asterisks (*) indicate statistical significance in comparison with the control condition ($p \leq 0.05$), i.e., absence of picloram.

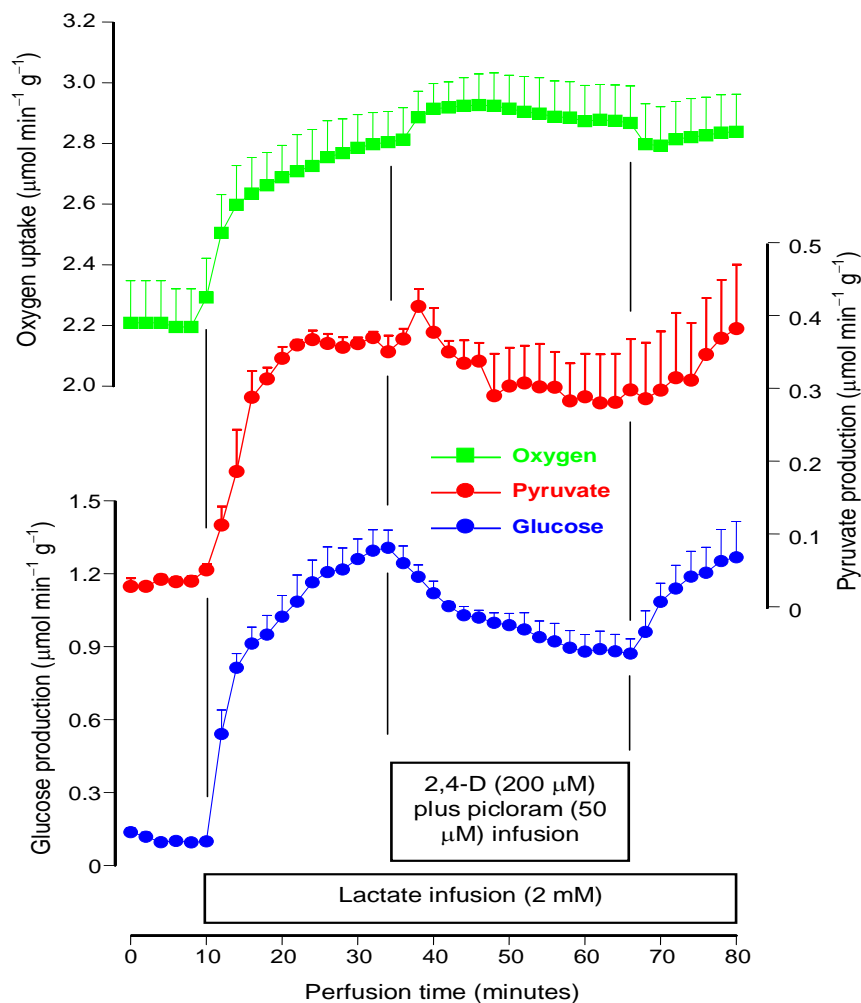


Figure 6. **Time courses and concentration dependences of the actions of picloram on lactate gluconeogenesis and related parameters.** Livers from fasted rats were perfused as described in the materials and methods section. Panel A shows the time courses of the changes caused by 100 μM picloram. Lactate (2 mM) was infused as indicated. The effluent perfusate was sampled in 2 min intervals and analyzed for its glucose and pyruvate contents. Oxygen consumption was followed polarographically. Panel B summarizes the results of similar experiments in which picloram was infused in the range between 50 and 1000 μM . Each datum point represents the mean of 3 liver perfusion experiments. Bars are standard errors of the mean. Asterisks (*) indicate statistical significance in comparison with the control condition ($p \leq 0.05$), i.e., absence of picloram.

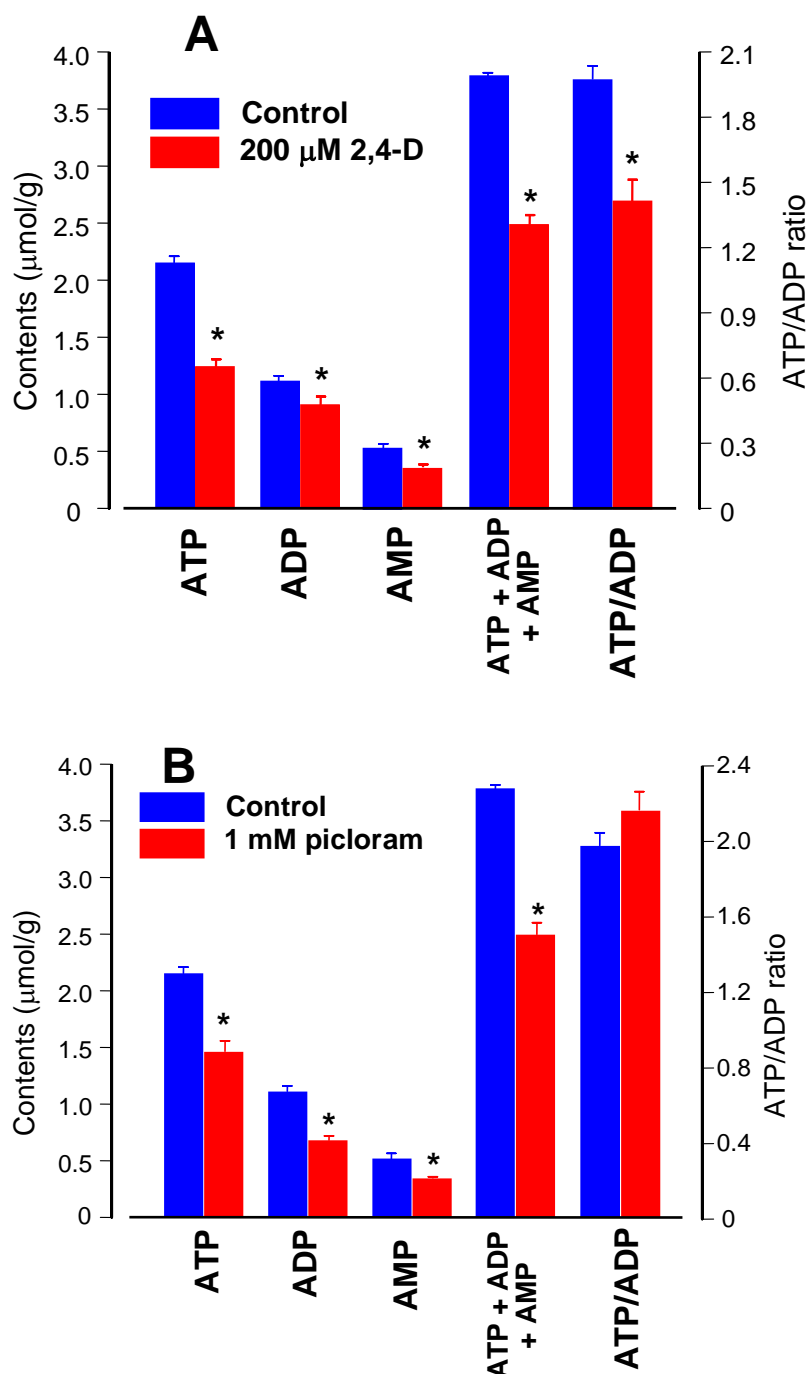


Figure 7. **Influence of 2,4-D and picloram on the hepatic contents of adenine mononucleotides in the liver from fasted rats.** Livers were perfused in an open system as described in the materials and methods section. Livers were pre-perfused with Krebs/Henseleit-bicarbonate buffer for 10 min. After that L-lactate (2 mM) was infused for 46 min with or without a simultaneous 2,4-D or picloram infusion during the last 20 minutes. At 56 minutes perfusion time the livers were freeze-clamped in liquid nitrogen and the adenine nucleotides were extracted with cold perchloric acid and determined by HPLC. Values are means \pm SEM. Asterisks indicate statistical significance in comparison with the corresponding controls.

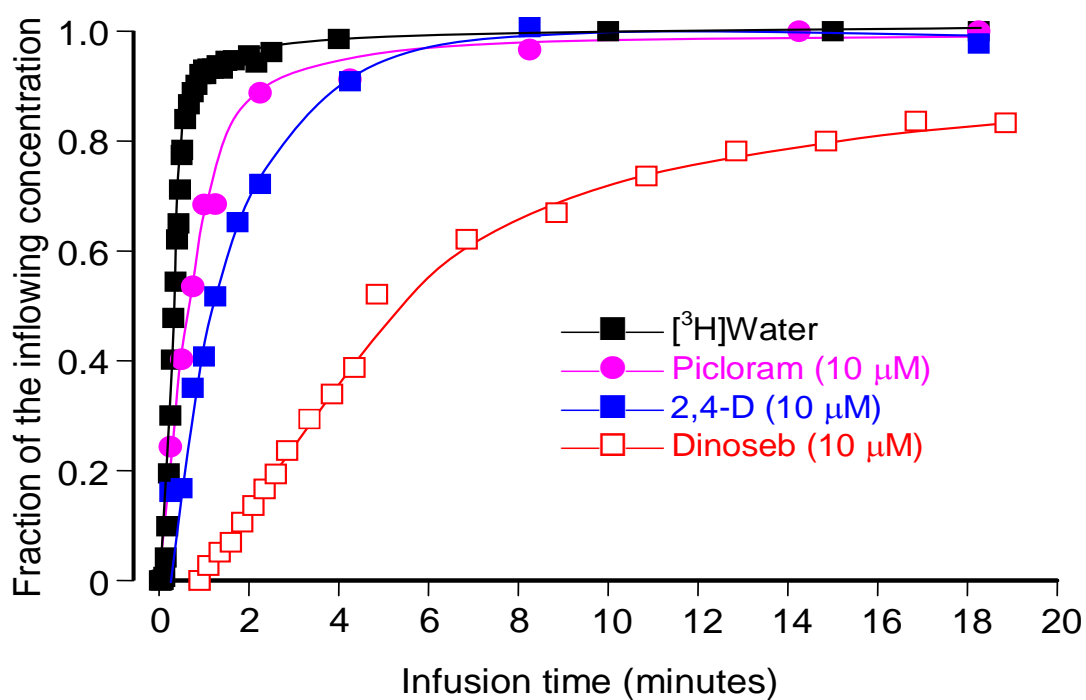


Figure 8. **Fractional outflow profiles of [³H]water, picloram and 2,4-D.** Each component was continuously infused into the portal vein at the indicated concentration. Samples of the effluent perfusate were collected for ³H counting and for the determination of the herbicides. The results were expressed as fractions of the inflowing concentration (venous portal ratio). Each curve represents the mean of 3 liver perfusion experiments.

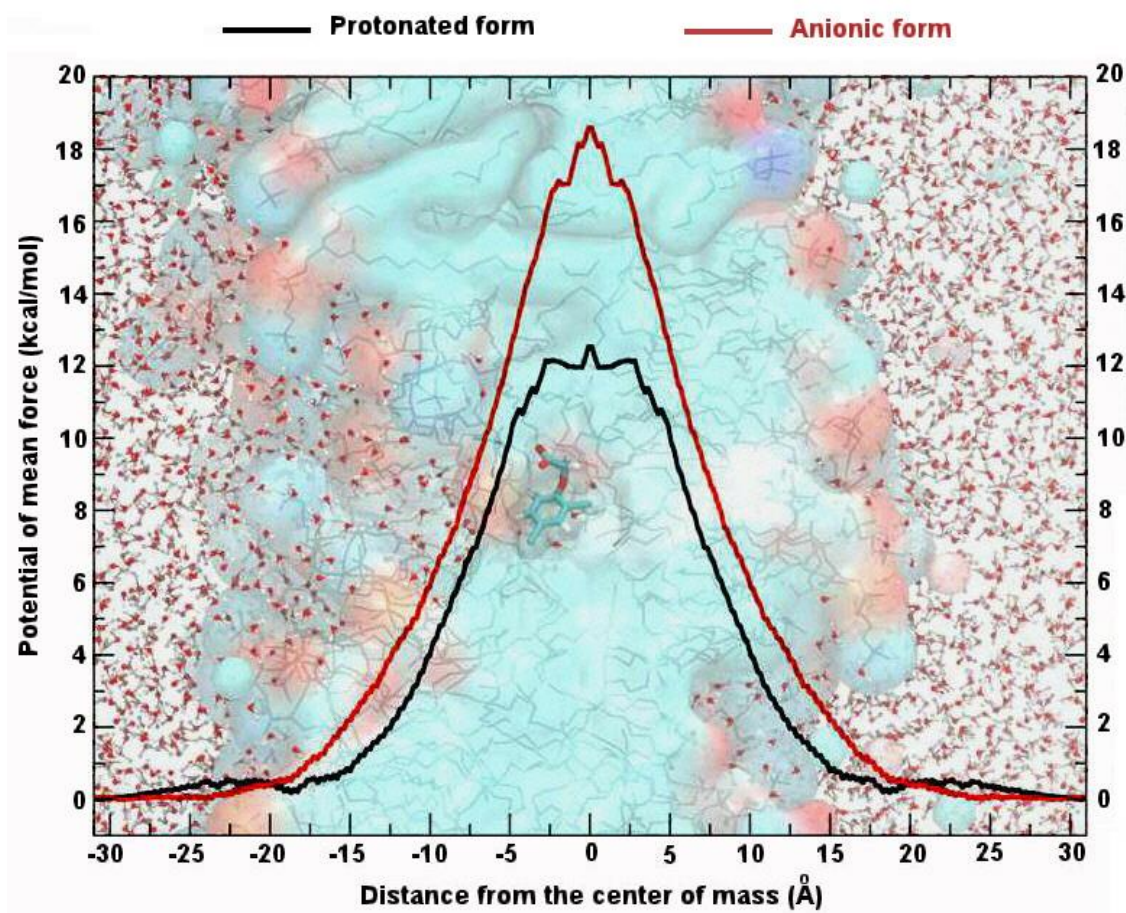


Figure 9. **Molecular dynamics simulation of the behaviour of 2,4-D in a phospholipid bilayer.** The lines represent the calculated potential of mean force (PMF) profile at each position of the 2,4-D molecule moving across the phospholipid bilayer. In the center is the 2,4-D molecule moving from left to right. Noteworthy are the slight invagination of the membrane towards the carboxylic group and the penetration of water molecules.